CONTROLLING SUBSTRATE SPECIFICITY AND STEREOSPECIFICITY OF ALCOHOL DEHYDROGENASES THROUGH MUTAGENESIS

by

CHRISTOPHER MICHAEL NEALON

(Under the Direction of ROBERT S. PHILLIPS)

ABSTRACT

This dissertation includes six chapters. Chapter 1 is an introduction and chapter 2 is a literature review that has been reprinted with permission from a published article. Chapter 3, chapter 4, and chapter 5 will be submitted for publication. Chapter 6 is the conclusion.

Chapter 3 of this dissertation discusses the enantioselective asymmetric reductions and kinetic assays of the I86A and I86A/C295A mutants of *Thermoanaerobacter ethanolicus* secondary alcohol dehydrogenase (TeSADH). The expansion of the active site small pocket allowed for ring-substituted acetophenones and heterocycles to react with the new TeSADH mutants to yield the *anti*-Prelog product, the *R*-alcohol. This broadened substrate specificity came at a cost of the specific activity, though the enantiomeric excess was >99%.

Chapter 4 of this dissertation utilizes the previously aforementioned TeSADH mutants for kinetic resolutions of racemic 1-arylethanols with the goal of converting *R*-alcohols into ketones, and leaving behind the unreacted *S*-alcohols. Due to the high

enantiomeric excess of the forward reaction, this is a creative route to generate the other alcohol isomer.

Chapter 5 of this dissertation involves the design and study of two new TeSADH mutants with the goal of expanding the active site small pocket in comparison to wild-type TeSADH. The two residues of interest, Met-151 and Thr-153, were near to each other. By mutation of each of these residues into an Alanine, the enantioselective asymmetric reductions and kinetic assays mostly yielded results that fell short from the wild-type TeSADH. Interestingly, the Met-151 residue isn't close enough to the Zn to be considered a Zn ligand, though the kinetic assay of M151A with acetone showed noticeable lag. The Met-151 residue is closer to the Asp-150, which could mean that the M151A mutant is unable to support the Asp-150 and keep it in place on the Zn.

INDEX WORDS: Alcohol deydrogenase, Asymmetric reduction, Biocatalysis, Kinetic assay, Kinetic resolution, Mutagenesis, *Thermoanaerobacter ethanolicus*

CONTROLLING SUBSTRATE SPECIFICITY AND STEREOSPECIFICITY OF ALCOHOL DEHYDROGENASES THROUGH MUTAGENESIS

by

CHRISTOPHER MICHAEL NEALON

B.S., University of Texas at Austin, 2006

A Dissertation Submitted to the Graduate Faculty of The University of Georgia in Partial Fulfillment of the Requirements for the Degree

DOCTOR OF PHILOSOPHY

ATHENS, GEORGIA

2015

CONTROLLING SUBSTRATE SPECIFICITY AND STEREOSPECIFICITY OF ALCOHOL DEHYDROGENASES THROUGH MUTAGENESIS

by

CHRISTOPHER MICHAEL NEALON

Major Professor:	Robert S. Phillips
Committee:	Geert-Jan Boons
	Vladimir Popik

Electronic Version Approved:

Suzanne Barbour
Dean of the Graduate School
The University of Georgia
August 2015

DEDICATION

To my parents, brother and sisters for all the love and support that they have shown me throughout my life.

ACKNOWLEDGEMENTS

First, I'd like to thank my research advisor, Professor Robert S. Phillips, for all of his guidance and support. I've learned so much while working in his research lab, which I'm immensely grateful for. Also, I'm thankful for the help and suggestions of my advisory committee, Professor Geert-Jan Boons and Professor Vladimir Popik.

I owe so much to my family for always being patient, encouraging and supportive to me. My groupmates have helped me with many things around the lab during my studies in the Phillips lab: Jay Patel, Quong Do, Yao Wang, Tung Dinh, Bryan Linn, Phanneth Som, Nathan Lott, Chandan Maitrani, and Sunil Kumar. Two visiting professors, Professor Musa Musa and Professor Chang Sup Kim, helped my studies through collaboration on the secondary alcohol dehydrogenase project. While working on the project, I've had help from undergraduate researchers, including Travis Welch and Anna Kim.

I must thank the Department of Chemistry and the University of Georgia for their support that allowed me to study here for my doctorate work. I'm grateful for all the friends that I've met in my time here in Athens, and I'm also grateful to the Catholic Center community for providing such a welcoming and friendly place, while I've lived in Athens, GA.

TABLE OF CONTENTS

LIST OF TABLES

Page

LIST OF FIGURES

Page

LIST OF ABBREVIATIONS

[BMIM][BF_4] ..... 1-butyl-3-methylimidazolium tetrafluoroborate

[BMIM][NTf_2] ..... 1-butyl-3-methylimidazolium bis((trifluoromethyl)sulfonyl)imide)

[BMIM][PF_6] ..... 1-butyl-3-methylimidazolium hexafluorophosphate

5-HMF 5-Hydroxymethyl-2-furfural

Abs. Conf. ..... Absolute Configuration

ADH ..... Alcohol Dehydrogenase

ADH-A ..... *Rhodococcus ruber* Alcohol Dehydrogenase

ADPR ..... Adenosine Diphosphoribose

Ala, A ..... Alanine

AR ..... Asymmetric Reduction

Arg, R ..... Arginine

Asn, N ..... Asparagine

Asp, D ..... Aspartic Acid

C ..... Celsius

C. antarctica ..... *Candida antarctica*

CalA ..... *Candida antarctica* lipase A

CalB ..... *Candida antarctica* lipase B

Conv. ..... Conversion

CPCR2 ..... *Candida parapsilosis* carbonyl reductase

CtXR .....*Candida tenuis* xylose reductase

Cys, C .....Cysteine

DTT .....Dithiothreitol

E ..... Enantiomeric Ratio

E. coli ..... *Escherichia coli*

ee, *ee* .....Enantiomeric Excess

Et .....Ethyl

g ..... Gram

GC .....Gas Chromatography/Gas Chromatograph

Gln, Q .....Glutamine

Glu, E .....Glutamic Acid

Gly, G .....Glycine

His, H .....Histidine

HLADH .....Horse Liver Alcohol Dehydrogenase

Ile, I ..... Isoleucine

J ..... Joule

K .....Kelvin

KR ..... Kinetic Resolution

L .....Liter

Leu, L .....Leucine

LladhA .....*Lactococcus lactis* alcohol dehydrogenase

Lys, K .....Lysine

M .....Molar

Me	Methyl
Met, M	Methionine
mg	Milligram
mL	Milliliter
mM	Millimolar
mmol	Millimole
mol	Mole
MPa	MegaPascal
NA	No Measurable Activity
NAD^+	Nicotinamide Adenine Dinucleotide
NADH	Nicotinamide Adenine Dinucleotide, Reduced
$NADP^+$	Nicotinamide Adenine Dinucleotide Phosphate
NADPH	Nicotinamide Adenine Dinucleotide Phosphate, Reduced
ND	Not Determined
nmol	Nanomole
OMe	Methoxy
Ph	Phenyl
Phe, F	Phenylalanine
Pro, P	Proline
s	Second
S. cerevisiae	*Saccharomyces cerevisiae*
S. pombe	*Schizosaccharomyces cerevisiae*
SADH	Secondary Alcohol Dehydrogenase

Sc ..... *Saccharomyces cerevisiae*

Ser, S ..... Serine

SsADH .....*Sulfolobus solfataricus* Alcohol Dehydrogenase

SsCR .....*Sporobolomyces salmonicolor* carbonyl reductase

T. brockii ..... *Thermoanaerobacter brockii*

T. ethanolicus .....*Thermoanaerobacter ethanolicus*

TbSADH ..... *Thermoanaerobacter ethanolicus* Secondary Alcohol Dehydrogenase

TeSADH .....*Thermoanaerobacter brockii* Secondary Alcohol Dehydrogenase

Thr, T ..... Threonine

Trp, W .....Tryptophan

Tyr, Y ..... Tyrosine

Val, V .....Valine

YADH .....Yeast Alcohol Dehydrogenase

CHAPTER 1

INTRODUCTION

This dissertation is composed of six chapters. Chapter 1 is an introduction, and chapter 2 is a literature review that has been reprinted with permission from a published article. Chapter 3, chapter 4, and chapter 5 will be submitted for publication. Chapter 6 is the conclusion.

Chapter 3 of this dissertation discusses the enantioselective asymmetric reductions and kinetic assays of the I86A and I86A/C295A mutants of *Thermoanaerobacter ethanolicus* secondary alcohol dehydrogenase (TeSADH). The expansion of the active site small pocket allowed for ring-substituted acetophenones and heterocycles to react with the new TeSADH mutants to yield the *anti*-Prelog product, the *R*-alcohol. While this broadened substrate specificity came at a cost of the specific activity, the enantiomeric excess was >99%. The combination of I86A and C295A provide a nice starting point for additional mutants.

Chapter 4 of this dissertation utilizes the previously aforementioned TeSADH mutants for kinetic resolutions of racemic 1-arylethanols with the goal of converting *R*-alcohols into ketones, which would leave behind the unreacted *S*-alcohols. Due to the high enantiomeric excess of the forward reaction, this would be a creative route to generate the other alcohol isomer. This would be of interest in the area of synthetic organic chemistry, because both the *R* and *S*-alcohols would be able to be produced selectively, as long as the substrates were able to fit inside of the active site.

Chapter 5 of this dissertation involves the design and study of two new TeSADH mutants with the goal of expanding the active site small pocket in comparison to wild-type TeSADH. The two residues of interest, Met-151 and Thr-153, were near to each other. By mutation of each of these residues into an Alanine, the enantioselective asymmetric reductions and kinetic assays mostly yielded results that fell short from the wild-type TeSADH. Interestingly, the Met-151 residue isn't close enough to the Zn to be considered a Zn ligand, though the kinetic assay of M151A with acetone showed noticeable lag. Because of this aforementioned lag, the kinetic parameters would be difficult to determine for any substituents. The Met-151 residue is closer to the Asp-150, which could mean that the M151A mutant is unable to support the Asp-150 and keep it in place on the Zn. Due to the asymmetric reductions behaving normally, the Zn must be able to reenter the active site, if it is in fact leaving the binding pocket. Even though the results were not ideal for M151A and T153A, the protein engineering sheds light on the negative impact of mutating the Met-151 residue.

CHAPTER 2

LITERATURE REVIEW: CONTROLLING SUBSTRATE SPECIFICITY AND STEREOSPECIFICITY OF ALCOHOL DEHYDROGENASES[1]

---

[1] Nealon, C. M.; Musa, M. M.; Patel, J. M.; Phillips, R. S. *ACS Catal.* **2015**, *5*, 2100-2114.

Abstract

The ability to control the substrate specificity and stereochemistry of enzymatic reactions is of increasing interest in biocatalysis. As this review highlights, this control can be achieved through various means, including mutagenesis of active site residues, alteration of physical variables like temperature and pressure, as well as through changing the reaction medium. While the focus of this article is on alcohol dehydrogenase reactions, each of these techniques can be readily applied towards other enzyme classes as well.

KEYWORDS**:** mutagenesis, substrate specificity, alcohol dehydrogenase, stereospecificity, protein engineering, medium engineering

Introduction

In recent years, biocatalysis, which is the use of enzymes as catalysts, has gained significant interest, since biocatalysis can be seen as a means of "green chemistry." For a process to be classified as green, it needs to generate or utilize few, if not zero, hazardous chemicals.[1] One very appealing aspect of enzymes is that they have been designed in nature for specific tasks, including recycling products and by-products into other more useful compounds. Even when an enzyme's active site has been optimized for a specific compound, the enzyme may show substrate promiscuity and thus accept a wide range of substrates in vitro. In order to expand substrate specificity, a wild-type enzyme can be modified by random or selective mutagenesis to expand the scope of the substrate specificity, some examples of which will be highlighted in this review. Two basic techniques of mutating an enzyme are through rational design and directed evolution.[1] Rational design entails altering a specific amino acid to cause a change in the enzyme selectivity, whether it is in the active site, the coenzyme binding pocket, or perhaps a spot

elsewhere on the enzyme. Directed evolution involves developing a library through random mutagenesis and then selecting the mutants that have features, which meet particular criteria, whether that be increased reactivity or decreased reactivity towards a desired substrate.

Another approach that is used to alter enzyme selectivity is changing the reaction medium (i.e. medium engineering). This approach is of great interest because it represents an alternative approach to the more laborious protein engineering. Besides protein engineering, this review will also cover a few examples of influencing stereoselectivity by switching reaction media from the traditional aqueous to nonaqueous media. The effect of temperature and pressure on stereospecificity of ADHs will also be described.

Alcohol Dehydrogenases

Alcohol dehydrogenases (ADHs, EC 1.1.1.X, X=1 or 2) are nicotinamide adenine dinucleotide (NAD^+)- or ($NADP^+$)-dependent oxidoreductases, which are enzymes that catalyze the transfer of electrons from a donor molecule to an acceptor molecule. They catalyze the reversible reduction of ketones and aldehydes to their corresponding alcohols. In an ADH-catalyzed redox transformation, a hydrogen molecule will be either added to a carbonyl or removed from an alcohol, as a hydride plus a proton. As shown in Figure 2.1, the hydride from the coenzyme (NADH/NADPH) can attack the carbonyl of an unsymmetrical ketone substrate from either the *Re* face or *Si* face, producing the corresponding optically active secondary alcohol, with only a few cases of enzymes allowing the hydrogen to come in from either face (i.e. not stereospecific).

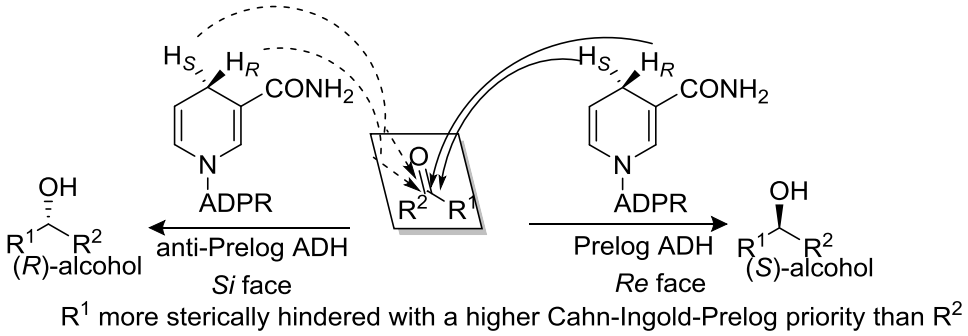

Figure 2.1. Prelog's rule explaining the stereochemistry of the hydride transfer from NAD(P)H to the carbonyl carbon of a ketone substrate in ADH-catalyzed transformations. ADPR = adenosine diphosphoribose

In order to understand better the orientation of the substrate in the enzyme active site, it is important to have a map of the active site. In pioneering studies of the 1960's, Prelog proposed using a diamond lattice structure to visualize oxidoreductase active sites.[2] To validate his hypothesis, he tested the reaction with a series of increasingly larger substrates, and was able to determine the maximum spatial limits of the active site in each direction. By overlaying the molecules, which gave successful results, the active site was effectively mapped. It was important to have a means to map the active site, since this would give a measure of the limit of stereospecificity, and in the future, substrate specificity.

In an extension of Prelog's diamond lattice model, Jones and coworkers further studied its utility towards horse liver alcohol dehydrogenase (HLADH) reactions.[3-7] In the early 1980's, Jones and Jakovac proposed a cubic space section model, due to the disadvantages of the diamond lattice for mapping an active site.[3] Among the disadvantages were the use of sp^3 hybridized carbon bond lengths and angles which could invariably limit researchers to use the diamond lattice model to choose substrates for analysis. With the cubic space section model, the cube sizes were flexible, which

allowed researchers to use blocks that were as large or small as desired. The results for simpler examples, which worked adequately with Prelog's diamond lattice, also worked satisfactorily with the cubic model. Jones and coworkers highlighted further examples that fit nicely with the new cubic shaped model.[4-7]

While mutagenesis can be accomplished routinely at present, it was not always the case. Hence, Jones studied the varying active sites of naturally occurring variants. Even though the cubic space model was useful, it was not widely adopted by other research groups due to the advent of more straightforward X-ray crystal structures, which give very clear information regarding the shape of the active site. Nonetheless, these early active site models have paved the way for current research, since they clearly showed that substrate specificity is controlled by the shape of the active site, and hence studying substrate specificity and then altering it is much more easily done with a model. For example, such a model has been proposed by Keinan *et al*.[8] for a thermophilic alcohol dehydrogenase from *Thermoanaerobium brockii*, and the model includes a small and a large pocket which is evident in the X-ray crystal structure.[9] The main focus for this article will be on alcohol dehydrogenases of the medium chain family, but we will include a few other examples. While there has been extensive research into enzyme mutation in order to alter cofactor specificity, that work falls outside of the scope of this review article, which will focus on altering substrate specificity through the use of mutagenesis, altering the temperature and pressure, and by changing the reaction medium.

Examples of Mutagenesis to alter substrate specificity

Medium Chain Alcohol Dehydrogenases

Site-directed mutagenesis has been widely utilized to study enzyme mechanisms, and less commonly to alter substrate specificity. Oftentimes, a crystal structure has been used to guide the mutagenesis. Generally speaking, there are four reasons for altering protein structure through mutagenesis.[10] Mutagenesis provides a means to study the rules that are in charge of protein structure and function. Mutation of an enzyme also can bring along a desired effect, which is one of the most common reasons. The last two reasons are the development of novel strategies in designing and working with proteins, and the opportunity to glimpse into the normal function of an enzyme.

Horse Liver ADH (HLADH)

HLADH has received a lot of attention over the years, in addition to having models applied to its active site as mentioned earlier in this review. In the 1970's, the isozymes of HLADH were discovered.[11] The Ethanol and Steroidal monomer units, "E" and "S", could be combined in three different dimers, "EE," "ES," and "SS." The EE and SS isozymes differ in that only the SS form reacts with steroidal alcohols. Interestingly, the E or S monomer units are inactive, but they become active when they dimerize. While the SS isozyme reacts with ethanol as well as steroids, the EE isozyme reacts only with ethanol. Thus, the structural differences between the EE and SS isozymes that lead to the changes in substrate specificity were of interest.

There were ten differences in amino acid sequence found between the two forms of HLADH.[12] As shown in Table 2.1, the differences are scattered throughout the structure. These amino acid differences control the substrate specificity of the E and S isozymes of HLADH.

Table 2.1. Differences in amino acid sequences of the two isozymes of HLADH

Residue	E	S	AA [a]	Location of residue in structure
17	E	Q	y [b]	Surface
43	T	A		Interior
59	T	A		Surface
94	T	I	y	Partly buried behind Phe-93 in the substrate pocket
101	R	S	y	Cleft; minor subunit-subunit interaction
110	F	L	y	Substrate pocket
115	D	Δ [c]	[d]	Buried behind Leu-116 in the substrate pocket
172	I	V		Interior
277	T	A		Surface; close to the adenine ring of coenzyme
366	E	K	y	Cleft between the two domains

[a] Determined by amino acid sequencing.[13] [b] y indicates agreement between the cDNA-derived sequence and the protein sequence. [c] Δ, deletion. [d] Residue ambiguous in Jörnvall's determination.

After Plapp and coworkers highlighted the differences between the two isozymes, they were able to interconvert the E and S isozymes.[14] Table 2.2 describes the mutations that were made for the E isozyme to react with a steroidal alcohol. As Plapp found, simply deleting the Asp-115 introduced some steroidal alcohol activity to the E isozyme. Surprisingly, the ESE mutant enzyme was found to have greater activity toward steroidal alcohols than the S isozyme, even though the substrate binding pockets are identical. This implies that other factors than the amino acids in direct contact to the bound substrate could be in play.

Table 2.2. Comparison of primary structures of the natural and mutant HLADH

Residue Number	E	E/D115Δ [a]	ESE	ESS	S/K366E	S [b]
17	Glu	Glu	Glu	Glu	GLN	GLN
43	Thr	Thr	Thr	Thr	ALA	ALA
59	Thr	Thr	Thr	Thr	ALA	ALA
94	Thr	Thr	ILE	ILE	ILE	ILE
101	Arg	Arg	SER	SER	SER	SER
110	Phe	Phe	LEU	LEU	LEU	LEU

115	Asp	Δ [a]	Δ [a]	Δ [a]	Δ [a]	Δ [a]
172	Ile	Ile	Ile	VAL	VAL	VAL
277	Thr	Thr	Thr	ALA	ALA	ALA
366	Glu	Glu	Glu	LYS	Glu	LYS
Relative charge per monomer	-2	-1	-2	0	-1	+1

[a] Δ, deletion. [b] Amino acids in capital letters correspond to S isozyme.

Adolph *et al.* reported a ternary crystal structure of SS HLADH complexed with NAD^+ and cholic acid and then compared the structure with that of the EE isozyme.[15] Their study revealed that the major structural difference was the widening of the substrate channel.[15] This allowed space for the steroidal alcohol to fit in the substrate pocket, whereas the EE isozyme lacks the space for the steroidal alcohol to fit in the pocket. These results emphasized the importance of the shape of the active site in substrate specificity of ADHs, and demonstrated that there can be dramatic effects on substrate specificity with a relatively small number of mutations.

Yeast ADH (YADH)

YADH, an NAD^+-dependent ADH, has *in vivo* activity towards acetaldehyde and ethanol during anaerobic fermentation of glucose. Just as with other ADHs, the active site of YADH accommodates various other aldehydes and their corresponding primary alcohols. Examples of unnatural substrates for YADH include acyclic aldehydes and their corresponding primary alcohols. Some of these unnatural substrates include 1-propanol and ethylene glycol, among many others.[16,17]

In an effort to alter the substrate specificity of YADH, Murali *et al.* introduced the double mutant T48S/W93F YADH, and found that this mutation opened up the active site as planned, thus allowing larger alcohols to fit inside the active site of the designed

mutant.[18] They also found that the Phe-93 position reduced the substrate affinity, possibly due to the hydrophobicity of the phenylalanine.

Three isozymes (I, II, and III) of YADH from *Saccharomyces cerevisiae*, and the ADH from *Schizosaccharomyces pombe* have nearly identical active sites.[19] The only difference found was at residue 294. Isozyme I and *S. pombe* ADH have a methionine at this position, whereas isozymes II and III have a leucine. Mutagenesis of the Met-294 in isozyme I allowed for comparison of the three isozymes, which yielded very similar kinetic parameters. The kinetic study was conducted with ethanol as the substrate and all of the wild type enzymes and the mutant were tested. Isozyme II was found to have a 10-20 fold smaller Michaelis constant and inhibition constant than the others. This showed that an amino acid mutation outside the active site caused a significant change in enzyme activity, even though the active site sequences all matched.

In continuation of the previous work, Plapp and coworkers studied *S. cerevisiae* YADH I and compared it to the liver ADHs of horse and monkey.[20,21] They also mutated residues within the active site of the YADH I. Table 2.3 shows the V/K_m values for these dehydrogenases with a range of primary alcohols containing 2-9 carbons. Interestingly, *S. cerevisiae* wild type YADH and its T48S mutant had decreasing activity from ethanol to pentanol, and then wild type activity increased with the larger alcohols, while T48S YADH exhibited activity for hexanol and no activity beyond this. *S cerevisiae* W57M YADH showed less ethanol specific activity, and the activity declined quickly as the primary alcohol was extended. Even though the single mutant *S. cerevisiae* W93A YADH had low activity for ethanol, the active site was enlarged enough that the larger primary alcohols reacted much more easily. Combining this mutation with the T48S

mutant to generate the double mutant T48S/W93A YADH gave activity that was nearer to that of HLADH (see Table 2.3) with primary alcohols. However, the triple mutant (*S. cerevisiae* T48S/W57M/W93A) YADH had significantly lower activity towards most of the tested substrates. The secondary alcohol and branched chain alcohol specific activities shown in Table 2.4, demonstrate that the *S. cerevisiae* YADH mutants tested had little improvement with smaller alcohols, but had some improvement with the larger secondary and branched alcohols. The activity was much lower than what was observed with HLADH.

Table 2.3. Kinetic parameters for various primary alcohols with YADHs

ADH	V/K_m ($M^{-1}s^{-1}$)							
	Alcohols							
	Ethyl	**Propyl**	**Butyl**	**Pentyl**	**Hexyl**	**Heptyl**	**Octyl**	**Nonyl**
Sc I[a]	20,000	4400	930	780	1700	1800	3300	5100
Sc T48S	12,000	2500	1300	330	480	ND[b]	ND	ND
Sc W57M	5,000	260	340	450	70	ND	ND	ND
Sc W93A	57	61	150	500	5100	26,000	29,000	13,000
Sc T48S/W93A	37	43	220	3500	16,000	34,000	54,000	38,000
Sc T48S/W57M/W93A	530	140	160	90	90	460	820	930
HLADH	10,000	21,000	19,000	29,000	50,000	135,000	58,000	ND

[a] *Sc*: *Saccharomyces cerevisiae*, [b]ND: not determined

Table 2.4. Kinetic parameters for various secondary and branched chain alcohols with YADHs

ADH	V/K_m ($M^{-1}s^{-1}$)								
	2-Propanol	**2-Butanol**		**2-Methyl-1-propanol**	**2-Methyl-1-butanol**		**3-Methyl-1-butanol**	**Benzyl alcohol**	**Cyclohexanol**
		R	***S***		***S***	***RS***			
Sc I	25	0.8	18	7.6	NA[a]	NA	NA	NA	NA

Sc T48S	24	1.2	27	40	2.7	4.2	NA	14	NA
Sc W57M	12	1.4	3.3	2.5	NA	NA	NA	ND [b]	ND
Sc W93A	1.5	0.61	0.49	3.1	2.8	9.3	52	17	0.041
Sc T48S/W93A	ND	0.14	0.22	ND	16	57	230	5.0	1.1
Sc T48S/W57M/W93A	0.79	0.50	4.2	3.8	3.3	2.3	2.7	9.2	0.17
HLADH	24	110	290	13,000	18,000	10,000	19,000	78,000	5,500

[a] NA, no measurable activity; [b] ND, not determined

Benner and coworkers tried to alter the substrate specificity of YADH in order to allow reactions with branched chain alcohols.[22] There were a few residues that could have been potentially altered to increase the activity. The residues chosen (W54, L116, M270, I290) were pointed out by Branden *et al.* as side chains that could be modified to improve activity, since they are located at the entrance of the active site.[23] While HLADH has the same residues at locations 116 and 290, the methionine at site 270 for YADH is a valine in HLADH. At site 54, the tryptophan in YADH had been replaced by a leucine in HLADH. Benner investigated Trp-54 further to improve the activity of YADH.[22] With the W54L mutation, the ethanol specificity dropped down 10-fold compared with the wild type, as shown in Table 2.5. The greatest specificity for the W54L mutant was found with cinnamyl alcohol. Less change was found between the wild type and mutant enzymes for secondary alcohols exhibiting low activity. The W54L mutant showed improvement with longer straight chain alcohols and branched alcohols, which was very interesting.

Table 2.5. YADH - Substrate specificity of YADH I and its W54L mutant with various alcohols[a]

	Wild type ADH I			**Mutant W54L**		
	k_{cat} **(s^{-1})**	K_m **(mM)**	k_{cat}/K_m **($s^{-1}mM^{-1}$)**	k_{cat} **(s^{-1})**	K_m **(mM)**	k_{cat}/K_m **($s^{-1}mM^{-1}$)**
Primary						

alcohols						
Ethanol	308±11	4.0±0.5[b]	76.3±7.1[b]	102.1±2.8	13.4±0.6	7.64±0.13
Cinnamyl alcohol	133±8	4.58±0.35	29.0±0.6	98.0±3.9	1.5±0.1	67.3±2.9
Secondary Alcohols						
2-Propanol	53.1±10.1	268±58	0.198±0.005	5.8±0.9	193±33	0.030±0.001
(*S*)-2-Butanol	11.9±3.5	93.3±33.9	0.127±0.008	0.31[b]		

[a] Determined with 10 mM NAD^+ in sodium pyrophosphate buffer (32 mM, pH 8.2), containing 100 mM Na_2SO_4 at varying alcohol concentrations at 25°C. [b] With an alcohol concentration of 50 mM.

Lactococcus lactis alcohol dehydrogenase (LladhA)

LladhA is of interest since it can be used for the conversion of isobutyraldehyde to isobutanol, a possible biofuel, with NADH, when expressed in *E. coli*. Arnold and coworkers altered the active site of LladhA by site-saturation mutagenesis.[24] Even though the initial intent was to increase the specificity for isobutyraldehyde, the researchers also conducted kinetic assays with other aldehydes against LladhA, $LladhA^{RE1}$ (Y50F/I212T/L264V) and $LladhA^{29C8}$ (Y50F/N110S/I212T/L264V), with the results shown in Table 2.6.[24] As the wild-type LladhA was mutated to the triple and then quadruple mutant, the k_{cat} and k_{cat}/K_m for isobutyraldehyde went up considerably. Acetaldehyde and 2-furaldehyde both showed a decrease in k_{cat}/K_m, while k_{cat} for 5-hydroxymethylfurfural increased for both $LladhA^{RE1}$ and $LladhA^{29C8}$. Interestingly, while the k_{cat} values for cinnamaldehyde showed little change, there was a 3-4 fold drop in the K_m values, which translated to a corresponding boost in k_{cat}/K_m. In addition, the researchers found more substrates that worked for these three enzymes (wild type and two mutants), including cinnamaldehyde and 5-hydroxymethyl-2-furaldehyde.

Table 2.6. Kinetic data for wild-type and mutants of *Lactococcus lactis* ADH[a]

Aldehydes	LladhA (wild-type)			LladhA^{RE1} (Y50F/I212T/L264V)			LladhA^{29C8} (Y50F/N110S/I212T/L264V)		
	K_m (mM)	k_{cat} (s^{-1})	k_{cat}/K_m ($mM^{-1}s^{-1}$)	K_m (mM)	k_{cat} (s^{-1})	k_{cat}/K_m ($mM^{-1}s^{-1}$)	K_m (mM)	k_{cat} (s^{-1})	k_{cat}/K_m ($mM^{-1}s^{-1}$)
Isobutyraldehyde	12	30	2.8	1.70	140	82	0.68	300	440
Acetaldehyde	0.4	35	94	0.5	31	57	0.92	58	63
5-HMF[b]	22	19	0.88	0.67	23	34	0.57	29	51
2-Furaldehyde	0.39	22	57	0.26	6.0	21	0.20	7	37
Cinnamaldehyde	0.7	27	39	0.24	28	140	0.16	31	210

[a]The enzyme assays were conducted in 100 mM Tris-HCl buffer, pH 7 with 1 mM DTT, 200 µM NADH, and 10 mM substrate. [b] 5-Hydroxymethyl-2-furfural

Sulfolobus solfataricus ADH (SsADH)

SsADH is a thermostable zinc-dependent ADH that has been isolated from *Sulfolobus solfataricus*, obtained from a hot spring near Naples, Italy. Using error-prone PCR mutagenesis with screening for increased activity, Giordano *et al.* made the N249Y mutant SsADH, but unexpectedly, the mutation altered the substrate affinity as well, as shown in Table 2.7.[25] The Asn-249 residue resides closer to the cofactor, as evidenced by the crystal structure shown in Figure 2.2. The substrate specificity decreased for most of the tested substrates, with a slight increase for 1-propanol. Interestingly, the values of k_{cat} and K_m both increased, resulting in net decreases in k_{cat}/K_m values for most substrates. The increase in k_{cat} was actually due to faster product release of the NADH cofactor in

the steady state. Subsequently, Raia and coworkers did further studies with wild-type SsADH, as well as trying out further mutations.[26] To determine if Trp-95 plays a role in the stereospecificity, they mutated the tryptophan to a leucine, which has hydrophobic properties but less steric bulk. As shown in Table 2.8, the W95L mutation of SsADH reduced the specific activity with all of the alcohols tested, with some of the alcohols giving no measurable activity. Combining N249Y with the W95L mutation, the specific activity improved on each substrate tested, but was still much lower than the wild-type SsADH. However, the *E* values for 2-butanol and 2-pentanol decreased from 42 and 7, respectively, for wild-type SsADH, and to 4 and 5 for W95L/N249Y mutant enzyme.

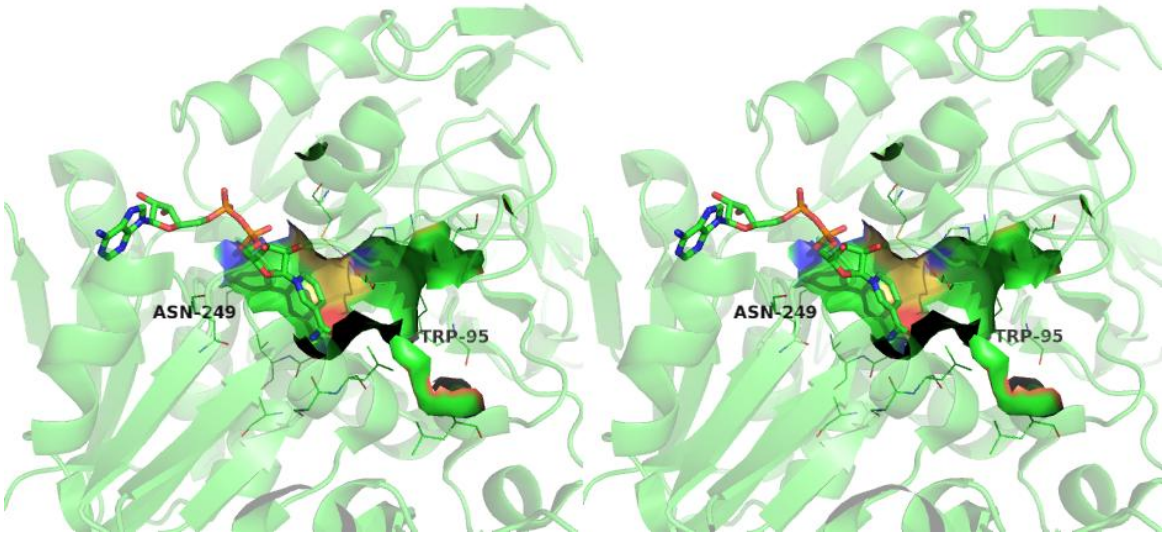

Figure 2.2. Crossed-eye stereoview of SsADH, along with two residues of interest labeled. NAD^+ shown in stick-form. This image was prepared with Pymol (The PyMOL Molecular Graphics System, Version 1.3 Schrödinger, LLC.) using the PDB file (1R37).

Table 2.7. Kinetic Constants for wild-type SsADH and N249Y SsADH (mSsADH)

Substrate	k_{cat}/K_m ($mM^{-1}s^{-1}$)	
	SsADH	**N249Y SsADH**

1-Propanol	4.3	9.7
Cyclohexanol	40	8.4
Benzyl alcohol	13.8	14.5
4-Methoxybenzyl alcohol	14.3	20.5
Benzaldehyde	376.0	98.0
4-Methoxybenzaldehyde	137.0	23.8

Table 2.8. Substrate specificity for wild-type and mutant SsADHs [a]

Substrate	k_{cat}/K_m ($s^{-1}mM^{-1}$)		
	Wild-type	**W95L/N249Y**	**W95L**
Ethanol	0.67	0.06	/ [b]
1-Propanol	10.4	2.4	/ [b]
1-Butanol	38.7	9.4	/ [b]
(*S*)-2-Butanol	100.0	0.16	/ [b]
(*R*)-2-Butanol	2.4	0.044	/ [b]
1-Pentanol	92.6	8.5	2.0
(*S*)-2-Pentanol	37.1	0.76	/ [b]
(*R*)-2-Pentanol	5.0	0.16	/ [b]
1-Hexanol	57.1	15.1	10.5
1-Heptanol	42.1	17.7	2.4
2-Ethoxyethanol	6.4	/ [b]	/ [b]
3-Pentanol	5.5	/ [b]	/ [b]
Cyclohexanol	40.0	2.7	/ [b]
Benzyl alcohol	13.8	5.2	2.9
4-Methoxybenzyl alcohol	41.4	12.9	3.1
Butyraldehyde	281.4	72.9	2.77
Isobutyraldehyde	111.5	23.8	2.50
Benzaldehyde	376.6	46.7	5.14
trans-Cinnamaldehyde	233.3	82.1	2.30

[a] The activity was measured at 65 ^{o}C as described.[23] [b] No measurable activity

Thermoanaerobacter brockii ADH and *Thermoanaerobacter ethanolicus* secondary ADH (SADH)

Two research groups independently isolated what were originally thought to be two different thermophilic bacteria, *Thermoanaerobacter ethanolicus* and *Thermoanaerobium brockii*, from hot springs in Yellowstone National Park.[27,28] When *T. ethanolicus* was isolated, it was targeted because a thermophile would allow anaerobic fermentations to be

performed at temperatures near the boiling point of ethanol, theoretically increasing the efficiency of ethanol production. More recently, the two organisms were determined to be in the same genus, Thermoanaerobacter.[29] Bryant *et al.* isolated and characterized two alcohol dehydrogenases from *T. ethanolicus.*[30] It was observed that while one of the ADHs preferred primary alcohols, the other ADH was more active towards ketones and secondary alcohols than it was towards ethanol, and henceforth, this enzyme is referred to as secondary ADH (SADH). A similar SADH was reported by Keinan *et al.* from *T. brockii.*[8] At first, the SADHs from the two organisms were thought to differ by four amino acids.[31] However, they have been found recently to have identical sequences.[32] The robustness of this thermophilic ADH has been of particular interest in designing mutants without affecting the protein folding or thermal stability. The crystal structure of wild-type SADH was published in 1998 by Frolow and coworkers under the PDB code 1YKF.[9] Figure 2.3 displays the active site from the crystal structure in stereoview. The active site of SADH has a large pocket and small pocket, as predicted in Prelog's model and later by Keinan *et al.*.[8] Depending on how the ketone is oriented within the active site, the product alcohol would either be of *R* or *S* configuration. With this in mind, we mutated the Ser-39 into a threonine in order to modify the substrate specificity of SADH.[33] This mutation introduces a methyl group into the large pocket, decreasing the size of the large pocket, and hence was predicted to favor *R*-alcohols. The S39T mutation was selected because it did not disrupt the hydrogen bonding network in SADH, which is essential for the enzyme activity. As predicted, the stereospecificity for *R*-2-butanol and *R*-2-pentanol was increased significantly in S39T SADH. The relative specificity of wild-type and S39T mutant enzymes for secondary and primary alcohols

was also of interest. The k_{cat}/K_m values for ethanol, 1-propanol and 2-propanol decreased, with ethanol activity decreasing by 5-fold from wild-type to S39T SADH (Table 2.9). There was a 370-fold specificity ratio between 2-propanol relative to 1-propanol for wild-type SADH, while S39T only had a 145-fold specificity ratio between 2-propanol to 1-propanol.

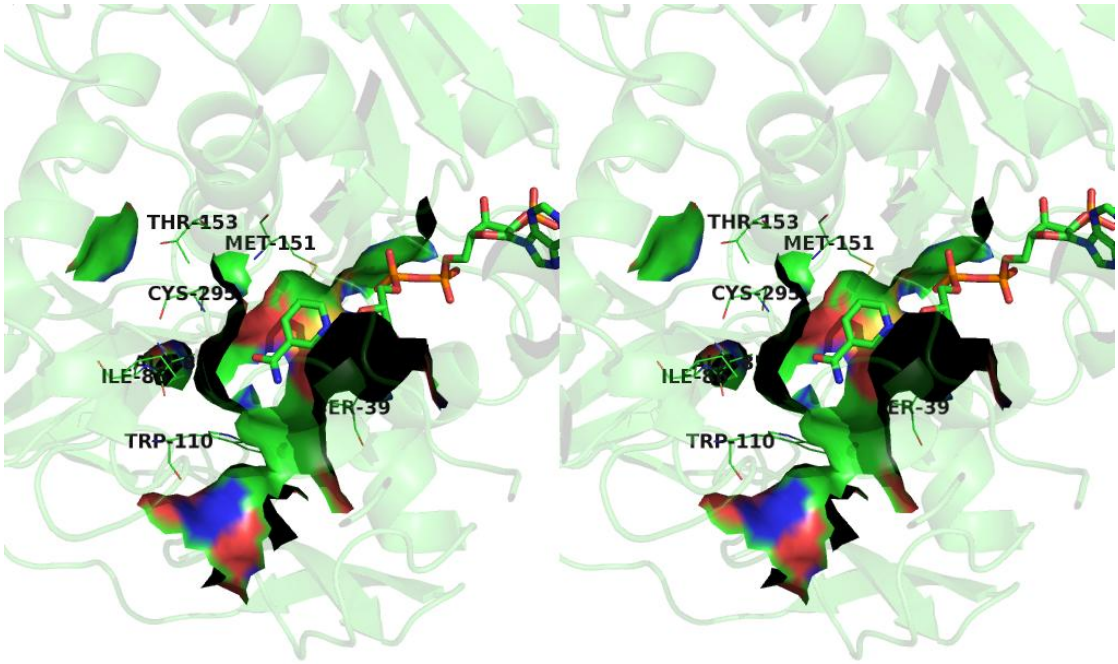

Figure 2.3. Crossed-eye stereoview of SADH, with residues of interest labeled. $NADP^+$ shown in stick-form. This image was prepared with PyMOL (The PyMOL Molecular Graphics System, Version 1.3 Schrödinger, LLC.) using the PDB file (1YKF).

We designed the C295A SADH mutant in an unsuccessful effort to eliminate the irreversible inactivation that occurred during asymmetric reduction of ethynyl ketones by wild-type SADH, which was thought to be due to the irreversible nucleophilic attack of the sulfur in Cys-295 on the ethynyl moiety of the substrates.[34] The C295A mutation introduced a non-nucleophilic residue in the small pocket, which improved the reaction

but did not eliminate the inactivation noticed in wild-type SADH. Thus, the inactivation by ethynyl ketones may involve the reaction of Cys-37, which is an active site Zn ligand, and hence cannot be mutated. However, many of the substrates gave better results with C295A SADH than with the wild type enzyme, and some substrates that show no activity with wild-type SADH were substrates for the mutant, as shown in Table 2.10.[35] The C295A mutation opened up the small pocket, thus allowing this mutant enzyme to accommodate butyl and substituted butyl moieties within the small pocket, which are not accommodated by the small pocket of wild-type SADH. Thus, the butyl and isobutyl ethynyl ketones in Table 2.10 gave products with opposite stereochemical configuration from wild-type and C295A SADH. Furthermore, ketones with a large substituent containing an α-branch, such as *sec*-pentyl in Table 2.10, are good substrates for C295A SADH but are inactive with wild-type enzyme. It should be noted that the ethynyl group, which is smaller than the other substituent of the ketone, has higher Cahn-Ingold-Prelog priority for stereochemical assignment than alkyl groups, which leads to inversion of the stereochemical assignment (i.e., *S*-configured alcohols represent *anti*-Prelog products). Asymmetric reduction of methyl-4-oxohex-5-ynoate using C295A SADH resulted in the formation of the corresponding *R*-alcohol with a decrease in enantioselectivity when compared with reduction using wild-type SADH, as shown in Table 2.10. The higher affinity of the small pocket of the active site of SADH toward alkyl groups was first explained by Keinan *et al.* for SADH.[8] When the ketone has only two small substituents, as methyl, ethyl, propyl or isopropyl, the larger substituent paradoxically prefers to bind in the small pocket, probably because of stronger van der Waals interactions of the larger substituent in the small pocket.

Table 2.9. k_{cat}/K_m values for oxidation of ethanol, 1-propanol, and 2-propanol at 50 ^{o}C by wild-type & S39T SADH

Substrate	k_{cat}/K_m (M^{-1} s^{-1})	
	wild-type	**S39T**
Ethanol	222±36	45±5
1-Propanol	273±35	206±25
2-Propanol	$(1.0x10^5)\pm(2x10^4)$	$(3.0x10^4)\pm(0.7x10^4)$

Table 2.10. C295A SADH-catalyzed reductions of ethynylketones [a]

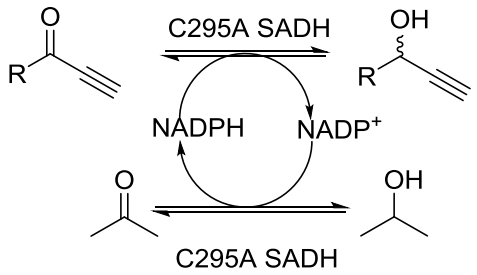

R	Yield (%)[b]	Abs. Conf.[c]	*ee* (%)
CH_2CH_3	39 (32)	*S* (*S*)	76 (80)
$CH(CH_3)_2$	88 (50)	*S* (*S*)	>98 (>98)
$C(CH_3)_3$	39 ([d])	*S* (*S*)	85 (85)
$CH_2CH_2CH_3$	51 (28)	*S* (*S*)	76 (51)
$CH_2CH(CH_3)_2$	42 (20)	*S* (*R*)	56 (50)
$CH_2C(CH_3)_3$	0 ([d])	- (*R*)	- (66)
$CH_2CH_2CH_2CH_3$	60 (32)	*S* (*R*)	67 (42)
$CH(CH_3)CH_2CH_2CH_3$	43 (0)	*S* (-)	>98 (-)
$CH_2CH_2CO_2CH_3$	23 (35)	*R* (*R*)	60 (82)

[a]Results of the reductions with wild-type SADH are provided in parentheses. [b]Yield reported as isolated yield. [c]Abs. conf. = Absolute configuration. [d]Yield too low to isolate. ee determined by GC.

In order to broaden the substrate specificity of SADH, we next designed W110A SADH, which enlarged the large pocket of the active site.[36] The W110A mutation allows

for the reaction of phenyl-ring-containing ketone substrates and their corresponding (*S*)-configured alcohols that are not substrates for wild-type SADH. The stereochemistry of W110A SADH-catalyzed redox reactions follows Prelog's rule, in which NADPH delivers the pro-*R* hydride from the *Re* face of the prochiral ketone (Table 2.11). Surprisingly, phenylacetone was reduced with low enantioselectivity, suggesting that phenylacetone can fit in two orientations within the active site of W110A SADH allowing NADPH to deliver its hydride from either face of this substrate, and therefore leading to selectivity mistakes. The reduction of the α-chloroketone in Table 2.11 occurred with an unexpected dynamic kinetic resolution, probably due to the relatively high acidity of α-chloroketones. With the exception of β-tetralone, all reactions presented in Table 2.11 are reversible, which enabled the production of (*R*)-alcohols via kinetic resolution by stereospecific oxidation of their racemates. The apparent irreversibility of β-tetralone reduction possibly arises from the axial conformation of the substrate as initially formed in the active site, which then relaxes to the lower energy equatorial conformation when it leaves the active site.

Table 2.11. Asymmetric reduction of phenyl ring-containing ketones using W110A SADH.

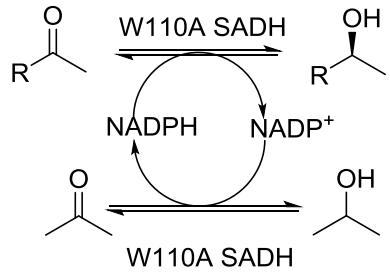

R	Abs. Conf. of Product	Conv. (%)	*ee* (%)
$PhCH_2CH_2$	*S*	99	>99
$Ph(C{=}O)CH_2$	*S*	98	>99
(*E*)-Ph-HC=CH	*S*	64	>99
p-$MeOC_6H_4(CH_2)_2$	*S*	87	91
$PhOCH_2$	*S*	>99	>99
p-$ClC_6H_4CH_2CHCl$	2*S*,3*R*	83[a]	>99
$PhCH_2$	*S*	95	37
p-$MeOC_6H_4CH_2$	*S*	97	>99
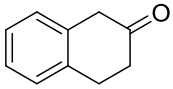	*S*	>99	71

[a] Isolated yield.

More recently, we used site-saturation mutagenesis of Trp-110 to study the effect of small changes in the large pocket of the active site of SADH on the stereoselectivity of aromatic ketone reductions.[37] Kinetic studies revealed that even a small alteration in the active site can make a significant change in stereoselectivity of ketone reduction. For example, there is a significant difference in kinetic parameters for W110V and those for W110G as shown in Table 2.12. Five of the designed mutants (W110I, W110Q, W110M, W110V, W110L) reduced phenylacetone, 1-phenyl-2-butanone, and 4-phenyl-2-butanone with very high enantioselectivity (>99% *ee*), which represents a significant improvement when compared with reductions catalyzed by W110A and W110G mutants (Table 2.13).

However, the W110M mutant did not show a higher *E* value than W110A, but showed a much lower value than the W110V, W110I and W110L mutants (Table 2.12), so steric bulk is not the only factor affecting stereochemistry because the valine, isoleucine, leucine, and methionine side chains are similar in size.

Table 2.12. Kinetic parameters for the oxidation of (*S*)- and (*R*)-1-phenyl-2-propanol with mutant SADH

Mutant SADH	**Enantiomer**	k_{cat} (s^{-1})	k_{cat}/K_m (M^{-1} s^{-1})	$E=(k_{cat}/K_m)_S/(k_{cat}/K_m)_R$
W110I	*S*	18.8 ± 1.9	15200 ± 2300	80.3 ± 16.2
	R	0.46 ± 0.05	188 ± 25	
W110Q	*S*	2.3 ± 0.2	551.4 ± 31.2	80.0 ± 17.5
	R	0.025 ± 0.006	6.9 ± 1.5	
W110M	*S*	4.5 ± 0.4	1990 ± 230	16.3 ± 3.5
	R	0.045 ± 0.003	121.0 ± 22.1	
W110V	*S*	38.6 ± 3.06	45300 ± 4500	134.5 ± 27.7
	R	1.2 ± 0.3	336.5 ± 61.0	
W110L	*S*	0.65 ± 0.03	2510.0 ± 560	104.4 ± 42.1
	R	0.0080 ± 0.00081	24.0 ± 9.0	
W110G	*S*	17.8 ± 3.1	5800 ± 940	9.02 ± 2.6
	R	1.4 ± 0.3	639.0 ± 149.0	
W110A	*S*	31.1 ± 8.1	4935 ± 715	17.4 ± 4.7
	R	0.56 ± 0.09	284 ± 65	

Table 2.13. Asymmetric reductions of phenylacetone, 1-phenyl-2-butanone, and 4-phenyl-2-butanone by mutant SADH

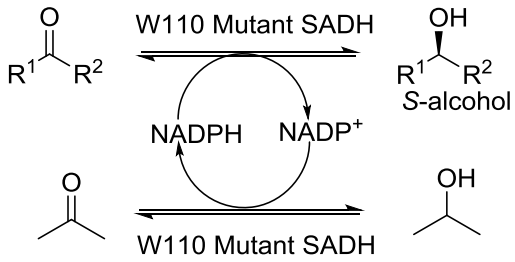

Mutant SADH	Phenylacetone		1-Phenyl-2-butanone		4-Phenyl-2-butanone	
	Conv. (%)	***ee* (%)**	**Conv. (%)**	***ee* (%)**	**Conv. (%)**	***ee* (%)**
W110I	>99.9	>99.9	99.4	>99.9	99.1	>99.9
W110Q	>99.9	>99.9	83.5	>99.9	99.1	>99.9
W110M	>99.9	>99.9	97.3	>99.9	99.3	>99.9
W110V	>99.9	>99.9	99.2	>99.9	99.1	>99.9
W110L	>99.9	>99.9	98.9	>99.9	99.2	>99.9
W110G	>99.9	79	95.8	91.6	99.1	70.5
W110A	>99.9	84.1	-	-	99	>99.9

In order to expand the small binding pocket of wild-type SADH, we mutated Ile-86 into alanine.[38] This mutant was designed to accommodate a phenyl ring within the small pocket, since the wild-type small pocket can accommodate only a three carbon substituent, and the mutation provides room for an additional three carbons. As predicted, I86A SADH shows high activity with acetophenone, which is not a substrate for the wild-type enzyme, and this mutant shows a reversal of stereochemistry, providing the *anti*-Prelog *R*-1-phenylethanol with >99% *ee* (Table 2.14). In contrast to other SADH

mutants at Trp-110, which follow Prelog's rule, I86A SADH cannot accommodate the phenyl ring in the large pocket, and therefore it follows *anti*-Prelog's rule in which NADPH delivers its pro-*R* hydride to the *Si* face of a prochiral ketone. Unfortunately, the largest substituent on the aromatic ring that the I86A mutant can accommodate is fluorine, since any larger atom or group on the phenyl ring resulted in very low or no activity. While the percent conversions in Table 2.14 provide estimates of the ease or difficulty of the substrates fitting into the active site, steric effects cannot be the only factor, since the acetylpyridine isomers are sterically similar, but 3-acetylpyridine has lower conversion. Thus, electronic effects may also be involved.

Table 2.14. Asymmetric production of *anti*-Prelog alcohols by the use of I86A SADH

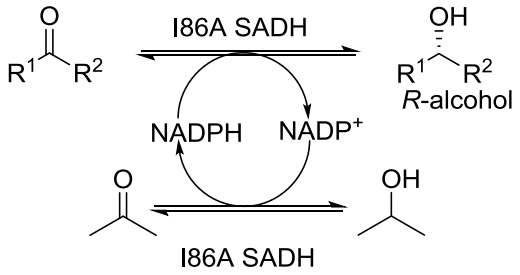

R^1	**R^2**	**Conv. (%)**	***ee* (%)**
C_6H_5	CH_3	79	98
C_6H_5	CH_3CH_2	60	>99
2,4-$F_2C_6H_3$	CH_3	33	>99
2-Pyridyl	CH_3	>99	>99
3-Pyridyl	CH_3	46	>99
4-Pyridyl	CH_3	>99	>99
3-Thienyl	CH_3	76	>99

Recently, Reetz and coworkers utilized saturation mutagenesis using the above mentioned work on SADH as a guide to identify mutation sites for asymmetric reduction

of 4-alkylidene cyclohexanone prochiral ketones to their corresponding axially chiral alcohols.[39] The data shown in Table 2.15 highlights the extensive list of mutants used for this study. As noticed with the previously published studies of SADH,[35-37] they found that, depending on the size of the substrate, and opening made by the mutation in the active site, the stereoselectivity would shift in favor of one alcohol stereoisomer or the other. The *R*-isomer was prevalent in the data from Table 2.14, with the conversions varying depending on the substrate. The best results were obtained with the Trp-110 mutants, which showed very high conversions and *ee*'s. The lowest results were with the C295E mutant, which had very low conversions, and moderate to high *ee*'s. The most interesting results were with the Ile-86 mutants, since they gave the *S*-isomer for the smaller substituents, and then eventually shifted to the *R*-isomer as the substituent got larger. The conversions and *ee*'s varied considerably with the smaller groups giving better results, and the larger groups showing a much lower conversion and *ee*.

Table 2.15. Performance of the best SADH mutants specifically evolved as catalysts in asymmetric reduction of 4-alkylidene cyclohexanone prochiral ketones.

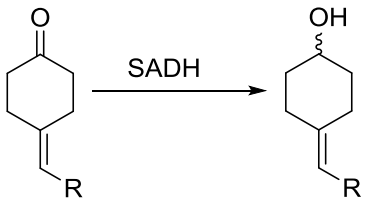

Mutation	R-group					
	Bromo	**Methyl**	**Phenyl**	**Methyl Ester**	**Ethyl Ester**	**Isopropyl Ester**

	Conv. (%)	***ee* (%)**	**Conv. (%)**	***ee* (%)**	**Conv. (%)**	***ee* (%)**	**Conv. (%)**	***ee* (%)**	**Conv. (%)**	***ee* (%)**	**Conv. (%)**	***ee* (%)**
none	≥95	66(*R*)	92	91(*R*)	38	77(*R*)	26	89(*R*)	33	87(*R*)	42	92(*R*)
A85V	≥95	95(*R*)	90	91(*R*)	28	63(*R*)	18	84(*R*)	22	91(*R*)	26	93(*R*)
I86A	≥95	98(*S*)	≥99	74(*R*)	33	65(*R*)	13	75(*R*)	18	85(*R*)	29	95(*R*)
I86G	≥95	98(*S*)	≥99	82(*S*)	30	66(*R*)	24	24(*S*)	25	8(*R*)	24	93(*R*)
I86E	≥95	95(*S*)	≥99	84(*S*)	22	88(*R*)	18	58(*R*)	30	89(*R*)	31	92(*R*)
I86M	≥95	92(*S*)	≥99	25(*S*)	27	73(*R*)	35	84(*R*)	52	86(*R*)	46	90(*R*)
I86T	≥95	92(*S*)	89	61(*S*)	15	74(*R*)	21	40(*R*)	23	57(*R*)	27	93(*R*)
W110A	≥99	82(*R*)	≥99	93(*R*)	≥99	99(*R*)	≥99	98(*R*)	≥99	99(*R*)	≥99	99(*R*)
W110E	≥99	91(*R*)	≥99	92(*R*)	≥99	89(*R*)	≥99	91(*R*)	≥99	92(*R*)	≥99	91(*R*)
W110M	≥99	97(*R*)	≥99	95(*R*)	≥99	99(*R*)	≥99	98(*R*)	≥99	99(*R*)	≥99	99(*R*)
W110T	≥99	97(*R*)	≥99	92(*R*)	≥99	97(*R*)	≥99	98(*R*)	≥99	99(*R*)	≥99	99(*R*)
C295E	16	84(*R*)	27	79(*R*)	10	88(*R*)	8	65(*R*)	10	64(*R*)	14	72(*R*)

While the SADH mutants mentioned so far in this section have given high enantiospecificity, there are uses that would require a less specific enzyme. More specifically, for an enzyme to racemize an *R* or *S* alcohol, the enzyme in question would have to have an open enough active site to allow the substrate to bind in both orientations. An alcohol racemase, an enzyme that gives a racemic mixture starting from the corresponding enantiopure compound, would be of interest in coupling with a kinetic resolution method to achieve a dynamic kinetic resolution. It is of interest to alter ADHs to play the role of racemases, as nature has very limited need for racemization, thus limiting the number of true racemases. The data in Table 2.16 show that *R* or *S* aromatic alcohols can be racemized by W110A SADH, at least partially.[40] This was made possible by facilitating the equilibrium in these redox reactions by including both $NADP^+$ and NADPH in the reaction media.

Table 2.16. W110A SADH-catalyzed racemization of enantiopure phenyl-ring-containing secondary alcohols

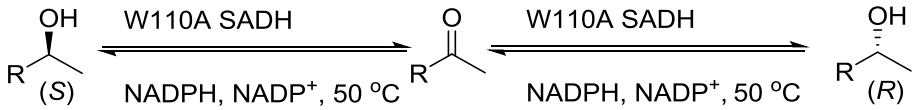

				***ee* (%)**	
Entry	**R**	**Substrate**	***E*-value (*S*/*R*)**	**Before**	**After**
1	$PhCH_2$	(*S*)	3.4	>99	6.3 (*S*)
2	$PhCH_2$	(*S*)	3.4	>99	4.3 (*S*)[a]
3	$PhCH_2$	(*R*)	3.4	>99	10.3 (*R*)
4	$PhCH_2$	(*R*)	3.4	>99	15.4 (*R*)[a]
5	*p*-$MeOC_6H_4CH_2$	(*S*)	12	91	44.0 (*S*)
6	$PhCH_2CH_2$	(*R*)	>100	>99	34.5 (*R*)
7	$PhCH_2CH_2$	(*S*)	>100	99	82.4 (*S*)
8	$PhCH_2CH_2$	(*S*)	>100	72	51.8 (*S*)
9	$PhOCH_2$	(*S*)	40	>99	>99 (*S*)

[a]DMF used instead of acetonitrile as the cosolvent.

Rhodococcus ruber ADH (ADH-A)

The ADH from *Rhodococcus ruber* DSM 44541, known as ADH-A, catalyzes the asymmetric reduction of ketones to secondary alcohols. This zinc-dependent enzyme is structurally similar to HLADH.[41] Gruber and coworkers published the crystal structure with an interest on the active site regions that would be ideal for mutagenesis in order to alter the substrate specificity.[41] Figure 2.4 shows a 2-octanone molecule docked into the active site of ADH-A. From the illustration, one possible mutation would be of the Trp-295 into either an alanine or glycine, which would open up space in the active site for a larger substituent than methyl on 2-octanone. With this in mind, Widersten and coworkers recently published kinetic data for wild-type ADH-A and included some data on the H39N mutant, which had several-fold lower substrate specificity (k_{cat}/K_m) than the wild type enzyme for acetophenone and *S*-1-phenylethanol.[42] They pointed out that the

H39N mutation had no effect on the K_m of NAD^+, meaning that the mutation substitutes well for the His-39, while altering the substrate specificity. It will be interesting to see if future mutations can affect the substrate specificity of this enzyme.

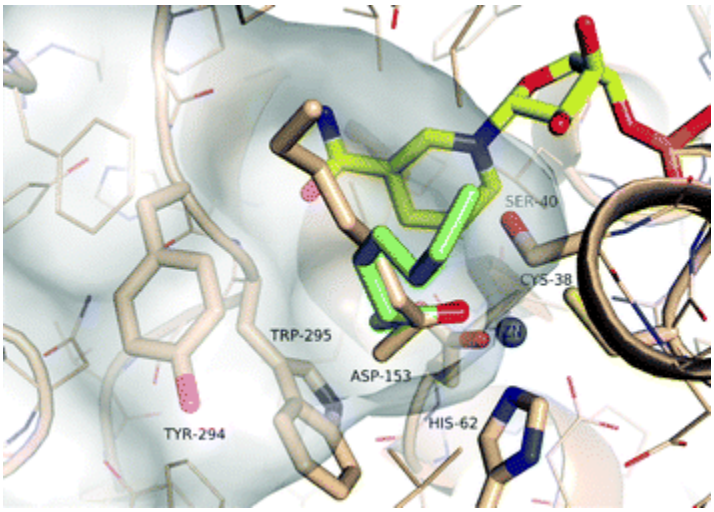

Figure 2.4. Results of docking 2-octanone into active site of ADH-'A' showing a comparison of representative binding modes from the two lowest energy docking clusters. The active site pocket is shown in a semi-transparent surface representation. Amino acids and the docked 2-octanone are shown in pink and green respectively, and the cofactor is in yellow. The zinc ion is shown as a grey sphere. The figure was prepared using PyMOL. (Figure and caption reprinted with permission of The Royal Society of Chemistry from reference [41]).

Candida parapsilosis carbonyl reductase (CPCR2)

The carbonyl reductase from *Candida parapsilosis*, a zinc-containing ADH, accommodates medium chain alcohols. Jakoblinnert and coworkers performed mutagenesis to expand the active site and thus widen the substrate scope of the enzyme.[43] The crystal structure and computational data were used to select residues (Leu-55, Pro-92, Gly-118, Leu-119, Leu-262) for site-saturation mutagenesis. They tested the resulting mutant library against poor substrates for the wild-type enzyme, and found an interesting mutation, L119M. With 2-methylcyclohexanone as the substrate, the specific

activity increased by seven-fold with L119M, as compared with wild-type CPCR2. Other substrates of interest listed in Table 2.17 showed an increase in activity with L119M CPCR2 as compared to wild-type CPCR2 for acetophenone. With cyclohexanone and 4-methylcyclohexanone, the increase in activity for L119M CPCR2 was around four-fold.

Table 2.17. Specific activities of wtCPCR2 and L119M-CPCR2.

Substrate	Specific Activity (U/mg)	
	Wt-CPCR2	**L119M-CPCR2**
Acetophenone	26.5	16.2
2-Methylcyclohexanone	3.0	8.5
3-Methylcyclohexanone	16.8	37.7
4-Methylcyclohexanone	18.3	95.6
Cyclohexanone	35.8	144.6

Activities were determined at 5 mM substrate concentration employing the standard NADH-depletion assay; measurements were conducted in triplicate.

Other ADH families:

***Sporobolomyces salmonicolor* Carbonyl Reductase (SsCR)**

Through the application of substrate-enzyme docking-guided point mutations, Zhu and coworkers have developed a set of useful *Sporobolomyces salmonicolor* carbonyl reductase (SsCR) mutants with different enantioselectivity from the wild-type enzyme.[44] As Table 2.18 demonstrates, the *R*-alcohols were the products from wild-type SsCR, while mutations at residue Gln-245 shifted the isomeric product to the *S*-alcohols. Li and coworkers subsequently found that mutation of Met-242 resulted in formation of *S*-alcohols for many of the substrates tested, as shown in Table 2.19.[45] Interestingly, the best mutant depended on the substrate being tested. Combining mutations at Met-242 and Gln-245 provided double mutant enzymes that gave the *S*-alcohols as the products, which also can be seen in Table 2.19. Expanding on the acetophenone study, Zhu and

coworkers tested the Gln-245 mutants against benzophenones, including 4-methylbenzophenone and 4-chlorobenzophenone, as shown in Table 2.20.[46] The wild type SSCR gave the *R* alcohol in high *ee* for each of the two substrates, but the Q245L mutant SSCR gave R alcohols with lower ee. Interestingly, the Q245P mutation shifted the preference towards the *S* alcohol for both 4-methylbenzophenone and 4-chlorobenzophenone in moderate *ee*. The Q245H mutation retained the *R* alcohol preference for 4-methylbenzophenone in moderate *ee*, while 4-chlorobenzophenone gave the *S* alcohol in low *ee*.

Table 2.18. Asymmetric reductions of *para*-substituted acetophenones catalyzed by SsCR and its Q245 mutants.

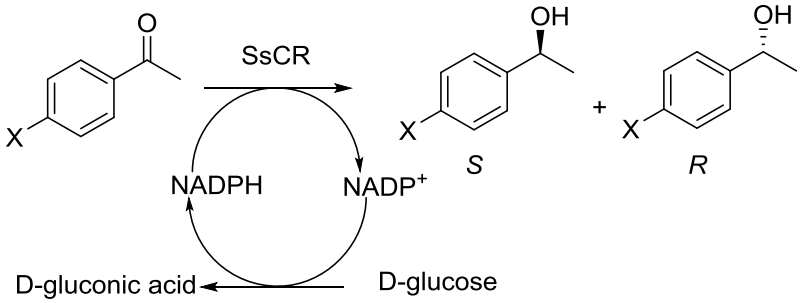

X	WT-SSCR		Q245H-SsCR		Q245P-SsCR		Q245L-SsCR	
	Specific Activity[a]	***ee* (%)**	**Specific Activity[a]**	***ee* (%)**	**Specific Activity[a]**	***ee* (%)**	**Specific Activity[a]**	***ee* (%)**
OCH_3	20	57 (*R*)	16	79 (*S*)	62	98 (*S*)	20	96 (*S*)
H	28	42 (*R*)	85	78 (*S*)	39	64 (*S*)	86	82 (*S*)
F	14	46 (*R*)	72	92 (*S*)	25	90 (*S*)	36	93 (*S*)
Cl	20	14 (*R*)	238	90 (*S*)	309	96 (*S*)	67	96 (*S*)
Br	13	42 (*R*)	203	92 (*S*)	403	98 (*S*)	47	97 (*S*)
CH_3	11	59 (*R*)	25	95 (*S*)	45	96 (*S*)	20	95 (*S*)
$C(CH_3)_3$	11	31 (*R*)	32	96 (*S*)	84	99 (*S*)	9	99 (*S*)

[a] The specific activity is defined as nmol/min^{-1}mg^{-1}

Table 2.19. Reduction of *para*-substituted acetophenones with M242/Q245-SSCR.

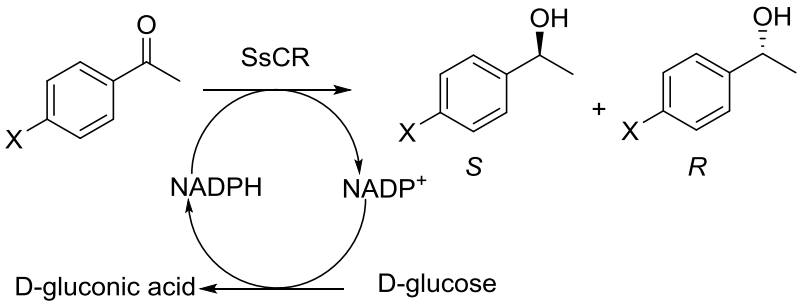

	Enantiomeric Excess (%)								
Substrate	**WT-SSCR**	**M242Y**	**M242D**	**M242C**	**M242G**	**M242L/Q245P**	**M242F/Q245T**	**M242C/Q245L**	**M242L/Q245T**
H	42 (*R*)	12 (*S*)	82 (*S*)	13 (*S*)	54 (*S*)	74 (*S*)	42 (*S*)	17 (*S*)	58 (*S*)
F	46 (*R*)	41 (*S*)	90 (*S*)	54 (*S*)	70 (*S*)	92 (*S*)	90 (*S*)	16 (*S*)	94 (*S*)
Cl	14 (*R*)	36 (*S*)	77 (*S*)	27 (*S*)	62 (*S*)	99 (*S*)	94 (*S*)	50 (*S*)	98 (*S*)
Br	42 (*R*)	22 (*S*)	61 (*S*)	4 (*R*)	52 (*S*)	>99 (*S*)	89 (*S*)	24 (*S*)	99 (*S*)
CH_3	59 (*R*)	21 (*R*)	43 (*S*)	38 (*R*)	4 (*S*)	99 (*S*)	72 (*S*)	20 (*S*)	95 (*S*)
OCH_3	57 (*R*)	7 (*R*)	39 (*S*)	18 (*R*)	6 (*R*)	99 (*S*)	92 (*S*)	36 (*S*)	97 (*S*)
$C(CH_3)_3$	31 (*R*)	93 (*S*)	>99 (*S*)	96 (*S*)	90 (*S*)	>99 (*S*)	95 (*S*)	99 (*S*)	99 (*S*)
CF_3	17 (*R*)	28 (*S*)	37 (*S*)	5 (*S*)	17 (*S*)	>99 (*S*)	98 (*S*)	94 (*S*)	99 (*S*)

Table 2.20. Reduction of 4-methylbenzophenone and 4-chlorobenzophenone with SSCR enzymes

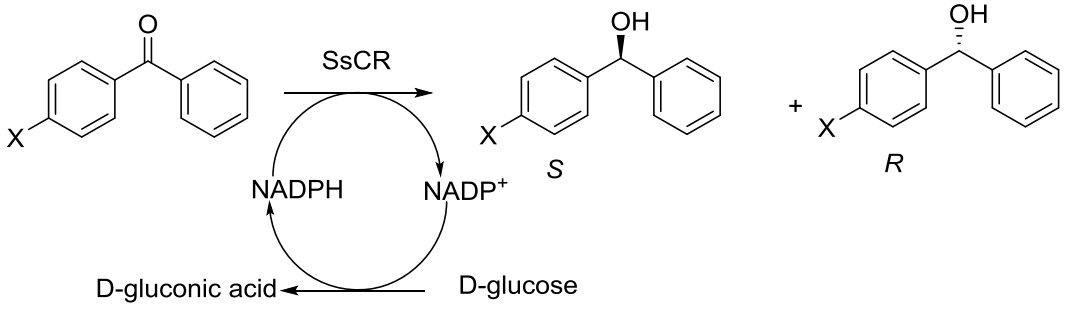

Enzyme	**X = Methyl**		**X = Chloro**	
	Conv. (%)	***ee* (%)**	**Conv. (%)**	***ee* (%)**
Wild-type	>99	84 (*R*)	95	78 (*R*)
Q245P	99	48 (*S*)	98	76 (*S*)
Q245L	98	46 (*R*)	>99	28 (*R*)

Q245H	94	46 (*R*)	>99	22 (*S*)

Candida tenuis Xylose Reductase (CtXR)

Candida tenuis xylose reductase (CtXR, EC 1.1.1.21),[47] a member of the NAD(P)-dependent aldo-keto reductase superfamily, was unexpectedly found to catalyze the asymmetric reduction of a series of aromatic α-keto esters to their corresponding optically active *α*-hydroxy esters as shown in Table 2.21.[48] The produced *α*-hydroxy esters had (*R*)-configuration (Prelog's mode) with very high enantioselectivities (>99% *ee*). An energy-minimized docking study revealed steric conflicts between the indole ring of Trp-23 and carbonyl group substituents as shown in Figure 2.5. Replacement of Trp-23 by smaller amino acids like Phe or Tyr using site-directed mutagenesis resulted in up to eightfold enhancement in catalytic efficiency for aromatic α-keto esters, as shown in Table 2.21. W23F and W23Y mutant variants of CtXR retain the high enantioselectivity of wild-type CtXR in asymmetric reduction of aromatic α-keto esters.

Table 2.21. Steady-state kinetic analysis of reduction of aromatic α-keto esters catalyzed by wild-type CtXR and W23F and W23Y mutants.

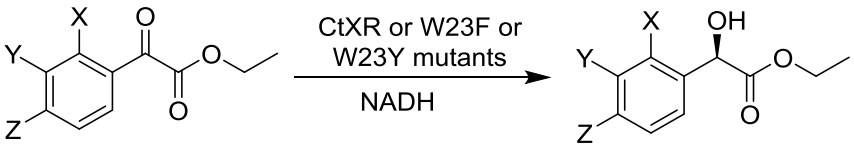

Substrate	k_{cat}/K_m ($M^{-1}s^{-1}$)		
	Wild-type CtXR	**W23F CtXR**	**W23Y CtXR**
D-xylose	136	2.4	0.8
X=H, Y=H, Z=H	269	911	636
X=Cl, Y=H, Z=H	576	4029	3158
X=H, Y=Cl, Z=H	53	369	186
X=H, Y=H, Z=Cl	2211	13835	11056
X=CN, Y=H, Z=H	27	208	128

X=H, Y=CN, Z=H	21	131	74
X=H, Y=H, Z=CN	197	955	717

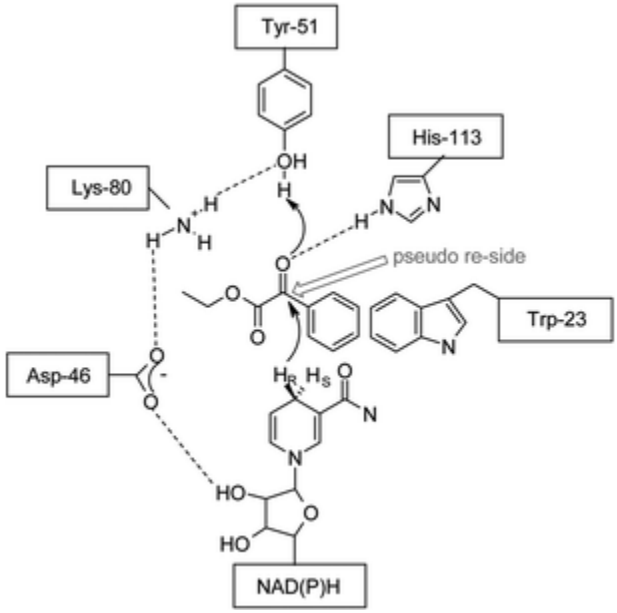

Figure 2.5. Proposed orientation of an aromatic α-keto ester in the active site of CtXR and stereochemical course of asymmetric production of *α*-hydroxy esters. Figure reprinted with permission of The Royal Society of Chemistry from *Chem. Commun.* **2007**, 1047-1049.

Nidetzky and coworkers also tested the wild type and aforementioned CtXR mutants against a series of ketones, which has been provided in Table 2.22.[49] The introduction of a phenylalanine or tyrosine mutation at Trp-23 caused mixed effects with the chosen ketones, including the largest increase with oxopantoyl-lactone giving a four to five fold specific activity increase compared with wild-type CtXR.

Table 2.22. Wild-type and mutant CtXR kinetic parameters with a series of ketones

Substrate	k_{cat}/K_m ($M^{-1}s^{-1}$)		
	Wild-type CtXR	**W23F CtXR**	**W23Y CtXR**
Acetophenone	0.5	0.2	0.2
Acetoin	1.8	0.8	0.8
4-Hydroxybutan-2-one	0.05	0.05	0.03

Diacetyl	800	282	121
Acetylacetone	0.07	0.03	0.03
Oxopantoyl-lactone	8.0	46	36
Ethyl pyruvate	542	160	57
Ethyl benzoylformate	269	911	636
Ethyl acetoacetate	0.7	0.3	0.2
Ethyl 4-chloroacetoacetate	34	68	62
Ethyl 4,4,4-trifluoroacetoacetate	0.3	0.6	0.3

Other factors affecting Activity and Stereoselectivity of ADHs

Effects of Temperature, pH and Pressure on Stereoselectivity

An important goal of research in biocatalysis is to exert a greater influence on the stereoselectivity of the enzymatic reaction. An obvious way to achieve it is by optimizing the physical conditions, i.e. temperature, pressure, pH, etc., of the given enzymatic reaction. However, for most enzymes, this is rather difficult to do, given that most enzymes are active only in a very narrow temperature range, and stability often rapidly declines past 42 °C. However, there are enzymes from thermophilic bacteria that can be used to study the effects of temperature on stereoselectivity, because these specific enzymes are stable over a much wider range of temperatures. One of the earliest such examples of ADHs was studied by Keinan *et al.*, who reported the reduction of 2-pentanone to (*S*)-2-pentanol by SADH at temperatures as high as 50 °C, although the highest stereoselectivity was observed at 5 °C.[8]

We found a strong temperature dependence on enantiospecificity of SADH, and it was observed that for 2-butanol, there was a reversal of stereospecificity from (*S*) below 26 °C to (*R*) above that temperature. As Keinan had reported,[8] (*S*)-2-pentanol was found to be the preferred substrate at temperatures up to 60 °C.[50,51] The effect of temperature on enantiospecificity was fit to Equation 2.1. The effect of temperature was found to be

the results of a relatively large $\Delta\Delta S^{\ddagger}$ which favors the reaction of the *R*-enantiomer, since $T\Delta\Delta S^{\ddagger}$ increases with temperature. This was the earliest report which quantitatively established the influence of temperature in stereospecificity of SADH, and showed great potential for its practical applications.

$$-RT\ln E = \Delta\Delta H^{\ddagger} - T\Delta\Delta S^{\ddagger} \quad (2.1)$$

Keinan *et al.* also studied the effect of pH on the reduction of 2-pentanone by SADH.[8] They observed a correlation between pH and stereospecificity of the formed product, 2-pentanol, with the best enantiopurity obtained at pH 7.5-8. We studied the effect of pH on stereospecificity of SADH on 2-butanol, and we observed that the *E* value for 2-butanol increases from 2.5 at pH 9 to 4.2 at pH 5.5.[52] The increase in stereospecificity was attributed to differences in catalytic commitments for the two enantiomers, which causes a change in the apparent kinetic pK_a of the enzyme for the two enantiomers. The catalytic commitment is the ratio of k_{cat} to the rate constant for release of the unreacted substrate from the enzyme. If this ratio, C, is greater than 1, the apparent kinetic pK_a for the reaction of the substrate is shifted to lower pH by log(1+C). This represented yet another correlation of a physical parameter change to stereospecificity, and it potentially imparted one more tool in hands of synthetic chemists to influence stereospecificity.

The next step was to study the cumulative effect of SADH mutations and physical parameters. We studied the effects of temperature on stereospecificity of 2-butanol and 2-pentanol oxidation using S39T SADH.[32] An interesting effect of this mutation was that it increased the preference for (*R*)-2-butanol and (*R*)-2-pentanol, and this represented a potential route for preparing both enantiomers of selected alcohols using the wild-type

and S39T mutant SADH, respectively. The thermodynamic parameters, $\Delta\Delta H^{\ddagger}$ and $\Delta\Delta S^{\ddagger}$, were compared for wild-type and S39T enzymes with 2-butanol and 2-pentanol, and the change in stereochemistry was found to be associated with a change in the $\Delta\Delta H^{\ddagger}$. The effects of temperature on the reaction of C295A SADH with 2-butanol and 2-pentanol were also determined.[53] Surprisingly, the temperature dependence of the enantiospecificity of 2-butanol and 2-pentanol is much less for C295A than for wild-type SADH, due to very small values of $\Delta\Delta S^{\ddagger}$. This is consistent with the $\Delta\Delta S^{\ddagger}$ arising from a difference in desolvation of the active site on substrate binding, since the crystal structure of wild-type SADH shows a structural water molecule hydrogen bonded to Cys-295.

There have been only a few reports on the effect of high pressure on enzymatic reactions. This should not be surprising, since temperature can be manipulated by common inexpensive instrumentation available in every laboratory, whereas application of high hydrostatic pressure requires expensive specialized instrumentation. Morita and Haight showed that malic dehydrogenase from *Bacillus stearothermophilus* was inactive at 101 ^{o}C from 0.1 to 70 MPa.[54] However, there was activity observed at 70 MPa with optimal activity at 130 MPa at 101 ^{o}C. This showed that pressure can increase enzyme activity, and Dallat and Legoy showed that SADH was activated by pressure up to 100 MPa.[55] Cho and Northrop also studied the kinetics of YADH under high pressure.[56] There are even fewer examples of hydrostatic pressure studies on enzyme stereochemistry. Kahlow *et al.* studied the effects of pressure on *Candida rugosa* lipase-catalyzed transesterification of menthol in chloroform at high pressure, and found the *E* value to significantly decrease with pressure from *E* of 55 at 0.1 MPa to about 9 at 10

MPa.[57] A model was developed based on molecular dynamics, and it showed that changes in active site solvation were responsible for the observed effect.

Recently, we studied the effects of hydrostatic pressure and temperature on stereospecificity of S39T SADH.[58] It was observed that the S39T SADH was active under high pressure and temperature conditions, e.g., 137.5 MPa and 325 K. The enantiomeric ratio, *E* value (*R*/*S*) was observed to be ~2 for 2-butanol and nearly 1 for 2-pentanol under different temperature and pressure conditions. A greater effect on pressure was observed for 2-hexanol, with the *S* isomer being the preferred enantiomer.

$$-RT\ln E = \Delta\Delta H^{\ddagger} - T\Delta\Delta S^{\ddagger} + P\Delta\Delta V^{\ddagger} \qquad (2.2)$$

The *E* value for 2- hexanol varied from 0.25 at 298 K and atmospheric pressure to 0.08 at 137.5 MPa, which was a three-fold decrease in the *R*/*S* ratio. The combined temperature and pressure data were fitted to Equation 2.2 to obtain the $\Delta\Delta S^{\ddagger}$ and $\Delta\Delta V^{\ddagger}$ values of +46 ± 15 J/mol and $+(2.0 \pm 0.4) \times 10^{-2}$ L/mol, respectively. Thus, the effects of temperature and pressure are opposite, with temperature favoring the *R*-enantiomer and pressure favoring the *S*-enantiomer. These results support our previously proposed solvation model,[59] which postulates that the positive entropy difference results from the expulsion of a water molecule that occupies the small pocket of the SADH active site in the crystal structure, when a larger alkyl group of the *R*-alcohol is bound in it. As further supporting evidence for this theory, the magnitude of $\Delta\Delta V^{\ddagger}$ from data fitting, 0.02 L/mol, is approximately the same as the volume of 1.0 mol of water.

Effect of Reaction Medium in Activity and Selectivity of ADHs

There are a number of advantages of using nonaqueous media instead of the natural aqueous medium in biotransformations.[60] There is no doubt that using enzymes in

nonaqueous media expands the scope of their use in production of enantiopure compounds because many of the interesting substrates are either water-insoluble or sparingly soluble. The use of nonaqueous media in biotransfomations also allows their use with other interesting reactions. Klibanov and co-workers reported the first example that shows that enzymes, including dehydrogenases, can function in nearly anhydrous nonaqueous media.[61] Since then, the concept of "reaction medium engineering" has gained significant interest in the field of biocatalysis.[62] A significant amount of research has been devoted to study the effect of reaction medium on enzyme activity and selectivity. Numerous examples of ADH-catalyzed transformations have been conducted in nonaqueous reaction media, including organic solvents, ionic liquids, and supercritical CO_2. In this review, we focus on examples that show the effect of reaction medium on stereoselectivity of ADH-catalyzed redox reactions.

Simpson and Cowan studied the effect of using organic cosolvents on enantioselectivity of asymmetric reduction of aliphatic ketones by secondary ADH from *Thermoanaerobacterium* sp. KET4B1.[63] They reported an enhancement in enantioselectivity of reduction reactions of 2-butanone to (*R*)-2-butanol when carried out in various organic solvents at different concentrations (Table 2.23). They noticed that solvents with lower log *P*, hydrophobicity constant, values have more significant influences on enantioselectivity; however, no direct correlation was observed. Surprisingly, the enantioselective reduction of 3-hexanone to (*S*)-3-hexanol in 10% (v/v) and 20% (v/v) of acetonitrile resulted in a small decrease in *ee* from 75% to 68% and 53%, respectively. Under the same conditions and using 10% (v/v) of acetonitrile, 3-methylbutan-2-one resulted in the formation of (*R*)-3-methylbutan-2-ol in 99.9% *ee*, in

comparison with 98.5% *ee* in pure aqueous medium, which, as claimed by the authors, could be within the error of the GC that was used to determine optical purity.

Table 2.23. Concentration effect of organic cosolvents on enantioselectivity of *Thermoanaerobacterium* sp. KET4B1.

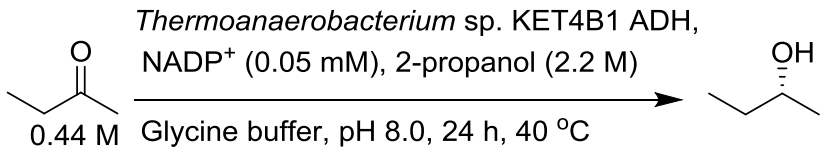

	% *ee*[a]					
Concentration of organic solvent (% v/v)	**Acetonitrile**	**Methyl propionate**	**Methanol**	**Methyl formate**	**Dimethyl sulfoxide**	**Heptane**
0	23	23	23	23	23	23
10	34	49	27	55	62	24
20	48	53	34	61	56	n.d.[b]
40	65	64	49	n.d.	n.d.	n.d.

[a] % *ee* values were determined at approximately 60% conversion. [b] n.d. indicates not determined due to high enzyme inhibition

Schumacher *et al.* studied the influence of water-miscible organic solvents on the enantioselective reduction of 2-butanone to (*R*)-2-butanol using the *anti*-Prelog *Lactobacillus brevis* ADH.[64] They noticed an enhancement in the enantioselectivity when acetonitrile or 1,4-dioxane are used as cosolvents. They studied the effect of varying organic solvent concentration from mole fraction of 0.015 to 0.1 mole with minimum enantioselectivity of 33% *ee* at $X_{acetonitrile}$= 0.015 and a slight increase to 43% *ee* at $X_{acetonitrile}$= 0.05, as shown in Table 1.24. They also noticed a minimum enantioselectivity of 32% *ee* when $X_{1,4\text{-dioxane}}$= 0.025 and an enhancement to 40% *ee* at $X_{1,4\text{-dioxane}}$= 0.1. It is worth mentioning that the same enantioselective reduction reaction gave (*R*)-2-butanol in 37% *ee* when carried out in phosphate buffer solution.

Table 2.24. Influence of different organic solvent content on enantioselectivity of 2-butanone reduction by *Lactobacillus brevis* ADH.

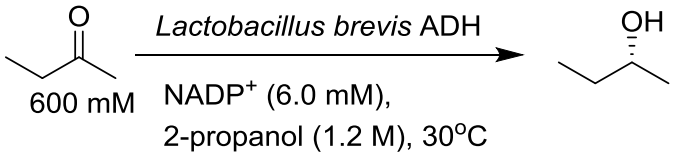

Entry	Solvent	X (mole fraction of organic solvent)	*ee* (%)
1	Acetonitrile	0.015	33
2		0.025	41
3		0.050	43
4		0.100	43
5	1,4-dioxane	0.015	34
6		0.025	32
7		0.050	34
8		0.100	40
9	Phosphate buffer	-	37

The high tolerance of SADH to elevated concentrations of organic solvents enabled us to use xerogel-encapsulated W110A SADH in hydrophobic organic solvents using 2-propanol as a cosubstrate.[65] A significant enhancement in *ee* of the enantioselective reduction of phenylacetone is noticed when the reaction is carried out using xerogel-encapsulated W110A SADH in organic solvents in comparison with conducting the same reaction using free enzyme in aqueous media, as shown in Table 2.25.

Table 2.25. Enantioselective reduction of phenylacetone in organic solvents using xerogel encapsulated W110A SADH.

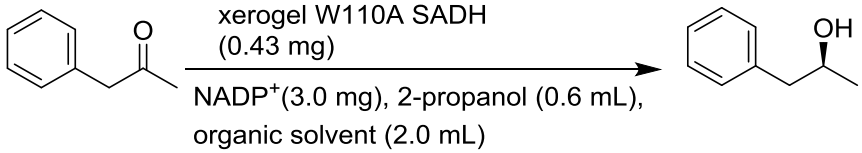

Entry	Solvent	Conv. (%)	*ee* (%)
1	Hexane	80	69
2	Toluene	24	55
3	Diisopropyl ether	37	73
4	*tert*-Butyl alcohol	38	63
5[a]	Tris-HCl buffer	95	37

[a] Reaction was conducted using free enzyme in aqueous medium

Eckstein *et al.* reported an ADH-catalyzed reduction reaction in a biphasic system containing the ionic liquid, [BMIM][NTf_2], as the nonaqueous phase.[66] They noticed that the *Lactobacillus brevis* ADH-catalyzed *anti*-Prelog enantioselective reduction of 2-octanone is faster in a biphasic system containing [BMIM][NTf_2] than when the same reaction is conducted using methyl *tert*-butyl ether as the nonaqueous solvent. They claimed that this improvement was due to the favorable partition coefficients of the cosubstrate 2-propanol and coproduct acetone, with the latter preferring to reside in the [BMIM][NTf_2] layer, which shifts the equilibrium towards the reduction pathway.

Driven by the high tolerance of SADH to elevated concentrations of nonaqueous solvents, we investigated the effect of various organic solvents and ionic liquids on enantioselectivity of asymmetric reduction of phenyl-ring-containing ketones using W110A SADH.[67] We noticed an improvement in *ee* in the enantioselective reduction of phenylacetone to (*S*)-1-phenyl-2-propanol using W110A SADH when reactions are conducted in media containing water-miscible organic solvents, with the best results obtained when acetonitrile was used, as shown in Table 2.26. The use of 1-butyl-3-methylimidazolium bis((trifluoromethyl)sulfonyl)imide ([BMIM][NTf_2]), a water-immiscible ionic liquid, leads to a comparable enhancement in enantioselectivity. No

such improvement is noticed when a water-miscible ionic liquid, 1-butyl-3-methylimidazolium tetrafluoroborate ([BMIM][BF_4]), was used. Similar results were obtained in the asymmetric reduction of 4-(4'-methoxyphenyl)-2-butanone to its corresponding (*S*)-alcohol. It was noticed that yield enhancement is observed in both the reduction and oxidation pathways of W110A SADH-catalyzed transformations when [BMIM][NTf_2] was used as the nonaqueous medium, thus demonstrating that the partition coefficients of the cosolvents between aqueous medium and [BMIM][NTf_2] are not the only factors influencing the percent conversion in such biphasic systems.

Table 2.26. Asymmetric reduction of phenyl-ring-containing ketones by W110A SADH in nonaqueous media.

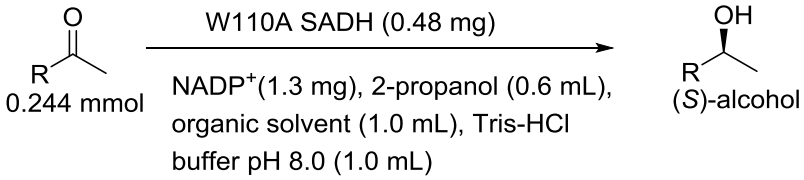

Entry	R	Solvent	Conv. (%)	*ee* (%)
1	$PhCH_2$	[BMIM][BF_4]	88	38
2	$PhCH_2$	DMF	97	56
3	$PhCH_2$	Acetonitrile	90	62
4	$PhCH_2$	[BMIM][NTf_2]	>99	60
5[a]	$PhCH_2$	-	95	37
6	4-$MeOC_6H_4(CH_2)_2$	[BMIM][BF_4]	40	87
7	4-$MeOC_6H_4(CH_2)_2$	DMF	35	86
8	4-$MeOC_6H_4(CH_2)_2$	Acetonitrile	28	94
9	4-$MeOC_6H_4(CH_2)_2$	[BMIM][NTf_2]	52	88
10[a]	4-$MeOC_6H_4(CH_2)_2$	-	87	91

a 36a

Shi *et al.* reported the influence of [BMIM][PF_6], a water-immiscible ionic liquid, and water-immiscible organic solvents on the enantioselectivity of the reduction of ethyl

2-oxo-4-phenylbutyrate by *Saccharomyces cerevisiae* (Scheme 2.1).[68] They noticed that (*R*)-ethyl 2-hydroxy-4-phenylbutyrate was obtained in 70.4% *ee* when benzene or diethyl ether were used as solvents. However, a shift to the (*S*)-configured product in 27.7% *ee* was noticed when [BMIM][PF_6] was used. Addition of water ([BMIM][PF_6]/water, 10:1, v/v) resulted in a shift to the (*R*)-configured alcohol (7% *ee*) that was increased to 82.5% *ee* by addition of ethanol (1%, v/v).

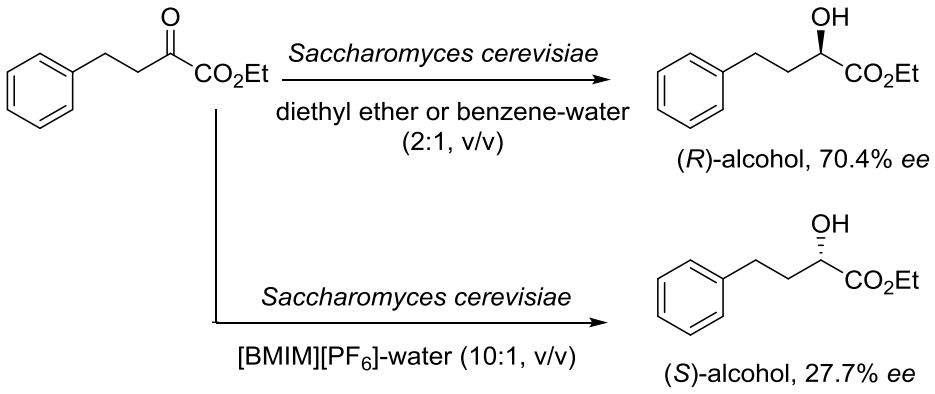

Scheme 2.1. Asymmetric reduction of 2-oxo-4-phenylbutyrate by *Saccharomyces cervisiae* ADH in organic solvents and [BMIM][PF_6]

Zhu and coworkers reported that both conversion and enantioselectivity of SsCR-catalyzed reduction of 4-chlorobenzophenone and 4-methylbenzophenone to their corresponding (*R*)-alcohols were dependent on the reaction medium, as shown in Table 2.27.[46] For both substrates, the best conversion and enantioselectivity results were obtained when 2-propanol or methanol were used as cosolvents. The addition of THF as the cosolvent resulted in significant improvement in enantioselectivity of the asymmetric reduction of both substrates; however, increasing the amount of THF to more than 10% (v/v) resulted in low or no conversions. Such high enantioselectivities in production of (*R*)-4-chlorobenzhydrol and (*R*)-4-methylbenzhydrol, important precursors for the synthesis of optically active forms of cetirizine hydrochloride and neobenodine,

respectively, using SsCR in media an organic cosolvent are remarkable because getting beyond 47% *ee* using chiral metal catalysts is not possible.

Table 2.27. Enantioselective reduction of 4-chlorobenzophenone and 4-methylbenzophenone using wild-type SsCR in reaction media with different organic cosolvents.[a]

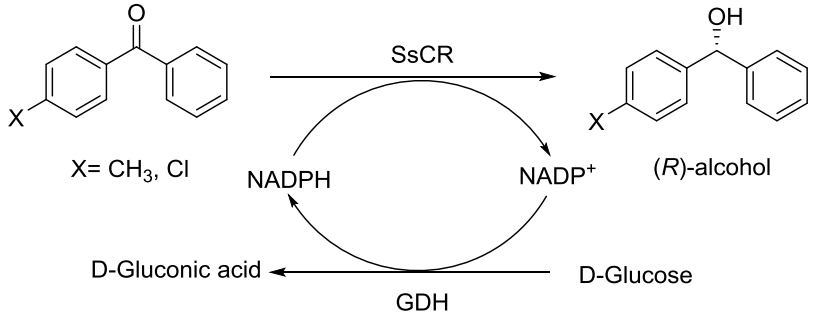

	4-chlorobenzophenone		4-methylbenzophenone	
Cosolvent	Conv. (%)	*ee* (%)	Conv. (%)	*ee* (%)
No solvent	47	50	45	82
DMSO	97	70	98	80
2-Propanol	93	74	>99	80
Methanol	95	78	>99	84
Butyl acetate	14	62	11	-
MTBE	46	58	52	78
THF	62	88	67	92

[a]Reactions were performed in phosphate buffer (100 mM, pH 7.0) containing 10% of organic cosolvent.

The relationship of reaction medium on activity and selectivity of ADHs with a physicochemical property of organic solvents has been the subject of interest, but no useful correlations have been found.[69,70,71] There is certainly more to be explored in medium engineering in order to simplify the selection of solvent in a certain enzymatic reaction, which could serve as a simpler alternative to the time consuming protein engineering approach.

Summary and Outlook

Over the course of this review, factors influencing substrate specificity and stereospecificity for ADHs have been discussed. Protein engineering, medium

engineering, reaction temperature, reaction pressure and pH show significant effects on ADH-catalyzed reactions. This review shows the importance of small alterations that could be made through protein engineering of the active site on expanding substrate specificity and stereospecificity. On the other hand, a simple and less laborious approach like medium engineering can be used to improve stereospecificity of ADHs. Reaction temperature and pressure have been shown to be important in altering stereospecificity of ADH-catalyzed reactions. Combining mutagenesis and medium engineering can even further improve reactions, as shown by several examples above. Expanding the substrate specificity and stereospecificity of ADHs will improve the effectiveness of redox reactions catalyzed by these enzymes, and thus make them good alternatives to other environmentally harsh methods. The pharmaceutical industry will probably find more uses in the future for ADHs due to their ability to produce enantiopure alcohols with either desired configuration, whereas typical chemical reaction conditions only produce one enantiomer under more severe conditions.

Abbreviations: ADH: alcohol dehydrogenase; NAD^+: nicotinamide adenine dinucleotide; $NADP^+$: nicotinamide adenine dinucleotide phosphate; HLADH: horse liver alcohol dehydrogenease; *S. cerevisiae*: *Saccharomyces cerevisiae*; *S. pombe*: *Schizosaccharomyces pombe*; YADH: yeast alcohol dehydrogenase; LlADH: *Lactococcus lactis* ADH; SsADH: *Sulfolobus solfataricus* ADH; SADH: *Thermoanaerobacter brockii* ADH and *Thermoanaerobacter ethanolicus* secondary ADH; SsCR: *Sporobolomyces salmonicolor* carbonyl reductase

References

[1] Rothenberg, G. *Catalysis: Concepts and* Green *Applications*, 1st edition; Wiley-VCH: Weinheim, 2008; pp.2, 16-7, 210-11.

[2] Prelog, V. *Pure Appl. Chem.* **1964**, *9*, 119-130.

[3] Jones, J. B.; Jakovac, I. J. *Can. J. Chem.* **1982**, *60*, 19-28.

[4] Lam, L. K.; Gair, I. A.; Jones, J. B. *J. Org. Chem.* **1988**,*53*, 1611-1615.

[5] Jones, J. B.; Takemura, T. *Can. J. Chem.* **1982**, *60*, 2950-2956.

[6] Krawczyk, A. R.; Jones, J. B. *J. Org. Chem.* **1989**, *54*, 1795-1801.

[7] Bridges, A. J.; Raman, P. S.; Ng, G. S.; Jones, J. B. *J. Am. Chem. Soc.* **1984**, *106*, 1461-1467.

[8] Keinan, E.; Hafeli, F. V.; Seth, K. K.; Lamed, R. *J. Am. Chem. Soc.* **1986**, *108*, 162-169.

[9] Korkhin, Y.; Kalb(Gilboa), A. J.; Peretz, M.; Bogin, O.; Burstein, Y.; Frolow, F. *J. Mol. Biol.* **1998**, *278*, 967-981.

[10] Coombs, G.S.; Corey, D.R. Site-Directed Mutagenesis and Protein Engineering. In *Proteins: Analysis and Design*, 1st edition; Angeletti, R.H., ed.; Academic Press: San Diego, 1998; pp.260-261.

[11] Theorell, H.; Åkeson, Å.; Liszka-Kopeć, B.; de Zalenski, C. *Arch. Biochem. Biophys.* **1970**, *139*, 241-247.

[12] Park, D. H., Plapp, B. V. *J. Biol. Chem.* **1991**, *266*, 13296-13302.

[13] Jornvall, H. *Eur. J. Biochem.* **1970**, *16*, 25-40.

[14] Park, D. H., Plapp, B. V. *J. Biol. Chem.* **1992**, *267*, 5527-5533.

[15] Adolph, H. W.; Zwart, P.; Meijers, R.; Hubatsch, I.; Kiefer, M.; Lamzin, V.; Cedergren-Zeppezauer, E. *Biochemistry* **2000**, *39*, 12885-12897.

[16] Wong, C. H.; Whitesides, G. M. Oxidoreductases. In *Enzymes in Synthetic Organic Chemistry*, 2nd edition; Baldwin, J.E.; Magnus, P.D., Eds; Tetrahedron Organic Chemistry Series; Pergamon: New York, 1995; 12, pp.142-150, 151-152.

[17] Leskovac, V.; Trivić, S.; Peričin, D. *FEMS Yeast Res.* **2002**, *2*, 481-494.

[18] Murali, C.; Creaser, E. H. *Protein Eng.* **1986**, *1*, 55-57.

[19] Ganzhorn, A. J.; Green, D. W.; Hershey, A. D.; Gould, R. M.; Plapp, B. V. *J. Biol. Chem.* **1987**, *262*, 3754-3761.

[20] Green, D. W.; Sun, H. W.; Plapp, B. V. *J. Biol. Chem.* **1993**, *268*, 7792-7798.

[21] Light, D. R., Dennis, M. S., Forsythe, I. J., Liu, C.-C., Green, D. W., Kratzer, D. A, Plapp, B. V. *J. Biol. Chem.* **1992**, *267*, 12592-12599.

[22] Weinhold, E. G.; Benner, S. A. *Protein Eng.* **1995**, *8*, 457-461.

[23] Brändén, C. I.; Jörnvall, H.; Eklund, H.; Furugren, B. *The Enzymes*, 3rd edition; Boyer,P. D. ed.; Academic Press: New York, 1975; 11, pp. 103-190.

[24] Liu, X.; Bastian, S.; Snow, C. D.; Brustad, E. M.; Saleski, T. E.; Xu, J. H.; Meinhold, P.; Arnold, F. H. *J. Biotechnol.* **2012**, *164*, 188-195.

[25] Giordano, A.; Cannio, R.; La Cara, F.; Bartolucci, S.; Rossi, M.; Raia, C. A. *Biochemistry* **1999**, *38*, 3043-3054.

[26] Pennacchio, A.; Esposito, L.; Zarari, A.; Rossi, M.; Raia, C. A. *Extremophiles* **2009**, *13*, 751–761.

[27] Zeikus, J. G.; Hegge, P. W.; Anderson, M. A. *Arch. Microbiol.* **1979**, *122*, 41-48.

[28] Wiegel, J.; Ljungdahl, L. G. *Arch. Microbiol.* **1981**, *128*, 343-348.

[29] Lee, Y. E.; Jain, M. K.; Lee, C.; Zeikus, J. G. *Int. J. Syst. Bacteriol.* **1993**, *43*, 41-51.

[30] Bryant, F. O.; Wiegel, J.; Ljungdahl, L. G. *Appl. Environ. Microbiol.* **1988**, *54*, 460-465.

[31] Burdette, D. S.; Vieille, C.; Zeikus, J. G. *Biochem. J.* **1996**, *316*, 115-122.

[32] We have found *T. ethanolicus* S39E SADH to have the identical sequence to the *T. brockii* SADH sequence from the reported crystal structure (1YKF). SADH from *T. ethanolicus* JW200 is 97% identical to the previously mentioned sequences.

[33] Tripp, A.E.; Burdette, D.S.; Zeikus, J.G.; Phillips, R.S. *J. Am. Chem. Soc*. **1998**, *120*, 5137-5141.

[34] Heiss, C.; Laivenieks, M.; Zeikus, J. G.; Phillips, R. S. *Bioorg. Med. Chem.* **2001**, *9*, 1659-1666.

[35] Heiss, C.; Phillips, R. S. *J. Chem. Soc., Perkin Trans. 1* **2000**, 2821-2825.

[36] a.) Musa, M. M.; Ziegelmann-Fjeld, K. I.; Vieille, C.; Zeikus, J. G.; Phillips, R. S. *J. Org. Chem.* **2007**, *72*, 30-34. b) Ziegelmann-Fjeld, K. I.; Musa, M. M.; Phillips, R. S.; Zeikus, J. G.; Vieille, C. *Protein. Eng., Des. Sel.* **2007**, *20*, 47-55.

[37] Patel, J. M.; Musa, M. M.; Rodriguez, L.; Sutton, D. A.; Popik, V.; Phillips, R. S. *Org. Biomol. Chem.* **2014**, *12*, 5905-5910.

[38] Musa, M. M.; Lott, N.; Laivenieks, M.; Watanabe, L.; Vieille, C.; Phillips, R. S. *ChemCatChem* **2009**, *1*, 89-93.

[39] Agundo, R.; Roiban, G. D.; Reetz, M. T. *J. Am. Chem. Soc.* **2013**, *135*, 1665-1668.

[40] Musa, M. M.; Phillips, R. S.; Laivenieks, M.; Vieille, C.; Takahashi, M.; Hamdan, S. M. *Org. Biomol. Chem.* **2013**, *11*, 2911-2915.

[41] Karabec, M.; Łyskowski, A.; Tauber, K. C.; Steinkellner, G.; Kroutil, W.; Grogan, G.; Gruber, K. *Chem. Commun.* **2010**, *46*, 6314-6316.

[42] Hamnevik, E.; Blikstad, C.; Norrehed, S.; Widersten, M. *J. Mol. Catal. B: Enzym.* **2014**, *99*, 68-78.

[43] Jakoblinnert, A.; Wachtmeister, J.; Schukur, L.; Shivange, A. V.; Bocola, M.; Ansorge-Schumacher, M. B.; Schwaneberg, U. *Protein Eng., Des. Sel.* **2013**, *26*, 291-298.

[44] Zhu, D.; Yang, Y.; Majkowicz, S.; Pan, T. H.; Kantardjieff, K.; Hua, L. *Org. Lett.* **2008**, *10*, 525-528.

[45] Li, H.; Yang, Y.; Zhu, D.; Hua, L.; Kantardjieff, K. *J. Org. Chem.* **2010**, *75*, 7559-7564.

[46] Li, H.; Zhu, D.; Hua, L.; Biehl, E. R. *Adv. Synth. Catal.* **2009**, *351*, 583-588.

[47] Kavanagh, K. L.; Klimacek, M.; Nidetzky, B.; Wilson, D. K. *Biochemistry* **2002**, *41*, 8785-8795.

[48] Kratzer, R.; Nidetzky, B. *Chem. Commun.* **2007**, 1047-1049.

[49] Kratzer, R.; Leitgeb, S.; Wilson, D.K.; Nidetzky, B. *Biochem. J.* **2006**, *393*, 51-58.

[50] Pham, V. T.; Phillips, R. S.; Ljugdahl, L. G. *J. Am. Chem. Soc.* **1989**, *111*, 1935-1936.

[51] Pham, V. T.; Phillips, R. S. *J. Am. Chem. Soc.* **1990**, *112*, 3629-3632.

[52] Secundo, F.; Phillips, R. S. *Enzyme Microb. Tech.* **1996**, *19*, 487-492.

[53] Heiss, C.; Laivenieks, M.; Zeikus, J. G.; Phillips, R. S. *J. Am. Chem. Soc.* **2001**, *123*, 345-346.

[54] Morita, R. Y.; Haight, R. D. *J. Bacteriol.* **1962**, *83*, 1341-1346.

[55] Dallet, S.; Legoy, M. D. *Biochim. Biophys. Acta* **1996**, *1294*, 15-24.

[56] Cho, Y. K.; Northrop, D. B. *Biochemistry* **1999**, *38*, 7470-7475.

[57] Kahlow, U. H.; Schmid, R. D.; Pleiss, J. *Protein Sci.* **2001**, *10*, 1942-1952.

[58] Patel, J. M.; Phillips, R. S. *ACS Catal.* **2014**, *4*, 692-694.

[59] Phillips, R. S. *J. Mol. Catal. B: Enzym.* **2002**, *19-20*, 103-107.

[60] Klibanov, A. M. *Nature* **2001**, *409*, 241-246.

[61] a) Carrea, G.; Riva, S. *Organic Synthesis with Enzymes in Non-Aqueous Media* Wiley-VCH, **2008**. b) Grunwald, J.; Wirz, B.; Scollar, M. P.; Klibanov, M. *J. Am. Chem. Soc.* **1986**, 108, 6732-6734.

[62] a) Wescott, C. R.; Klibanov, A. M. *Biochim. Biophys. Acta* **1994**, *1206*, 1-9. b) Carrea, G.; Riva, S. *Angew. Chem. Int. Ed*. **2000**, *39*, 2226.

[63] Simpson, H. D.; Cowan, D. A. *Protein Pept. Lett.* **1997**, *4*, 25-32.

[64] Schumacher, J.; Eckstein, M.; Kragl, U. *Biotechnol. J.* **2006**, *1*, 574-581.

[65] Musa, M. M.; Ziegelmann-Fjeld, K. I.; Vieille, C.; Zeikus, J. G.; Phillips, R. S. *Angew. Chem., Int. Ed.* **2007**, *46*, 3091-3094.

[66] Eckstein, M.; Filho, M. V.; Liese, A.; Kragl, U. *Chem. Commun.* **2004**, 1084-1085.

[67] Musa, M. M.; Ziegelmann-Fjeld, K. I.; Vieille, C.; Phillips, R. S. *Org. Biomol. Chem.* **2008**, *6*, 887-892.

[68] Shi, Y.-G.; Fang, Y.; Ren, Y.-P.; Wu, H.-P.; Guan, H. L. *J. Ind. Microbiol. Biotechnol.* **2008**, *35*, 1419-1424.

[69] Hirakawa, H., Kamiya, N.; Kawarabayashi, Y.; Naganume, T. *Biochim. Biophys. Acta* **2005**, *1748*, 94-99.

[70] Filho, M. V.; Stillger, M.; Muller, M.; Liese, A.; Wandrey, C. *Angew. Chem., Int. Ed.* **2003**, *42*, 2993-2996.

[71] Gonzalo, G.; Lavandera, I.; Faber, K.; Kroutil W. *Org. Lett.* **2007**, *9*, 2163-2166.

CHAPTER 3

BROADENING SUBSTRATE SPECIFICITY OF I86A SECONDARY ALCOHOL DEHYDROGENASE FROM *THERMOANAEROBACTER ETHANOLICUS*[1]

---

[1] Nealon, C. M.; Welsh, T. P.; Laivenieks, M.; Vieille, C.; Kim, C. S.; Phillips, R. S. To be submitted to *ACS Catalysis*.

Abstract

Through mutagenesis, the small pocket of the active site of *T. ethanolicus* secondary alcohol dehydrogenase (TeSADH) has been expanded to accommodate substituted acetophenones and heterocycles to produce the *anti*-Prelog products. The I86A and I86A/C295A mutations have broadened substrate specificity compared to wild-type. With respect to each other, the broadening of the substrate scope of I86A carries with it a decrease in the specific activity of the mutual substrates when I86A/C295A was tested, due to the substrates not fitting inside the active site as well with the additional space from the mutations. While the specific activity decreased some, the two mutants gave very high enantiomeric excess of the *R*-alcohol of the tested substrates.

Introduction

Two alcohol dehydrogenases, a primary and a secondary alcohol dehydrogenase, were isolated in the late 1980's from *Thermoanaerobacter ethanolicus*, which was isolated from a hot spring in Yellowstone National Park.[1,2] The wild-type secondary alcohol dehydrogenase (TeSADH) followed Prelog's rule in the reduction of ketones, and is known as a Prelog ADH, adding the *R*-hydride of the NADPH to the *Re*-face of the ketone. In an effort to broaden the substrate specificity of TeSADH, a number of active site residues have been altered. Some of the previously published mutations of TeSADH include S39T, C295A, W110A, and I86A.[3,4,5,6]

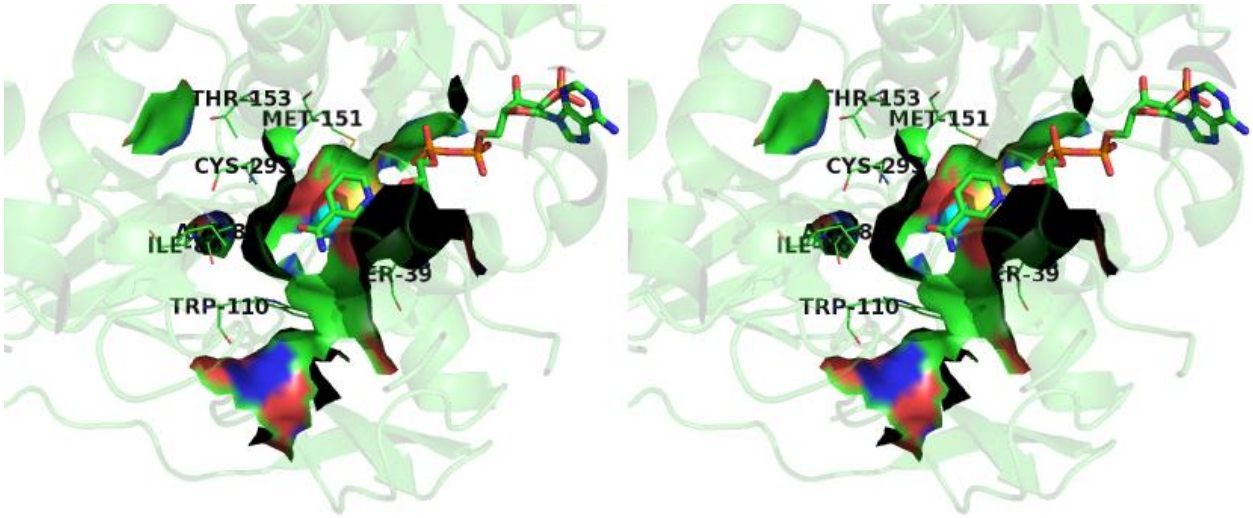

Figure 3.1. Stereoview of TbADH, with residues of interest labeled. $NADP^+$ shown in stick-form and Zinc as a cyan sphere. This image was prepared with Pymol[7] using the PDB file (1YKF).

The I86A mutation of TeSADH not only expanded substrate specificity to include acetophenone, which is a very poor substrate for wild-type TeSADH (Nealon, C; Phillips, R. unpublished results), but also reversed the usual preferred stereochemistry to produce the anti-Prelog product. However, I86A TeSADH exhibited limited reactivity with substituted acetophenones, fluorine being the only tolerable substituent found in the initial study.[6] Chiral 1-arylalkanols are useful intermediates in preparation of pharmaceuticals. Thus, it was of interest to expand the active site further to allow the reduction of substituted acetophenones.[5] The C295A mutant of TeSADH was studied previously by Heiss and coworkers, and was found to increase the size of the alkyl group which can bind in the "small pocket" by one carbon atom.[4] Due to the proximity of Cys-295 to Ile-86 (Figure 3.1), we predicted that having both mutations in the active site would expand the size of the small pocket. We have now prepared the I86A/C295A double mutant of TeSADH, and we have found, as expected, that it has broadened specificity for substituted acetophenones.

Results and Discussion

In order to further expand the active site of TeSADH, other enzymes with a broad substrate scope should be viewed for inspiration. The carbonyl reductase from *Candida parapsilosis* (CPCR2) contains a zinc ion just as the TeSADH, and also has activity with medium chain alcohols. Jakoblinnert and coworkers expanded the active site of their CPCR2, and as such affected the substrate specificity.[8] Five residues were selected for site-saturation mutagenesis (Leu-55, Pro-92, Gly-118, Leu-119, Leu-262). Of the active mutants at those aforementioned locations, only L119M gave activity that was greater than wild-type CPCR2. Even though methionine and leucine have side chains of similar size, the lack of branching within the methionine provided a less constraining CPCR2 active site.

Zhu and coworkers studied *Sporobolomyces salmonicolor* carbonyl reductase (SsCR), and desired to improve the activity of wild-type SsCR towards para-substituted acetophenones.[9] Through docking studies, they focused their site-saturation mutagenesis on the Gln-245 residue. The mutants with the greatest improvement were Q245H, Q245P, and Q245L, which all three interestingly switched the alcohol isomeric product from *R* to *S*.[9] Probing the SsCR active site further, Li and coworkers utilized site-saturation mutagenesis on the Met-242 residue, and found improvement for some of the substrates tested.[10] Also, M242Y, M242D, M242C and M242G reversed the stereospecificity of the alcohol product. Due to Met-242 and Gln-245 altering the substrate specificity separately, they opted to design a double mutant at the sites mentioned previously. From this study, M242L/Q245P and M242L/Q245T showed the largest boost in *ee*.[10] Broadening the substrate scope to include benzophenones, Li and

coworkers found that mutagenesis at the Gln-245 residue improved substrate specificity as well as providing a means for the *S*-isomer.[11] Zhang and coworkers recently reported a mutant SsCR study with *β*-amino ketones.[12] While there was a little activity with M242F/Q245T and *β*-amino acetophenone, a docking study followed by site-saturation mutagenesis yielded viable mutants at the Pro-170 and Leu-174. Of the SsCR mutants, L174Y and L174W were the single mutants of note with the greatest activity against *β*-amino acetophenone. In addition, the researcher designed double mutants of Pro-170 and Leu-174, with the interesting mutant SsCRs being P170R/L174Y, P170R/L174W, and P170H/L174W. When each of these mutants were tested against *β*-amino-2-acetylthiophene, only L174Y and P170R/L174Y gave high *ee* for each of the two substrates.[12]

Kavanagh and coworkers studied the active site of *Candida tenuis* xylose reductase (CtXR),[13] which was later found to react with alpha-keto esters.[14] Through modeling studies, the Trp-23 appeared to conflict with the alpha ketone of the substrates. With site-directed mutagenesis, the tryptophan was replaced by at first phenylalanine and then tyrosine. The activity increased for each of these when compared with wild-type against the various alpha-keto esters.[14] Kratzer and researchers studied the kinetics of acetophenone and other assorted ketones with W23F, W23Y and wild type CtXR.[15] While the mutants decreased the activity with most of the ketones, oxopantoyl-lactone and ethyl-benzoylformate interestingly had an increase in activity of four to five fold and two to three fold respectively. Due to the mixed kinetic results, the researchers rationalized that the Trp-23 has a role in selective binding and the specificity of the enzyme.[15]

As shown in Table 3.1, I86A TeSADH has the highest specificity constant, k_{cat}/K_m, with unsubstituted acetophenone, consistent with our previous results.[6] Extending the alkyl chain by one carbon to propiophenone results in only a 2-fold decrease in k_{cat}/K_m. With increasing substituent size, the specificity decreases. Interestingly, we found in this study that 3'-chloroacetophenone reacts with I86A mutant TeSADH, although the k_{cat}/K_m value is decreased by about 36-fold compared to I86A/C295A. As we had found previously, acetophenones with substituents larger than chlorine are not detectable as substrates for I86A TeSADH (Table 3.2). Another interesting result is that 2-acetylpyridine, 4-acetylpyridine and 3-acetylthiophene react much better than 3-acetylpyridine and 2-acetylthiophene. Due to their similar overall size, there has to be other effects involved besides sterics. It is likely that electronic effects are responsible. The electron-withdrawing effects of the pyridine ring are strongest in 2- and 4-acetylpyridine, due to resonance contributions, while the electron-donating effect of thiophene is weakest for 3-acetylthiophene. These observations suggest that hydride transfer to the carbonyl is facilitated by making the carbonyl carbon more electron-deficient.

To expand the active site further, the C295A mutation was incorporated into the I86A mutant TeSADH. While the I86A/C295A double mutant unexpectedly showed no reactivity with *para*-substituted acetophenones, *meta*-substitution was allowed, as shown in Table 2.2. Small *ortho*-substituents are also tolerated, since 2'-methylacetophenone was found to be a substrate (Table 3.2). It is interesting that the k_{cat}/K_m value for unsubstituted acetophenone is reduced about 8-fold for I86A/C295A TeSADH compared to I86A TeSADH. This means that the increase in substrate specificity is gained at the expense of reaction efficiency. The K_m values for acetophenones with I86A/C295A

TeSADH were generally around 8-10 mM, with some exceptions, so the k_{cat} is more affected by substitution. The reactivity of the acetophenones decreases with increasing size of the *meta*-substituent.

Table 3.1. I86A TeSADH Kinetic Assays

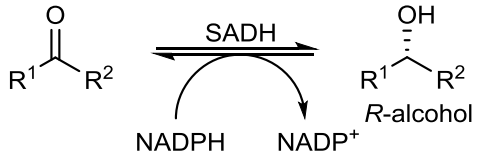

Substrate		I86A		
R^1	R^2	K_m (mM)	k_{cat} (s^{-1})	k_{cat}/K_m ($M^{-1}s^{-1}$)
CH_3	CH_3	0.76±0.29	1.01±0.16	1330±340
C_6H_5	CH_3	0.55±0.15	8.2±0.6	14900±3100
m-ClC_6H_5	CH_3	1.6±0.5	0.66±0.09	410±90
m-BrC_6H_5	CH_3	n.d.[b]	n.d.[b]	n.d.[b]
m-$CH_3C_6H_5$	CH_3	n.d.[b]	n.d.[b]	n.d.[b]
m-IC_6H_5	CH_3	n.d.[b]	n.d.[b]	n.d.[b]
o-$CH_3C_6H_5$	CH_3	n.d.[b]	n.d.[b]	n.d.[b]
2-pyridyl	CH_3	4.3±1.6	6.9±1.6	1600±260
3-pyridyl	CH_3	2.4±1.3	0.47±0.15	200±55
4-pyridyl	CH_3	1.5±0.2	1.7±0.1	1050±101
2-thienyl	CH_3	3.3±0.9	1.7±0.2	510±85
3-thienyl	CH_3	3.5±1.4	14.9±4.2	4300±730
C_6H_5	CH_2CH_3	0.79±0.24	6.5±5.5	8100±1700

2,4-$F_2C_6H_3$	CH_3	3.6±1.9	2.2±0.7	620±140
m-CH_3OC6H5	CH_3	n.d.[b]	n.d.[b]	n.d.[b]
m-$CF_3C_6H_5$	CH_3	n.d.[b]	n.d.[b]	n.d.[b]

[a]Substrate inhibiton. [b]Not detected

Table 3.2. I86A/C295A TeSADH Kinetic Assays

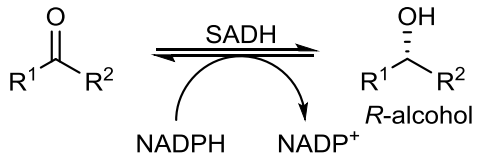

Substrate		I86A/C295A		
R^1	R^2	K_m (mM)	k_{cat} (s^{-1})	k_{cat}/K_m ($M^{-1}s^{-1}$)
CH_3	CH_3	32±8	3.5±0.6	1080±110
C_6H_5	CH_3	8.3±1.7	15.8±1.6	1900±220
m-ClC_6H_5	CH_3	9.4±3.5	12.3±2.4	1300±250
m-BrC_6H_5	CH_3	9.9±3.2	6.5±1.1	650±110
m-$CH_3C_6H_5$	CH_3	11±3.4	2.0±0.33	180±28
m-IC_6H_5	CH_3	3.7±0.9	0.61±0.06	160±30
o-$CH_3C_6H_5$	CH_3	10±4	0.18±0.04	18±3
2-pyridyl	CH_3	9.1±2	2.31±0.23	260±30
3-pyridyl	CH_3	N/A[a]	N/A[a]	630±14
4-pyridyl	CH_3	5.4±1.7	13.1±1.9	2400±400
2-thienyl	CH_3	5.7±2	1.5±0.2	260±60
3-thienyl	CH_3	N/A[a]	N/A[a]	350±60

C_6H_5	CH_2CH_3	15±5	23.3±5.5	1500±150
2,4-$F_2C_6H_3$	CH_3	13±6	2.9±0.7	230±60
m-CH_3OC6H5	CH_3	2.3±0.9	0.08±0.02	210±40
m-$CF_3C_6H_5$	CH_3	1.6±0.9	0.04±0.008	25±10

[a]Substrate inhibiton

Another means of comparison of the two mutant enzymes is through the determination of percent conversions and enantiomeric excesses in preparative reactions. Table 3.3 compares the previously published I86A TeSADH data[6], with two additional substrates, and the new I86A/C295A TeSADH data. In general, the preparative reaction results correlate with the kinetic results in Table 3.2. As expected, 3'-chloroacetophenone reacts much better with I86A/C295A than with I86A TeSADH, giving conversions of 95% and 14% respectively. 2-Acetylpyridine and 4-acetylpyridine gave fairly high conversion with I86A/C295A TeSADH, although slightly lower conversion than the previously published results with I86A.[5] One interesting observation was that the percent conversion with 2-acetylthiophene and 3-acetylthiophene rose with 2-acetylthiophene with I86A/C295A TeSADH, while the percent conversion fell with 3-acetylthiophene with I86A/C295A. 3'-Aminoacetophenone, 3'-nitroacetophenone, 3'-ethoxyacetophenone, and 4'-methylacetophenone did not show any reduction with I86A/C295A TeSADH, and would also be too large for the active site of I86A TeSADH. In all cases where reaction was observed, we found the product to be the anti-Prelog (R)-alcohol with >99% ee.

Table 3.3. I86A and I86A/C295 TeSADH GC Assays

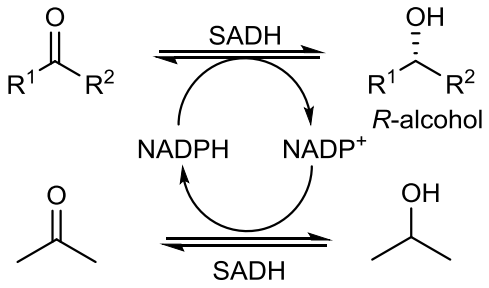

Substrate		I86A/C295A TeSADH			I86A TeSADH		
R^1	R^2	Conv. (%)	*ee* (%)	*R/S*	Conv. (%)	*ee* (%)	*R/S*
C_6H_5	CH_3	68	>99	*R*	47[a]	98[a]	*R*[a]
m-ClC_6H_5	CH_3	23	>99	*R*	0.62	>99	*R*
m-BrC_6H_5	CH_3	8	>99	*R*	n.d.[b]	n.d.[b]	n.d.[b]
m-IC_6H_5	CH_3	4	>99	*R*	n.d.[b]	n.d.[b]	n.d.[b]
m-$CH_3C_6H_5$	CH_3	23	>99	*R*	n.d.[b]	n.d.[b]	n.d.[b]
o-$CH_3C_6H_5$	CH_3	<1	>99	*R*	n.d.[b]	n.d.[b]	n.d.[b]
m-$CH_3OC_6H_5$	CH_3	5	>99	*R*	n.d.[b]	n.d.[b]	n.d.[b]
m-$CF_3C_6H_5$	CH_3	3	>99	*R*	n.d.[b]	n.d.[b]	n.d.[b]
2-pyridyl	CH_3	53	>99	*R*	>99[a]	>99[a]	*R*[a]
3-pyridyl	CH_3	75	>99	*R*	46[a]	>99[a]	*R*[a]
4-pyridyl	CH_3	98	>99	*R*	>99[a]	>99[a]	*R*[a]
2-thienyl	CH_3	27	>99	*R*	2.52	>99	*R*
3-thienyl	CH_3	39	>99	*R*	76[a]	>99[a]	*R*[a]
C_6H_5	CH_2CH_3	31	>99	*R*	60[a]	>99[a]	*R*[a]

2,4-$F_2C_6H_3$	CH_3	4	>99	*R*	33[a]	>99[a]	*R*[a]

[a]Musa et al.[5] [b]Not detected.

With the k_{cat} and k_{cat}/K_m data for the various acetophenones with I86A/C295A TeSADH in Table 3.2, Hammett-Taft analysis was performed. The three-dimensional fit to the general equation z=ax+by for each was as follows:

$$\text{Log}(k_{cat}/(k_{cat})_0)=1.531\sigma+1.312E_S \quad (3.1)$$

$$\text{Log}((k_{cat}/K_m)/(k_{cat}/K_m)_0)=1.52\sigma+1.105E_S \quad (3.2)$$

The sensitivity factors (a and b of the general equation above) define how impactful the σ and E_S values are on $\text{Log}(k_{cat}/(k_{cat})_0)$ and $\text{Log}((k_{cat}/K_m)/(k_{cat}/K_m)_0)$. From each of the best fit lines, there's just as much impact from the electronic effects as the sterics on the reaction. The value of ρ is similar for both k_{cat} and k_{cat}/K_m, showing that both parameters are affected similarly by electronic effects. The positive ρ indicates that electron-withdrawal increases reactivity, consistent with the results from acetylpyridine and acetylthiophene discussed above. However, the steric effects are greater on k_{cat}, as the steric parameter is larger. The plots of the results are shown in Figure 3.2.

Figure 3.2. I86A/C295A TeSADH Hammett-Taft Plot

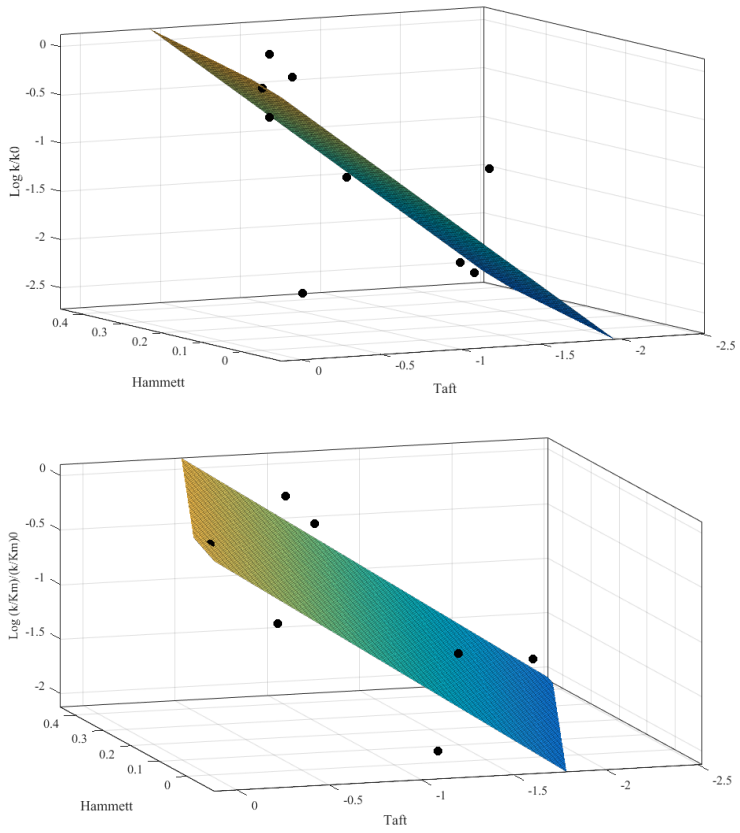

Considering that wild-type TeSADH active site cannot easily accommodate the phenyl moiety in the small pocket (Nealon, C.; Phillips, R. unpublished results), the discovery of a single mutant (I86A) through site-directed mutagenesis that can open the small pocket enough for a phenyl ring to fit inside is of interest. An additional mutation of a neighboring residue (C295A) in the I86A TeSADH active site has opened up the enzyme to additional reaction of substituted arylketones. It is of note that in increasing the active site size through multiple mutations, the efficiency of the enzyme decreased as the substrate pool was able to increase. This could merely be because the substrate has more room to move within the active site, and that the substrate doesn't fit as tightly. In conclusion, these additional mutations could provide a nice starting point for further expansion of the SADH active site.

Experimental Section

General Methods: Gas chromatography performed with a Varian 3300 GC (Agilent Tech; Santa Clara, CA) using a Supelco (Sigma Aldrich; St. Louis, MO) *β*-Dex 120 cyclodextrin chiral column (30 nm, 0.25 mm [i.d.], 0.25 µm film thickness) with Helium as the carrier gas and equipped with a flame ionization detector. Kinetic experiments and assays performed on a Varian Carey 1E UV-visible spectrophotometer (Agilent Tech; Santa Clara, CA) equipped with a Peltier thermoelectric temperature-controlled 12-cell holder. Any ^{1}H and ^{13}C NMR analyses ran on a 400MHz spectrometer with $CDCl_3$ as the solvent at room temperature with tetra-methylsilane or the solvent peak as the standard.

Materials: Substrates were used as purchased from commercial suppliers with the exception of 3'-bromoacetophenone, which was prepared by a published procedure.[16] Acetophenone was purchased from Fisher Scientific (Waltham, MA). 2'4'-Difluoroacetophenone was bought from Acros (Geel, Belgium). The 2-acetylpyridine was purchased from Pfaltz and Bauer (Waterbury, CT). The rest of the substrates tested were purchased from Sigma Aldrich (St. Louis, MO). Acetonitrile was purchased from Burdick and Jackson (Morristown, NJ). NADPH was purchased from Acros (Geel, Belgium). The antibiotics, kanamycin and ampicillin, were bought from Roche (Indianapolis, IN) and Fisher Biotech (Fair Lawn, NJ), respectively. Commercial grade solvents used were used without further purification.

Mutagenesis: The I86A plasmid was made with the method reported previously.[5] Using the Quikchange method, the I86A plasmid using the pADHB25 was further mutated with the following forward and reverse primers: C295A-f

(ATAAAAGGCGGGCTA**GCC**CCCGGTGGACG), and C295A-r (TTTCCGCCCGAT**CGG**GGGCCACCTGCAGA).

Purification or Secondary Alcohol Dehydrogenase: The method used for this protein expression and purification was based on a previously published method.[3] Differences to this method include usage of the 50 mM Tris HCl pH 8.0 buffer with 5 mM DTT and 10 μM $ZnCl_2$, a 5 mL Red A agarose column and optimization of the low salt (0.02 M $NaClO_4$) and high salt (0.2 M $NaClO_4$) solutions. No further purification was needed after the Red A agarose column as the polyacrylamide gel showed a single band. The fractions were stored at -80 ^oC.

Enzyme Assays: The enzyme assay method was performed as published previously.[5] There were a number of changes that must be noted. The enzyme assays were performed at 50 ^oC in triplicate. The enzyme activity was measured in 50 mM Tris-HCl buffer (8.0 pH at 50 ^oC) with 0.4 mM $NADP^+$ (alcohol oxidation) or 50 mM potassium phosphate buffer (6.5 pH at 50 ^oC) with 0.4 mM NADPH (ketone reduction). The initial velocity was recorded on a Varian Cary 100 UV/Vis spectrophotometer at 340 nm for 10 min by monitoring NADPH consumption (ketone reduction) or NADPH generation (alcohol oxidation). Preincubation of the assay samples was in the appropriate 50 mM Buffer solution and the enzyme sample with 5 mM DTT and 10 μM $ZnCl_2$ added before allowing the samples to warm up to 50 ^oC in the UV/Vis sample compartment for 10 min. Each assay contained approximately 5% acetonitrile, since raising this concentration too high ruined the enzyme activity.

Asymmetric Reduction with I86A and I86A/C295A: Reactions were performed on a 1 mL scale. 0.21 mmol substrate, 1 mg NADPH, 0.5 mL Tris-HCl buffer (8.0 pH with 10

μM $ZnCl_2$), 0.2 mL 2-propanol, 1 mg DTT and I86A or I86A/C295A TeSADH (0.654 mg). The reactions were kept at 24 hr at 50 ^oC. After completion of 24 hr, the reactions were quenched by addition of dichloromethane. This organic extract could be used to quantify the percent conversions. Acetylation with acetic anhydride and pyridine was performed as referenced.[17] Enantiomeric excess of the products found after acetylation of reaction product.

Hammett-Taft calculations: The curve fitting tool (cftool) in MATLAB[18] was used to fit the three sets of data (Hammett, Taft, and either $\text{Log}(k_{cat}/(k_{cat})_0)$ or $\text{Log}((k_{cat}/K_M)/(k_{cat}/K_M)_0)$) to the custom equation z=ax+by. Equation 1 fitting parameters: 1.013 (SSE), 0.1435 (R^2), 0.02113 (Adj. R^2), 0.3805 (RMSE). Equation 2 fitting parameters: 0.2519 (SSE), 0.6082 (R^2), 0.5522 (Adj. R^2), 0.1897 (RMSE).

Abbreviations: ADH: alcohol dehydrogenase; $NADP^+$: nicotinamide adenine dinucleotide phosphate; TeSADH: *Thermoanaerobacter ethanolicus* secondary ADH

Supporting Information Available: Chromatographic data, Hammett-Taft plot data and kinetic assay data. This material is available free of charge via the Internet at http://pubs.acs.org.

References

[1] Zeikus, J. G.; Hegge, P. W.; Anderson, M. A. *Arch. Microbiol.* **1979**, *122*, 41-48.

[2] Wiegel, J.; Ljungdahl, L. G. *Arch. Microbiol.* **1981**, *128*, 343-348.

[3] Tripp, A. E.; Burdette, D. S.; Zeikus, J. G.; Phillips, R. S. *J. Am. Chem. Soc*. **1998**, *120*, 5137-5141.

[4] Heiss, C.; Laivenieks, M.; Zeikus, J. G.; Phillips, R. S. *Bioorgan. Med. Chem.* **2001**, *9*, 1659-1666.

[5] Musa, M. M.; Ziegelmann-Fjeld, K. I.; Vieille, C.; Zeikus, J. G.; Phillips, R. S. *J. Org. Chem*. **2007**, 72, 30-34.

[6] Musa, M. M.; Lott, N.; Laivenieks, M.; Watanabe, L.; Vieille, C.; Phillips, R. S. *ChemCatChem* **2009**, *1*, 89-93.

[7] The PyMOL Molecular Graphics System, Version 1.3 Schrödinger, LLC.

[8] Jakoblinnert, A.; Wachtmeister, J.; Schukur, L.; Shivange, A. V.; Bocola, M.; Ansorge-Schumacher, M. B.; Schwaneberg, U. *Protein Eng., Des. Sel.* **2013**, *26*, 291−298.

[9] Zhu, D.; Yang, Y.; Majkowicz, S.; Pan, T. H.; Kantardjieff, K.; Hua, L. *Org. Lett.* **2008**, *10*, 525−528.

[10] Li, H.; Yang, Y.; Zhu, D.; Hua, L.; Kantardjieff, K. *J. Org. Chem*. **2010**, *75*, 7559−7564.

[11] Li, H.; Zhu, D.; Hua, L.; Biehl, E. R. *Adv. Synth. Catal*. **2009**, *351*, 583−588.

[12] Zhang, D.; Chen, X.; Chi, J.; Feng, J.; Wu, Q.; Zhu, D. *ACS Catal.* **2015**, *5*, 2452-2457.

[13] Kavanagh, K. L.; Klimacek, M.; Nidetzky, B.; Wilson, D. K. *Biochemistry* **2002**, *41*, 8785−8795.

[14] Kratzer, R.; Nidetzky, B. *Chem. Commun*. **2007**, 1047−1049.

[15] Kratzer, R.; Leitgeb, S.; Wilson, D. K.; Nidetzky, B. *Biochem. J*. **2006**, *393*, 51−58.

[16] Pearson, D. E.; Pope, H. W.; Hargrove, W. W. *Org. Syn.* **1960**, *40*, 7.

[17] Ghanem, A.; Schuring, V. *Tetrahedron: Asymmetry* **2003**, *14*, 57-62.

[18] Mathworks, 2014 (MATLAB Version R2014b).

CHAPTER 4

KINETIC RESOLUTION OF 1-ARYLETHANOLS BY MUTANT *THERMOANAEROBACTER ETHANOLICUS* SECONDARY ALCOHOL DEHYDROGENASE[1]

---

[1] Nealon, C. M.; Laivenieks, M.; Vieille, C.; Kim, C. S.; Phillips, R. S. To be submitted to *Bioorg. Med. Chem. Lett.*

Abstract

Kinetic resolution provides a means of producing the normally unreactive product alcohol by the enzymatic conversion of one alcohol of a racemic mixture. This study compares the I86A and I86A/C295A mutants of *Thermoanaerobacter ethanolicus*, and demonstrates their utility generating the S-alcohols of the various substituted 1-arylethanols. The smaller and less substituted substrates reacted with each of the mutants to give *S*-alcohol in near quantitative yield. Halogens positioned meta on the 1-arylethanol yielded better results with the I86A/C295A SADH than with the I86A mutant.

Introduction

The active site of the secondary alcohol dehydrogenase from *T. ethanolicus* (SADH) has been investigated extensively to broaden substrate specificity. Beginning with the wild-type secondary alcohol dehydrogenase, mutations have been introduced in order to see the effect they have on the small and large pockets of the active site.[1] Mutations of the large pocket include S39T and W110A, while the small pocket mutations are I86A and C295A. The S39T mutation was one of the earlier examples that allowed for the altering of the secondary alcohol dehydrogenase active site.[2] In an effort to prevent the irreversible reaction of alkynes with the enzyme active site, the C295A mutation was introduced.[3] While the anticipated result was not found, the C295A mutant enzyme did show some alteration of substrate specificity due to expansion of the small pocket of secondary alcohol dehydrogenase. In the case of the I86A mutant SADH, the small pocket of the active site was able to accept a phenyl-ring, whereas the wild type secondary alcohol dehydrogenase was unable to accommodate the phenyl ring.[4] Further

investigating the large pocket of the secondary alcohol dehydrogenase, mutating the tryptophan-110 into an alanine opened the large pocket to fit a benzyl substituent.[5] Each of these SADHs give relatively high ee, which is ideal when reducing ketones to the preferred alcohol product.

Results and Discussion

For kinetic resolution assays, the percent conversion ideally should be no higher than 50%, since as previously mentioned, the main goal of a kinetic resolution is to yield the reactive isomer product and the unreacted isomer. As shown in Table 4.1, the reaction of less sterically hindered substrates with I86A/C295A SADH gave higher ee values as well as percent conversions nearer to 50%. Not surprisingly, 1-phenylethanol (**a**) gave 47% and 50% conversion with I86A and I86A/C295A, respectively. With the addition of a chlorine atom in the meta-position (**b**), both of the mutants show a decrease in conversion, but I86A/C295A is more efficient. 2,4-Difluoro-1-phenylethanol (**l**) reacted with I86A SADH to give a 3.3% conversion of R-isomer, while the I86A/C295A mutant gave 18% conversion of the *R*-isomer. As the size of the meta-substituent increases (**c-e**), both the percent conversion and ee generally decreases, as shown for the I86A/C295A mutant. Interestingly, 2-pyridinyl-1-ethanol (**f**) gave low conversion and ee with both of the two mutants tested. As the ethanol moiety moves around the pyridine, I86A results remained generally the same. For the I86A/C295A mutant, 3-pyridinyl-1-ethanol (**g**) and 4-pyridinyl-1-ethanol (**h**) showed improvement in the percent conversions and the ee. Even though sterics could explain differences between the two mutants, it wouldn't explain the differences within the substrates amongst the same mutant. The three different pyridinyl-1-ethanols have the same relative size, so the difference in reactivity

could arise from electronic effects. For the thiophene based substrates (**i-j**), the reaction was nearly quantitative for both 2-thiophenyl-1-ethanol and 3-thiophenyl-1-ethanol for each of the mutants. The steric argument would explain this boost in percent conversion and the ee. Lastly, 1-phenyl-1-propanol (**k**) reacted nearly quantitatively for each of the mutant SADH's.

Table 4.1. Kinetic resolution assays for I86A and I86A/C295A SADH

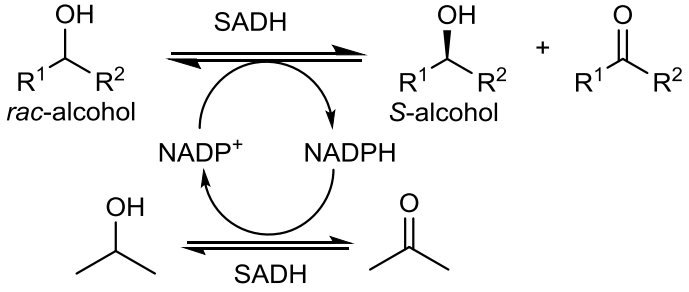

	R^1	R^2	*R* or *S* Product	I86A		I86A/C295A	
				Conv (%)	*ee* (%)	Conv (%)	*ee* (%)
a	C_6H_5	CH_3	*S*	47	89	50	>99
b	*m*-ClC_6H_5	CH_3	*S*	4.4	4.6	30	44
c	*m*-BrC_6H_5	CH_3	*S*	-	-	35	53
d	*m*-$CH_3C_6H_5$	CH_3	*S*	-	-	47	89
e	*m*-IC_6H_5	CH_3	*S*	-	-	8.7	9.5
f	2-pyridyl	CH_3	*S*	9.1	8.8	2.5	2.5
g	3-pyridyl	CH_3	*S*	7.5	8.1	37 [A]	58
h	4-pyridyl	CH_3	*S*	13	15	20 [A]	24
i	2-thienyl	CH_3	*S*	50 [A]	>99	50 [A]	>99
j	3-thienyl	CH_3	*S*	50 [A]	>99	48	93
k	C_6H_5	CH_2CH_3	*S*	49	94	49 [A]	95
l	2,4-$F_2C_6H_3$	CH_3	*S*	3.2	3.3	18	22

[A] 0.424mg enzyme used

In order to broaden the substrate specificity of the *T. ethanolicus* SADH, combining two useful mutations would open the active site further.[6] Separately, the C295AA and I86A mutants broadened the substrate specificity.[3,4] The I86A/C295A mutant was designed with a combination of mutations in the small pocket of the active site. It was

unclear how stable and useful the newly designed double mutant would be, due to the possibility of conformational changes that could even cause the inactivity of the mutant. The resulting mutant saw a drop in the activity for some of the substrates. The obvious rationale would be that the larger active site allows for more space which provides a broader substrate scope, but the substrates have more wiggle room which explains why activity would decrease.

While studying the asymmetric reduction of W110A and various ketones, Musa and coworkers also investigated the kinetic resolution of W110A SADH with racemic alcohols.[5] Even though a great deal of research has been done on SADH, very little kinetic resolution research has been done with alcohol dehydrogenases. Kinetic resolution provides a route for the generation of the opposite stereoisomer through reaction of the enzyme with the reactive isomer in a racemic mixture. In contrast, lipases have been widely used in kinetic resolutions.

Among lipases, *Candida antarctica* lipase B (CalB) has been the most widely studied. After starting with an initial library from saturation mutagenesis at W104, S105, A281 and A282, Wu and coworkers continued further iterative saturation mutagenesis in order to improve *R*-selectivity for one route and *S*-selectivity for the other route.[7] Each of the mutants were screened against a multitude of aromatic and aliphatic substrates. As a result, the researchers found that the thermostability of WT-CalB carried on into the mutants, while expanding the mutant library substantially.[7] Qin and coworkers improved kinetic resolution of CalB with various profen esters through site-saturation mutagenesis centered around the I189 and V190 residues.8 These substrates required extended reaction times with WT-CalB of twenty hours to yield a low yield of the *R*-product, while

the mutants that were screened gave varying degrees of conversion to give S-product. One of the best mutants found for the profen esters was referred to as M5 (I189F/V190L/V154G/Q157S).[8] While CalB has been studied the most, *C. antarctica* lipase A (CalA) also has activity towards alcohols. Wikmark and coworkers studied the mutagenesis of CalA and found that the activity of the lipase with various secondary alcohols improved with the double mutation of Y93L/L367I.[9] The lipase from *Burkholderia cepacia* has also been studied through kinetic resolution against poor substrates.[10] The preference of this lipase gave the R-product, while still providing some of the S-isomer to a smaller degree. Initially, single mutants were designed around residue isoleucine-287, and tested against racemic phenyl alcohols. The I287F mutant gave the best results, which then provided a starting point for double and triple mutant variants designed with additional mutations at isoleucine-290 and glutamine-292. Of the additional mutants, the I287F/I290A mutant gave near quantitative conversion to the *R*-acetate. Many of the substrates that reacted quite well with the double mutant above hardly reacted with the wild-type of the *B. cepacia* lipase, which demonstrated an improvement in the enzyme activity.[10]

Within the esterases, Ma and researchers have improved kinetic resolution enzyme activity of carboxyl esterase from *Rhodobacter sphaeroides* through directed evolution.[11] The activity was improved from wild type the most with the N62C/M121V/L145H mutant with the various tested substrates. The esterase from *Pseudomonas putida* was improved through the design of mutants at the W187 and D287.[12] Of these residues, the largest increase in substrate specificity of the S-isomer was seen with the W187H mutant, as compared with the wild-type.

The goal of a kinetic resolution is to open up a route to the unreacting isomer, amongst a racemic mixture. From this current study, the results show an improvement for many of the substrates with the additional mutation while preserving the high stereospecificity. This further demonstrates the utility of SADH-catalyzed kinetic resolutions for reaching each product and should be further researched with additional *T. ethanolicus* SADH mutants.

Experimental Section

General Methods: A Varian 3300 GC (Agilent Tech; Santa Clara, CA) with a Supelco (Sigma Aldrich; St. Louis, MO) β-Dex 120 cyclodextrin chiral column (30 nm, 0.25 mm [i.d.], 0.25 μm film thickness) and flame ionization detector was used for gas chromatography with Helium carrier gas.

Materials: Racemic alcohol substrates were prepared from $NaBH_4$ reduction of the phenyl-ring containing ketones.[13] With the exception of 3'-bromoacetophenone, which was prepared as a found in publication,[14] the ketones used without further purification prior to reduction. Acetophenone was purchased from Fisher Scientific (Waltham, MA). 2'4'-Difluoroacetophenone and the NADPH were bought from Acros (Geel, Belgium). The 2-acetylpyridine was purchased from Pfaltz and Bauer (Waterbury, CT). The rest of the substrates tested were purchased from Sigma Aldrich (St. Louis, MO). Acetonitrile was purchased from Burdick and Jackson (Morristown, NJ). The kanamycin was bought from Roche (Indianapolis, IN), and the ampicillin was from Fisher Biotech (Fair Lawn, NJ). Commercial grade solvents used were used without further purification.

Kinetic Resolution: Reactions were performed on a 1mL scale. 0.136 mmol substrate, 0.2 mg $NADP^+$, 0.1 mL acetone, 0.2 mg DTT, TeSADH (0.212 mg) and raised up to 1

mL with Tris-HCl buffer (8.0 pH with 10 μM $ZnCl_2$). The reactions were kept at 24 hr at 50 ^oC. After completion of 24 hr, the reactions were quenched by addition of dichloromethane. This organic extract could be used to quantify the percent conversions. Acetylation with acetic anhydride and pyridine was performed as referenced.[15] Enantiomeric excess of the products was found after acetylations.

Supporting information: The kinetic resolution gas chromatograph data has been made available free of charge on http://www.elsevier.com.

References and notes

[1] Prelog, V. *Pure Appl. Chem*. **1964**, *9*, 119-130.

[2] Tripp, A. E.; Burdette, D. S.; Zeikus, J. G.; Phillips, R. S. *J. Am. Chem. Soc*. **1998**, *120*, 5137-5141.

[3] Heiss, C.; Laivenieks, M.; Zeikus, J. G.; Phillips, R. S. *Bioorgan. Med. Chem.* **2001**, *9*, 1659-1666.

[4] Musa, M. M.; Lott, N.; Laivenieks, M.; Watanabe, L.; Vieille, C.; Phillips, R. S. *ChemCatChem* **2009**, *1*, 89-93.

[5] Musa, M. M.; Ziegelmann-Fjeld, K. I.; Vieille, C.; Zeikus, J. G.; Phillips, R. S. *J. Org. Chem.* **2007**, *72*, 30-34.

[6] Nealon Dissertation Chapter 3

[7] Wu, Q.; Soni, P.; Reetz, M. T. *J. Am. Chem. Soc.* **2013**, *135*, 1872-1881.

[8] Qin, B.; Liang, P.; Jia, X.; Zhang, X.; Mu, M.; Wang, X.; Ma, G.; Jin, D.; You, S. *Catal. Commun.* **2013**, *38*, 1-5.

[9] Wikmark, Y.; Humble, M. S.; Bäckvall, J. *Angew. Chem. Int. Ed.* **2015**, *54*, 4284-4288.

[10] Ema, T.; Nakano, Y.; Yoshida, D.; Kamata, S.; Sakai, T. *Org. Biomol. Chem.* **2012**, *10*, 6299-6308.

[11] Ma, J.; Wu, L.; Guo, F.; Gu, J.; Tang, X.; Jiang, L.; Liu, J.; Zhou, J.; Yu, H. *Appl. Microbiol. Biotechnol.* **2013**, *97*, 4897-4906.

[12] Ma, B.; Kong, X.; Yu, H.; Zhang, Z.; Dou, S.; Xu, Y.; Ni, Y.; Xu, J. *ACS Catal.* **2014**, *4*, 1026-1031.

[13] Yadav, V. K.; Babu, K. G. *Tetrahedron.* **2003**, *59*, 9111-9116.

[14] Pearson, D.E.; Pope, H.W.; Hargrove, W.W. *Org. Syn.* 1960, 40, 7.

[15] Ghanem, A.; Schuring, V. *Tetrahedron: Asymmetry* **2003**, *14*, 57-62.

CHAPTER 5

INVESTIGATION OF MET-151 AND THR-153 MUTATIONS OF *THERMOANAEROBACTER ETHANOLICUS* SADH[1]

[1] Nealon, C. M.; Kim, C. S.; Phillips, R. S. To be submitted to *Protein Eng. Des. Sel.*

Abstract

In an effort to broaden the substrate specificity of wild-type *T. ethanolicus* secondary alcohol dehydrogenase (TeSADH), M151A and T153A mutants were designed in hopes of expanding the small pocket of the active site. Interestingly, Met-151 being adjacent to the Zn^{2+} in the active site made the kinetic assays with M151A troublesome. Since M151A did not lose activity altogether, the Met-151 residue may stabilize the Zn coordination. The two mutants have activity that is comparable with wild-type SADH, though some substrates fell short.

Introduction

Through the use of protein engineering, the active site from secondary alcohol dehydrogenase of *Thermoanaerobacter ethanolicus* (TeSADH) has been altered to broaden substrate specificity. The active site has both a small and large pocket, and thus obeys Prelog's Rule, which, depending on the orientation of the ketone substrate, can result in a product that will be either the *R* or *S* isomeric alcohol.[1] One of the earliest studied examples of mutagenesis with TeSADH was the S39T mutation that increased the *R*-stereospecificity, in comparison to wild-type, but suffered a decrease in specific activity against ethanol, 1-propanol and 2-propanol.[2] With the C295A mutation, the small pocket of TeSADH was expanded, which led to the stereochemical preference reversal for the isobutyl and butyl ethynyl ketones, along with a greater percent conversion for many of the other tested ethynyl ketones.[3] Another mutation studied was W110A, which opened up the large pocket enough to allow substrates containing a benzyl group to react to give the *S*-alcohol, while wild-type TeSADH does not react with these substrates.[4] Subsequently, Musa and coworkers studied the I86A mutation of

TeSADH, and found that the active site small pocket was expanded enough for a phenyl moiety, but only fluoro substituents were tolerated on the ring.[5] Combining the I86A mutation with C295A to a double mutant, I86A/C295A, broadened the substrate scope of TeSADH, and allowed reaction of acetophenones substituted in the *meta* position with substituents such as Cl, Me, and Br, but larger substituents such as OMe did not react well, neither did para-substituted acetophenones.[6] In the present study, we identified Met-151 and Thr-153 as potential sites for additional mutations to further expand the active site of TeSADH and allow the reactions of a broader range of arylketones. The effects of M151A and T153A mutations of TeSADH are reported herein.

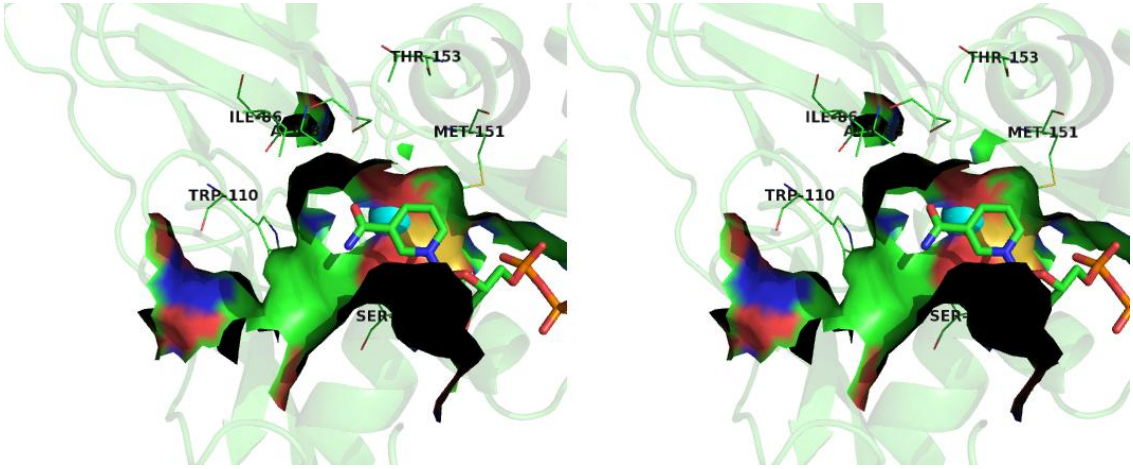

Figure 5.1. Crossed-eyed stereoview of the *T. ethanolicus* wild type active site with residues of interest labeled. $NADP^+$ is shown in stick form, and the cyan sphere is zinc cation. This image was prepared with PyMOL[7] (The PyMOL Molecular Graphics System, Version 1.3 Schrödinger, LLC) using the PDB file (1YKF).

Results and Discussion

In an effort to expand the small pocket of *T. ethanolicus* SADH and discover other interesting residues to combine with the already studied mutations, I86A and C295A, two residues were chosen, Met-151 and Thr-153, to be replaced with alanine. Both of these

residues make up part of the small pocket, as can be seen in **Figure 5.1**. The new TeSADH mutants, M151A and T153A, were compared with wild type TeSADH, in order to see how these mutations affect the catalytic properties. As shown in **Table 5.1 and 5.2**, wild type TeSADH generally has higher conversion with substrates that are shorter and that have α-branching. In order for the *S*-product to be formed, the R^1-group would have to be situated in the large pocket of the active site. While the R^1-group of straight chain ketones residing in the large pocket is not surprising, adding a methyl branch on 2-butanone shifts the R^1-group to the small pocket, thereby giving the *R*-product. This effect of α-branching of small substrates was first observed by Keinan.[8] Adding additional branching, to the t-butyl group, R^1 is too bulky to be in the small pocket, which was why it shifts back to the *S*-product, but in low yield. Heiss and Phillips also found that the small pocket of wild-type TeSADH can bind alkyl groups of 3 carbons or less, and allows α-branching. Most of the percent conversions of the substrates tested for the two mutants were less than those of wild type TeSADH. Interestingly, T153A TeSADH reacted slightly better with 3-methyl-2-butanone, while M151A TeSADH reacted a little less than wild type. Introduction of the M151A mutation into the wild type active site shifted the preference of product from *S* to *R* for 4-methyl-2-pentanone, similar to what was observed with C295A TeSADH. This may be because the mutation enlarges the small pocket, which then allows the preference towards α-branching in the small pocket to take over. Also, 3,3-dimethyl-2-butanone reacts better with M151A TeSADH and gives the opposite product from wild type, while this substrate fails to react with T153A.

Table 5.1. Asymmetric Reduction of WT, and M151A TeSADH[a]

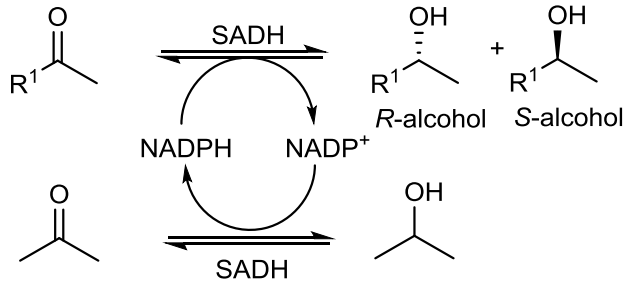

R[1]	M151A TeSADH		
	Conv.[b]	$E=(A_S)/(A_R)$ [b]	Major Product [b]
$CH_3(CH_2)_3$	1.7 (24)	2.8 (23)	*S* (*S*)
$CH_3(CH_2)_4$	1.9 (25)	6.6 (200)	*S* (*S*)
$CH_3(CH_2)_5$	0.95 (12)	3.4 (67)	*S* (*S*)
$CH_3(CH_3)CHCH_2$	2.2 (2.9)	0.11 (13)	*R* (*S*)
$CH_3O_2CCH_2$	6.9 (15)	1.9 (2.9)	*S* (*S*)
$CH_3(CH_3)CH$	72 (78)	0.05 (0.54)	*R* (*R*)
$(CH_3)_3C$	7.8 (0.78)	0.05 (1.5)	*R* (*S*)
$CH_3CH_2O_2CCH_2$	1.9 (5.9)	56 (109)	*S* (*S*)
C_6H_5	0 (0)	0.78 (-)	*R* (-)

[a]WT SADH values within parentheses. [b]Calculated through GC

Table 5.2. Asymmetric Reduction of WT, and T153A TeSADH[a]

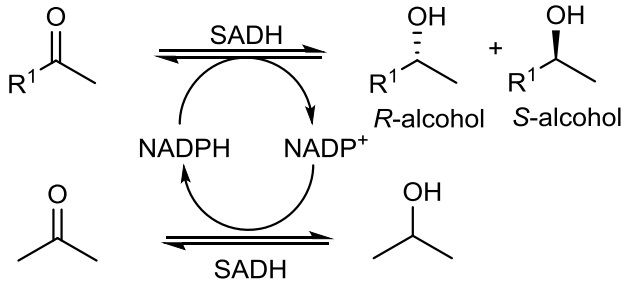

R[1]	T153A TeSADH		
	Conv.[b]	$E=(A_S)/(A_R)$ [b]	Major Product [b]
$CH_3(CH_2)_3$	1.3 (24)	26 (23)	*S* (*S*)
$CH_3(CH_2)_4$	3.5 (25)	53 (200)	*S* (*S*)
$CH_3(CH_2)_5$	1.1 (12)	4.5 (67)	*S* (*S*)
$CH_3(CH_3)CHCH_2$	2.1 (2.9)	14 (13)	*S* (*S*)
$CH_3O_2CCH_2$	3.1 (15)	1.2 (2.9)	*S* (*S*)
$CH_3(CH_3)CH$	86 (78)	0.39 (0.54)	*R* (*R*)
$(CH_3)_3C$	0 (0.78)	- (1.5)	- (*S*)
$CH_3CH_2O_2CCH_2$	1.8 (5.9)	71 (109)	*S* (*S*)

C_6H_5	(0)	0.16 (-)	*R* (-)

[a]WT SADH values within parentheses. [b]Calculated through GC

Next, we performed kinetics experiments to determine the kinetic parameters for wild type TeSADH and the two mutants. In the course of these studies, we found that M151A behaved strangely with the acetone substrate. Due to little change in the initial slope with varying substrate concentration, the M151A acetone assay was ran for longer than the usual ten minutes. **Figure 5.2** shows the initial thirty minutes of the assay, which shows a lag before reaching the maximum rate with acetone and M151A TeSADH, which is not seen with wild-type TeSADH. Upon closer inspection of Met-151 in **Figure 5.1**, it is seen that the Met-151 sits next to the Zn^{2+} in the TeSADH active site. It is possible that the mutation of Met-151 to Ala weakens binding of the Zn^{2+}, which then would inactivate TeSADH. **Figure 5.3** shows a proposed model for the observed kinetics with a slow activation of the enzyme and a fast addition of the substrate. From **Figure 5.2**, the lag was approximated graphically (**Table 5.3**) by the intersection of the initial linear portion and the linear regression of the steady-state rate for each of the concentrations. The estimated lag time generally increases with increasing concentration of ketone substrate, possibly due to binding to the apoenzyme and preventing Zn^{2+} binding. However for the asymmetric reductions shown in **Table 5.1 and 5.2**, the reaction takes place for 24 hours, which means that a small amount of lag will have minimal impact on the results. Due to this complication with the simplest substrate, measurement of kinetic parameters for M151A TeSADH with substrates was not performed.

The ligands that bind to the Zn^{2+} have been studied previously by Burdette and researchers.[10] Any mutations to Asp-150, Cys-37 and His-59 caused the inactivation of

the enzyme. The three zinc ligands are within 2.0-2.6 Å, which is about half the distance of the Met-151 sulfur from the metal ion (4.0 Å). Actually, the Met-151 methyl group is 3.3 Å away from the Asp-150 oxygen bound to the zinc cation. As **Figure 5.4** shows, there are van der Waals interactions between the Met-151 and Asp-150. By mutating the Met-151 into an alanine, the lack of the van der Waals forces between Met-151 and Asp-150 might cause a loosening of the zinc cation.

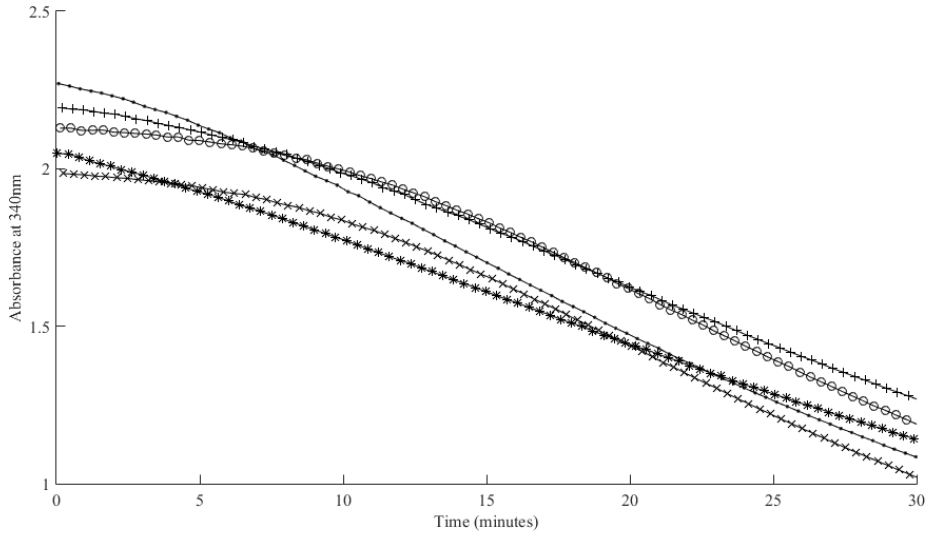

Figure 5.2. Reaction progression of M151A with Acetone. Figure legend: 2mM Acetone (*), 4mM Acetone (•), 8mM Acetone (○), 16mM Acetone (+), 32mM Acetone (x).

Table 5.3. Estimated lag time for M151A - Acetone kinetic assay

Concentration	Estimated Lag time (minutes)
2mM Acetone	6.4
4mM Acetone	7.1
8mM Acetone	10.1
16mM Acetone	7.9
32mM Acetone	10.3

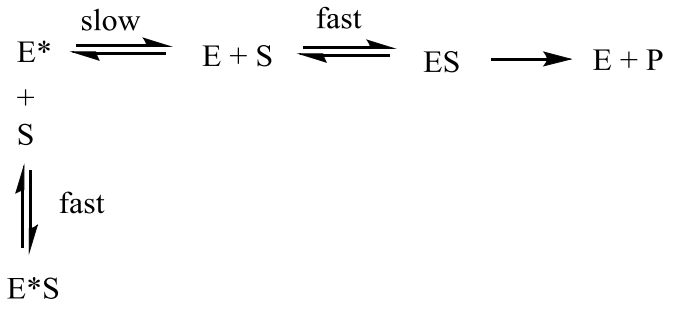

Figure 5.3. Proposed model for M151A and Acetone. E* refers to inactive form.

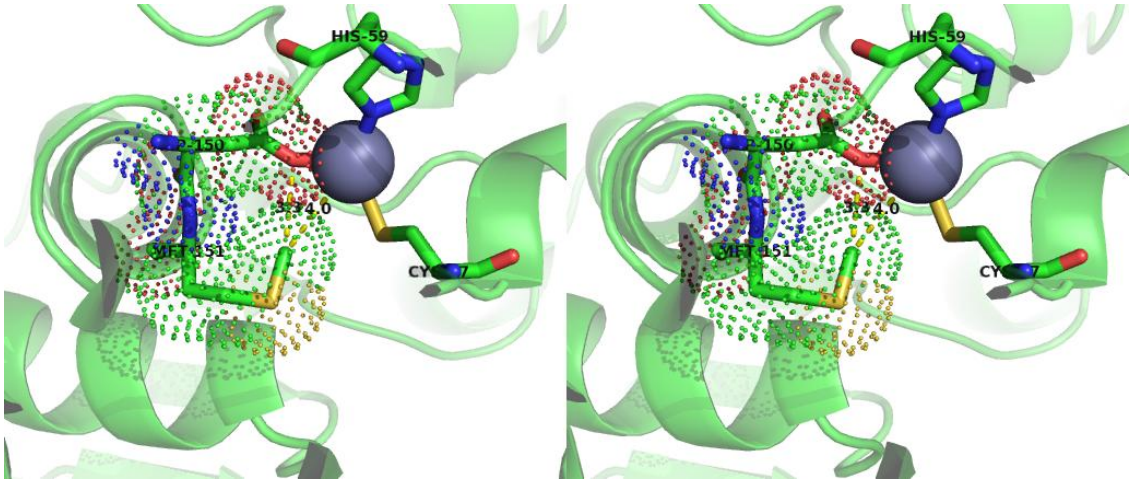

Figure 5.4. Cross-eyed stereoview of the TeSADH active site with van der Waals interactions between Met-151 and Asp-150 shown with dots. Residues of interest are in stick form, and Zn^{2+} shown as a grey sphere. This image was prepared with PyMOL[7] (The PyMOL Molecular Graphics System, Version 1.3 Schrödinger, LLC) using the PDB file (1YKF).

Wild type and T153A TeSADH behaved more normally, and kinetic parameters were obtained. **Table 5.4 and 5.5** summarizes the kinetic parameters for wild-type and T153A TeSADH. For acetone, wild type TeSADH has a factor of ten increase over T153A in k_{cat}/K_m. With methyl acetoacetate and ethyl acetoacetate, wild type TeSADH was 17- and 226-fold higher, respectively, than T153A. 3-Methyl-2-butanone actually showed a

slightly higher k_{cat}/K_m for T153A than wild-type TeSADH. Not surprisingly, for acetophenone and 3,3-dimethyl-2-butanone, the wild-type active site can barely accommodate each of the substrates. The k_{cat}/K_m for each was very low with wild type TeSADH. Acetophenone and 3,3-dimethyl-2-butanone showed no measurable activity with T153A.

Table 5.4. Kinetic Analysis of WT SADH

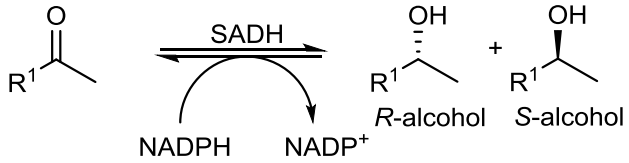

R^1	Wild Type		
	K_m (mM)	k_{cat} (s^{-1})	k_{cat}/K_m ($M^{-1}s^{-1}$)
CH_3	0.43±0.16	4.4±0.3	10000±3200
$CH_3(CH_3)CHCH_2$	1.9±0.5	1.19±0.11	620±120
$CH_3O_2CCH_2$	3.9±1.5	6.51±0.86	1600±450
$CH_3CH_2O_2CCH_2$	0.41±0.19	2.43±0.29	5900±2200
$CH_3(CH_3)CH$	1.6±0.5	1.57±0.22	970±190
$CH_3(CH_2)_3$	3.9±0.9	0.48±0.05	120±17
$CH_3(CH_2)_4$	1.3±0.3	0.82±0.09	660±120
$CH_3(CH_2)_5$	1.20±0.4	0.28±0.04	240±55
$(CH_3)_3C$	0.44±0.27	0.004±0.001	8±4
C_6H_5	0.22±0.11	0.005±0.001	24±10

Table 5.5. Kinetic Analysis of T153A SADH

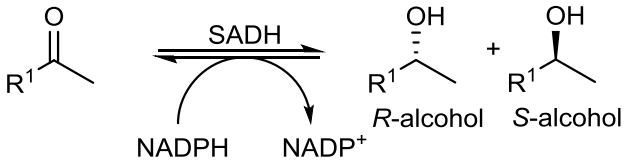

R^1	T153A		
	K_m (mM)	k_{cat} (s^{-1})	k_{cat}/K_m ($M^{-1}s^{-1}$)
CH_3	0.25±0.13	0.27±0.04	1100±450
$CH_3(CH_3)CHCH_2$	3.9±1.4	0.11±0.02	280±5

$CH_3O_2CCH_2$	12±4.2	1.2±0.2	92±13
$CH_3CH_2O_2CCH_2$	5.2±1.6	0.12±0.01	23±5
$CH_3(CH_3)CH$	0.43±0.14	0.52±0.05	1200±300
$CH_3(CH_2)_3$	2.1±1.3	0.11±0.03	51±23
$CH_3(CH_2)_4$	2.5±1.1	0.04±0.01	15±5
$CH_3(CH_2)_5$	0.33±0.22	0.012±0.002	36±20
$(CH_3)_3C$	NR	NR	NR
C_6H_5	NR	NR	NR

The carbonyl reductase from *Sporobolomyces salmonicolor* (SSCR) has an active site that accommodates para-substituted acetophenones. By incorporating a mutation at Gln-245, not only did the specific activity and ee increase, but the stereospecificity reversed as well (*R* to *S*).[11] Expanding on this aforementioned mutant, Li and researchers combined a mutation at the Met-242 residue with the Gln-245 mutants. The stereospecificity was still reversed to *S*, and the ee increased as well with para-substituted acetophenones for two double mutants, M242L/Q245P and M242L/Q245T.[12] Zhang and coworkers found protein engineering at residues Pro-170 and Leu-174 could improve SSCR activity towards β-amino ketones.[9] The combination of mutations at each of those sites, P170R/L174Y gave even a reversal of stereochemistry (*S* to *R*) for the aryl ketone. The 2-thienyl derivative saw a reversal (*R* to *S*) for both the L174W and the P170R/L174W, and surprisingly, little difference between the two mutants.[13] A carbonyl reductase (CPCR2) from *Candida parapsilosis* was reengineered by Jakoblinnert and coworkers to have increased cyclohexanone reactivity by the mutation of the leucine at the 119 position into a methionine.[14] Using the previously published crystal structure for *Candida tenuis* xylose reductase (CtXR)[15], Nidetzky and coworkers found that mutation at the Trp-23 residue altered the substrate specificity for various aryl ketones, though some of the substrates reacted better than wild-type and others reacted poorer.[16] The

reaction of Trp-23 mutants with alpha-keto esters however, improved substantially over wild type.[17] The mutant W23F gave the best results against the alpha-keto esters tested.

In conclusion, these studies were carried out to determine if Met-151 and/or Thr-153 are good targets to expand the active site of wild type TeSADH. However, the results suggest that these residues are not good targets, since the M151A and T153A mutant TeSADHs have low activity and/or abnormal catalytic properties. Also, the methionine-151 residue being adjacent to the Zn^{2+} could be the reason why the kinetic assays were troublesome. In future directions, additional mutations will be studied in order to expand the active site further. Due to the success of the previously studied residues I86A and C295A, considering other neighbors of these two residues could lead to mutations with a larger small pocket. Ala-85, Thr-154, Tyr-267, and Leu-294 are a few possible mutants to consider for expanding the active site.

Experimental Section

General Methods: The gas chromatography experiments were performed on a Varian 3300 GC (Agilent Tech; Santa Clara, CA) using Helium as the carrier gas and equipped with a Supelco (Sigma Aldrich; St. Louis, MO) *β*-Dex 120 cyclodextrin chiral column (30 nm, 0.25mm [i.d.], 0.25 μm film thickness) and with a flame ionization detector. The kinetic experiments and assays were ran on a Varian Carey 100 UV-visible spectrophotometer (Agilent Tech; Santa Clara, CA) equipped with a Peltier thermoelectric temperature-controlled 12-cell holder.

Materials: Acetophenone and acetone were both from Fisher Scientific (Waltham, MA). Acetonitrile was purchased from Burdick and Jackson (Morristown, NJ). The rest of the

substrates were purchased from Sigma Aldrich (St. Louis, MO). The kanamycin was bought from Roche (Indianapolis, IN), and the ampicillin was from Fisher Biotech (Fair Lawn, NJ). Commercial grade solvents used were used without further purification.

Mutagenesis: The wild type plasmid was designed as reported previously.[18] An improvement on the Quikchange site-directed mutagenesis procedure was used to introduce the partially overlapping primers into the pADHB25 plasmid.[19] Initially, fully overlapping primers were tried with site-directed mutagenesis with the Quikchange method. Since fully overlapping primers only use the wild type plasmid as the template for the mutagenesis, it was found that the concentration of the mutated plasmid was too low for the transformation. In an effort to improve the mutagenesis, an improvement on Quikchange was used for the site-directed mutagenesis with partially overlapping primers.[19] By using partially overlapping primers, the mutagenesis became more like a PCR, since not only would each wild type plasmid function as a template, but also each mutated plasmid as well. The transformation gave little trouble for each of the mutants by using the improved Quikchange method.

The partially overlapping primers were as follows: M151A-f (GATTCCCGAT**GCG**ATGACCACTGGTTTTCACGGAGCTGAACTG), M151A-r (GGTCAT**CGC**ATCGGGAATCATAACTGCAGCTTCCAATGG), T153A-f (CCCGATATGATG**GCC**ACTGGTTTTCACGGAGCTGAACTGGC), and T153A-r (CCAGT**GGC**CATCATATCGGGAATCATAACTGCAGCTTCC).

Purification for Secondary Alcohol Dehydrogenase (M151A, T153A and WT): Cell debris was removed after sonication at 4,000 rpm (3082Xg) for 90 min. The heat treatment was applied on the supernatant for 10 min at 65 ^{o}C. The post heat-treatment

centrifugation was done at 4,000 rpm (3082Xg) for 90 min. No ammonium sulfate was used. Rather, the supernatant was loaded on a single Red A agarose column using a BioLogic LP pump with Model 2110 fraction collector. Once the TeSADH was on the red agarose column, the impurities were removed by washing with Tris-HCl buffer (pH 8.0, 5 mM DTT, 10 µM $ZnCl_2$) and then the Tris-HCl buffer with $NaClO_4$ (0.2 M $NaClO_4$, pH 8.0, 5 mM DTT, 10 µM $ZnCl_2$) eluted the enzyme off the column. A polyacrylamide gel of the pooled fractions showed a single band. The fractions were stored at -80 ^oC.

Enzyme Assays: The enzyme activity was analyzed in 50 mM Tris-HCl buffer (pH 8.0 at 50 ^oC) with 0.4 mM $NADP^+$ (alcohol oxidation) or 50mM potassium phosphate buffer (pH 6.5 at 50 ^oC) with 0.4 mM NADPH (ketone reduction) in triplicate. The initial velocity was recorded on a Varian Cary 100 UV/Vis spectrophotometer at 340 nm for 10 min by monitoring NADPH consumption (ketone reduction) or NADPH generation (alcohol oxidation). Preincubation of the assay samples was in the appropriate 50 mM buffer solution and the enzyme sample with 5 mM DTT and 10 µM $ZnCl_2$ added before allowing the samples to warm up to 50 ^oC in the UV/Vis sample compartment for 10 min. Since it was found that high acetonitrile concentration reduced activity, the concentration didn't exceed 5% for the enzyme assays.

Asymmetric Reductions: Reactions were performed on a 1 mL scale. Substrate (0.21 mmol), 1 mg NADPH, 0.5 mL Tris-HCl buffer (pH 8.0 with 10 µM $ZnCl_2$), 0.2 mL 2-propanol, 1 mg DTT and M151A, T153A or wild-type TeSADH (0.327 mg). The reactions were kept at 24 hr at 50 ^oC with shaking. After completion of 24 hr, the addition of dichloromethane quenched the reactions. This organic extract could be used

to quantify the percent conversions. Acetylation with acetic anhydride and pyridine was performed as described, in order to aid in measuring of the enantiomeric excess of the products.[20]

M151A - Acetone Assays and Analysis: The assays were prepared the same way as the above enzyme assays and then allowed to run for one hour in the Cary 100 UV-Vis spectrophotometer. The data was plotted in MATLAB[21], and fit to the equation (1).

References

[1] Prelog, V. *Pure Appl. Chem*. **1964**, *9*, 119-130.

[2] Tripp, A. E.; Burdette, D. S.; Zeikus, J. G.; Phillips, R. S. *J. Am. Chem. Soc*. **1998**, *120*, 5137-5141.

[3] Heiss, C.; Laivenieks, M.; Zeikus, J. G.; Phillips, R. S. *Bioorgan. Med. Chem.* **2001**, *9*, 1659-1666.

[4] Musa, M. M.; Ziegelmann-Fjeld, K. I.; Vieille, C.; Zeikus, J. G.; Phillips, R. S. *J. Org. Chem.* **2007**, *72*, 30-34.

[5] Musa, M. M.; Lott, N.; Laivenieks, M.; Watanabe, L.; Vieille, C.; Phillips, R. S. *ChemCatChem* **2009**, *1*, 89-93.

[6] Nealon Dissertation Chapter 2.

[7] The PyMOL Molecular Graphics System, Version 1.3 Schrödinger, LLC.

[8] Keinan, E.; Hafeli, F. V.; Seth, K. K.; Lamed, R. *J. Am. Chem. Soc.* **1986**, *108*, 162-169.

[9] Hiromi, K. *Kinetics of Fast Enzyme Reactions*; John Wiley and Sons: New York, 1979; p 223.

[10] Burdette, D. S.; Secundo, F.; Phillips, R. S.; Dong, J.; Scott, R. A.; Zeikus, J. G. *Biochem. J.* **1997**, *326*, 717-724.

[11] Zhu, D.; Yang, Y.; Majkowicz, S.; Pan, T. H.; Kantardjieff, K.; Hua, L. *Org. Lett.* **2008**, *10*, 525−528.

[12] Li, H.; Yang, Y.; Zhu, D.; Hua, L.; Kantardjieff, K. *J. Org. Chem*. **2010**, *75*, 7559−7564.

[13] Zhang, D.; Chen, X.; Chi, J.; Feng, J.; Wu, Q.; Zhu, D. *ACS Cat.* **2015**, *5*, 2452-2457.

[14] Jakoblinnert, A.; Wachtmeister, J.; Schukur, L.; Shivange, A. V.; Bocola, M.; Ansorge-Schumacher, M. B.; Schwaneberg, U. *Protein Eng., Des. Sel.* **2013**, *26*, 291−298.

[15] Kavanagh, K. L.; Klimacek, M.; Nidetzky, B.; Wilson, D. K. *Biochemistry* **2002**, *41*, 8785−8795.

[16] Kratzer, R.; Leitgeb, S.; Wilson, D. K.; Nidetzky, B. *Biochem. J*. **2006**, *393*, 51−58.

[17] Kratzer, R.; Nidetzky, B. *Chem. Commun*. **2007**, 1047−1049.

[18] Burdette, D. S.; Vieille, C.; Zeikus, J. G. *Biochem. J.* **1996**, *316*, 115-122.

[19] Liu, H.; Naismith, J. H. *BMC Biotechnol.* **2008**, *8*, 91.

[20] Ghanem, A.; Schuring, V. *Tetrahedron: Asymmetry* **2003**, *14*, 57-62.

[21] Mathworks, 2014 (MATLAB Version R2014b).

CHAPTER 6

CONCLUSION

The aim of this research has been to learn more about the active site of *Thermoanaerobacter ethanolicus* SADH, which has been accomplished. Wild type SADH has good reactivity with straight chain ketones and small substrates with branching on the R-group, due to the small pocket's affinity towards α-branched alkyl groups. However, if the R-group is an aromatic ring, the activity plummets considerably and gives barely quantifiable yield. The lack of activity of acetophenone with wild type SADH inspired the I86A work that led us to the I86A/C295A asymmetric reduction study. It had been found that a phenyl ring could fit into the small pocket of the active of I86A SADH. With the additional C295A mutation, the active site allowed even larger substrates, however with substitution only in the *meta*-position. Due to the locations of the mutations in the active site of SADH, it was initially believed that the area opened up in the active site would be around the *para*-position. This could be from a conformational change since the resident amino acids may form interactions with their neighbors that the mutation cannot replicate. In the future, a crystal structure of these mutants and other mutants would help demonstrate what happens within the active site upon site-directed mutagenesis. This would be invaluable for leading the investigators to substrates that might not have been previously considered. Also, due to the stability of the I86A/C295A SADH mutant, a logical step would be to design triple and even quadruple mutants that would open up the door to a even larger "small" pocket.

With the orientation of the substrate in the active site, typically one of two isomeric alcohols would be produced because it is unlikely that the substrate would bind to the small and large pocket equally. This means that for the enzyme reactions, the product would be either the *R* or the *S*-isomer. Ketone reduction provides one of these isomers. Kinetic resolution of racemates provides a means to generate the alcohol that would not normally be formed. While kinetic resolution had been studied with the W110A SADH mutant, this type of study had not been attempted previously with the I86A and I86A/C295A system. The kinetic resolution project allowed a route to make the *S*-isomers, with the only concern being the amount of conversion of the reaction. If the reaction reached 50% conversion, then the reaction solution would be composed of the ketone and the unreacted *S*-alcohol. Presumably, the kinetic resolution wouldn't work as well when the substrate has difficulty fitting inside the active site. It would be interesting to study a mutant that expands the active site further and compare the kinetic resolution data for that mutant with the mutants of this study. By enlarging the small pocket, some of the substrates may fit inside the active site better, although as was found with the overall study, by opening the active site further and accommodating more substrates, the substrate would not bind as tightly.

In an interest of finding new mutations worth pursuing, the M151A and T153A mutations were designed and tested against wild type SADH, in hopes of active site expansion. The Met-151 neighbored the Zn within the active site, creating trouble for the kinetic studies. Even though the asymmetric reduction reactions proceeded well for each of these two mutants, the mutants appeared to not be very good mutations on their own, since wild type SADH gave fairly solid results. While these two mutants didn't proceed

too well, there are other residues that may improve activity considerably. The same procedures of testing the wild type, M151A and T153A mutants could readily be applied towards a new mutant.

APPENDIX A

CHAPTER 3 SUPPORTING INFORMATION

TABLE OF CONTENTS

Page

S3.1. Asymmetric Reduction Chromatographic Data After Acetylation

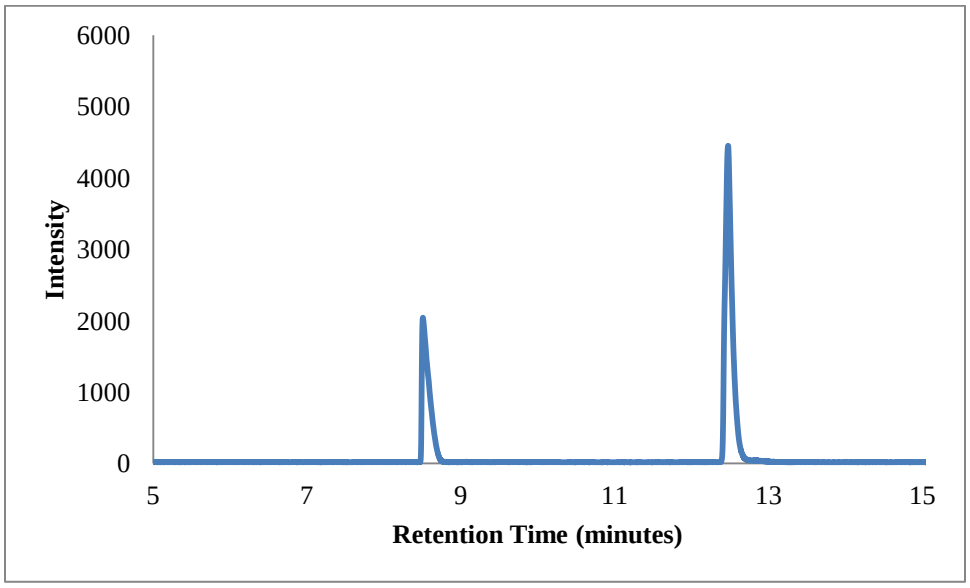

Figure S3.1: AR of acetophenone with I86A/C295A. Retention time (area): 8.5025 (220.73), 12.4675 (471.28)

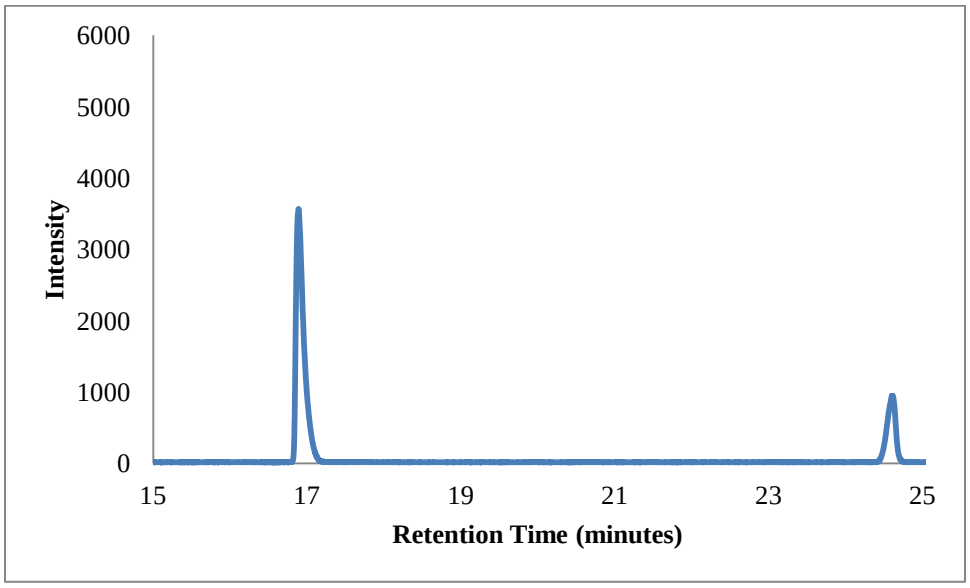

Figure S3.2: AR of 3'-Chloroacetophenone with I86A/C295A. Retention time (area): 16.8842 (428.59), 24.6083 (125.82)

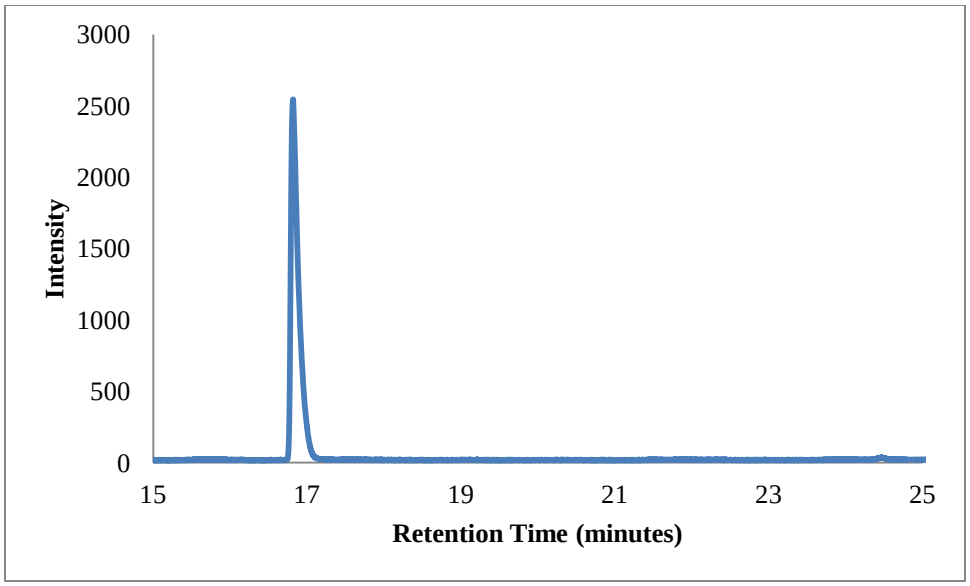

Figure S3.3: AR of 3'-Chloroacetophenone with I86A. Retention time (area): 16.8117 (297.97), 24.4492 (1.87)

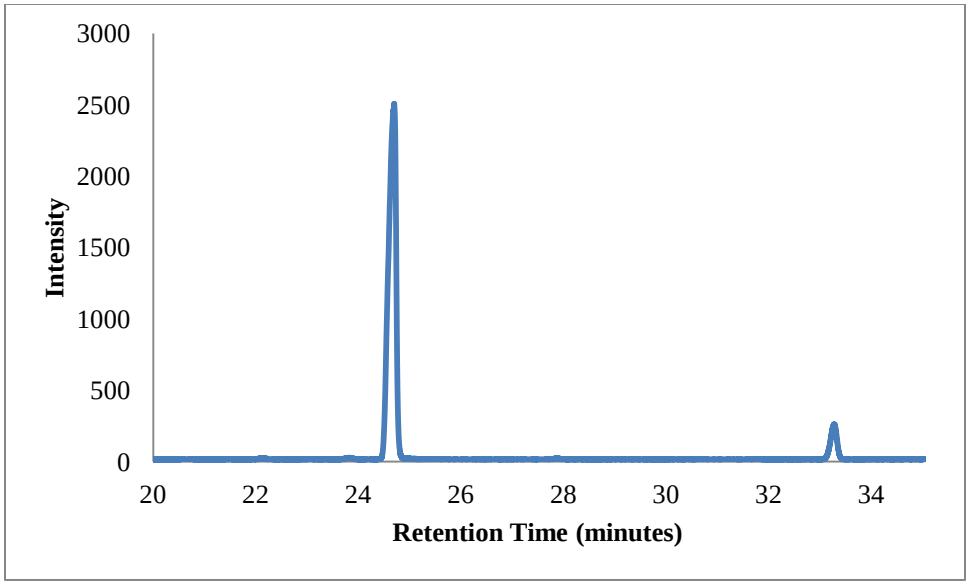

Figure S3.4: AR of 3'-bromoacetophenone with I86A/C295A. Retention time (area): 24.69 (424.14), 33.2675 (39.02)

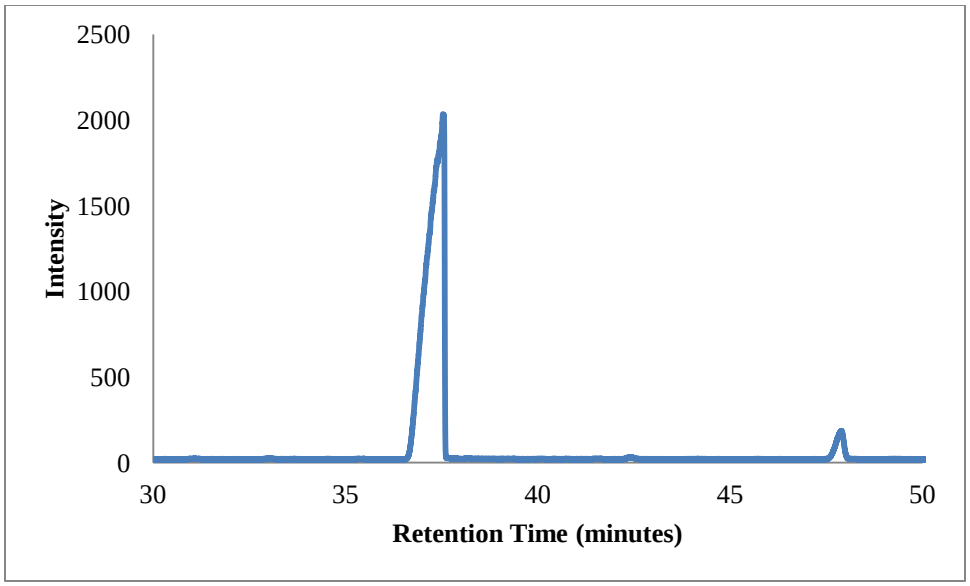

Figure S3.5: AR of 3'-iodoacetophenone with I86A/C295A. Retention time (area): 37.5342 (1031.82), 47.9083 (39.67)

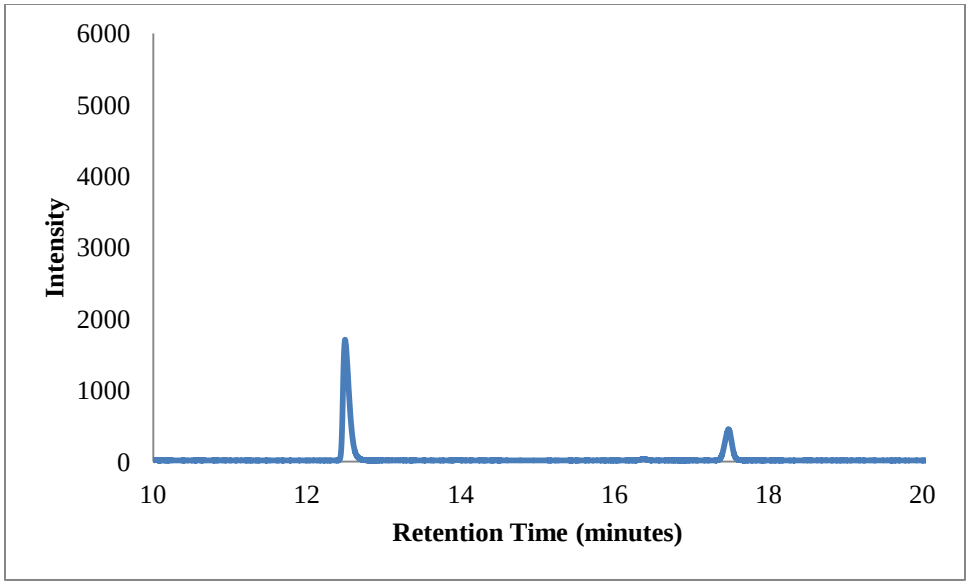

Figure S3.6: AR of 3'-methylacetophenone with I86A/C295A. Retention time (area): 12.4867 (160.89), 17.4683 (47.11)

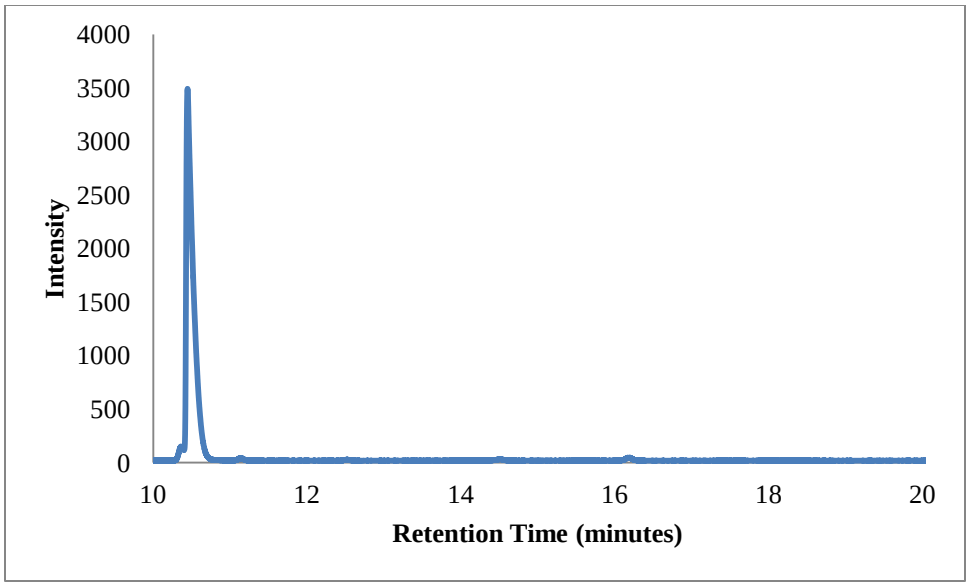

Figure S3.7: AR of 2'-methylacetophenone with I86A/C295A. Retention time (area): 10.4392 (363.32), 16.1583 (3.14)

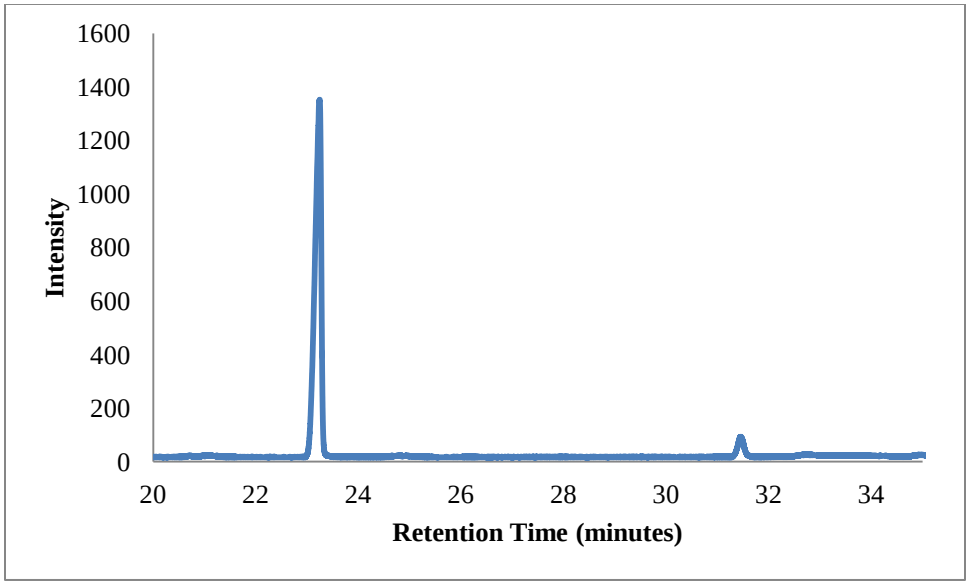

Figure S3.8: AR of 3'-methoxyacetophenone with I86A/C295A. Retention time (area): 23.2375 (190.17), 31.4367 (10.93)

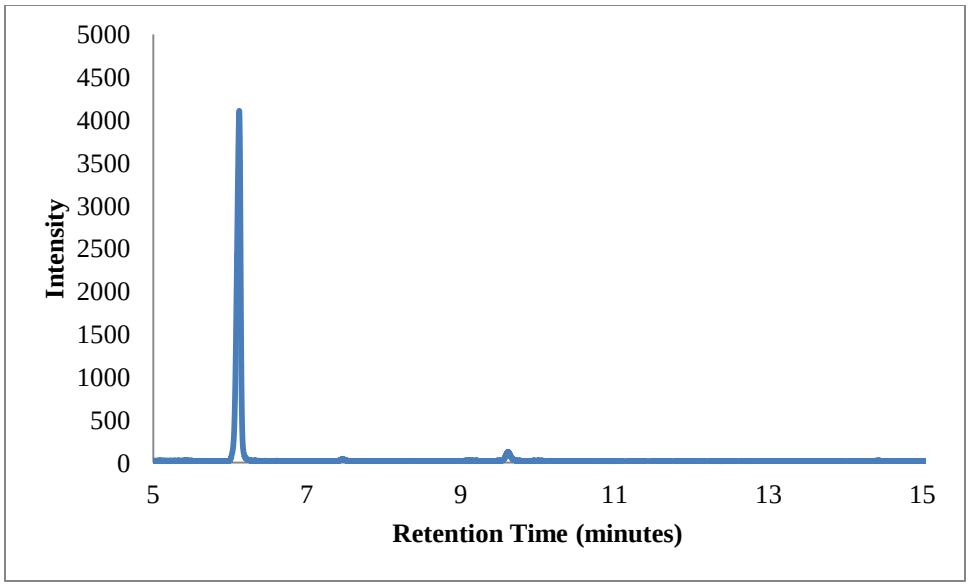

Figure S3.9: AR of 3'-trifluoromethylacetophenone with I86A/C295A. Retention time (area): 6.115 (240.38), 9.6042 (8.57)

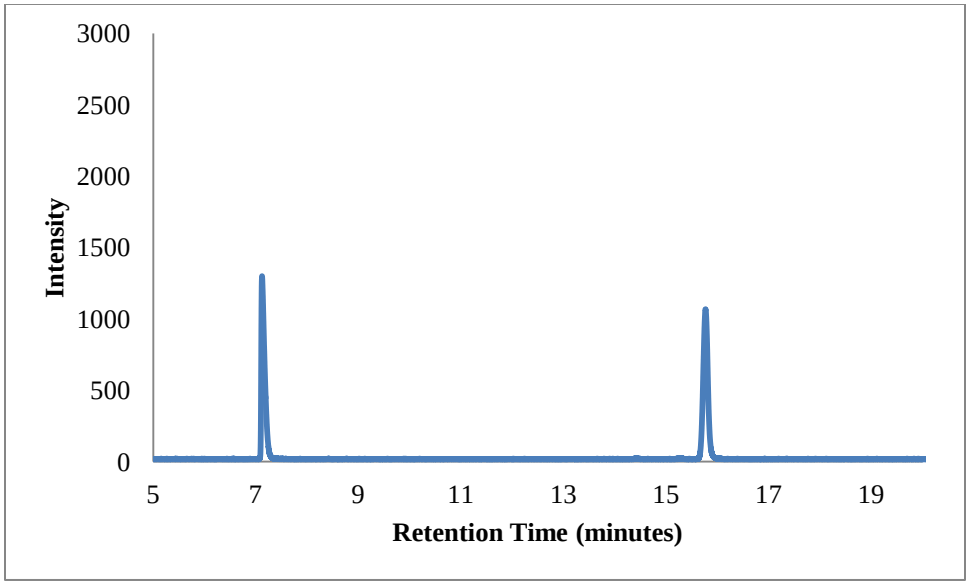

Figure S3.10: AR of 2-acetylpyridine with I86A/C295A. Retention time (area): 7.1217 (98.49), 15.7633 (112.09)

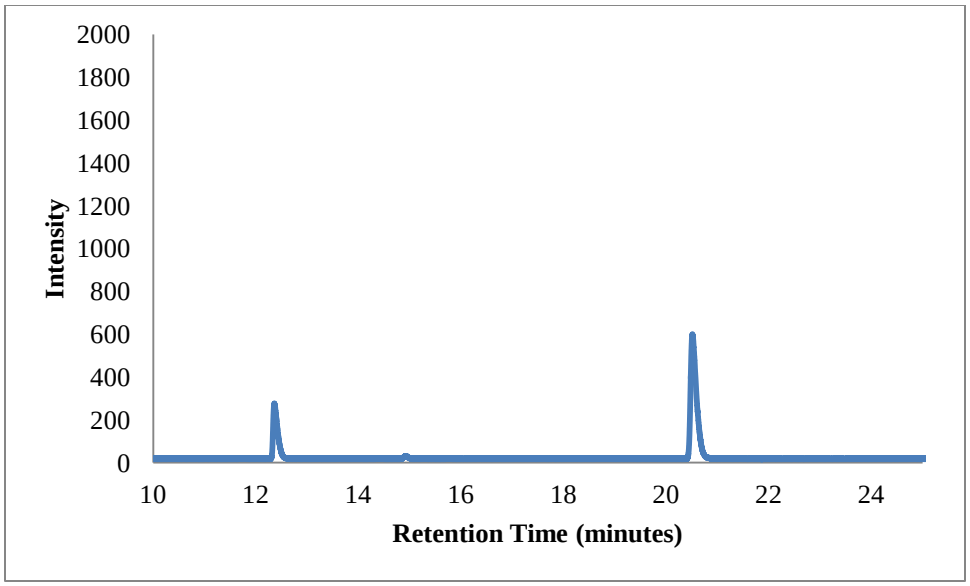

Figure S3.11: AR of 3-acetylpyridine with I86A/C295A. Retention time (area): 12.3542 (26.74), 20.5067 (78.64)

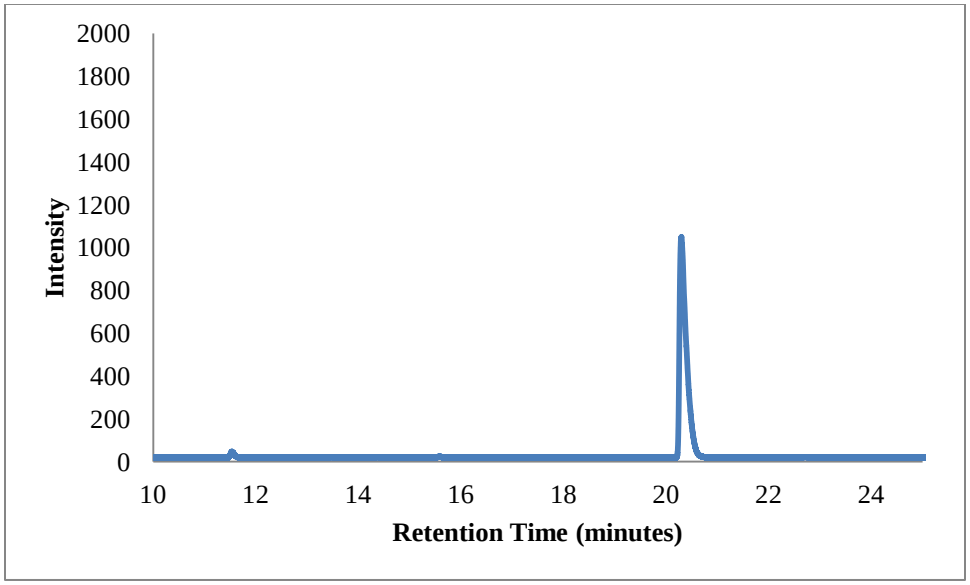

Figure S3.12: AR of 4-acetylpyridine with I86A/C295A. Retention time (area): 11.525 (2.96), 20.2892 (159.99)

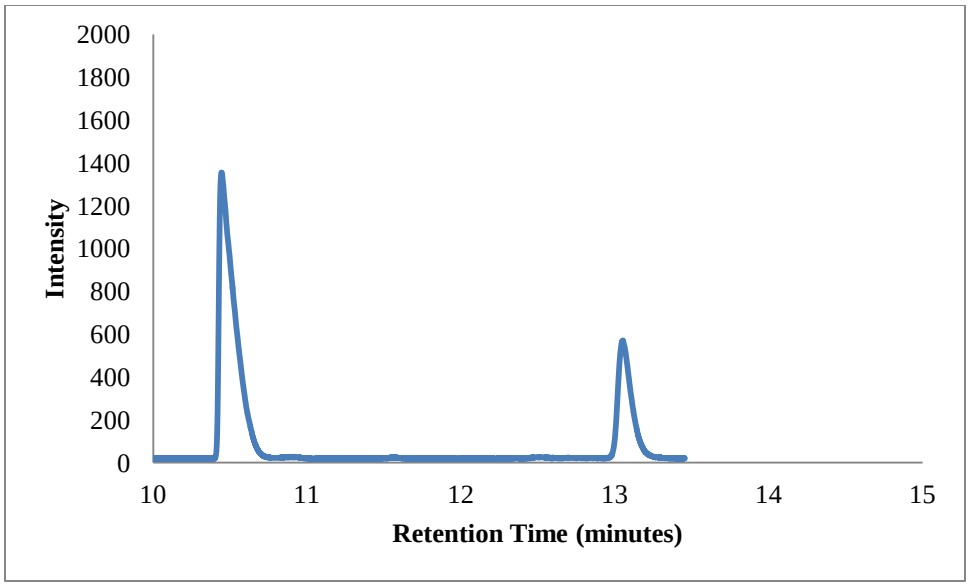

Figure S3.13: AR of 2-acetylthiophene with I86A/C295A. Retention time (area): 10.4417 (157.76), 13.0483 (57.09)

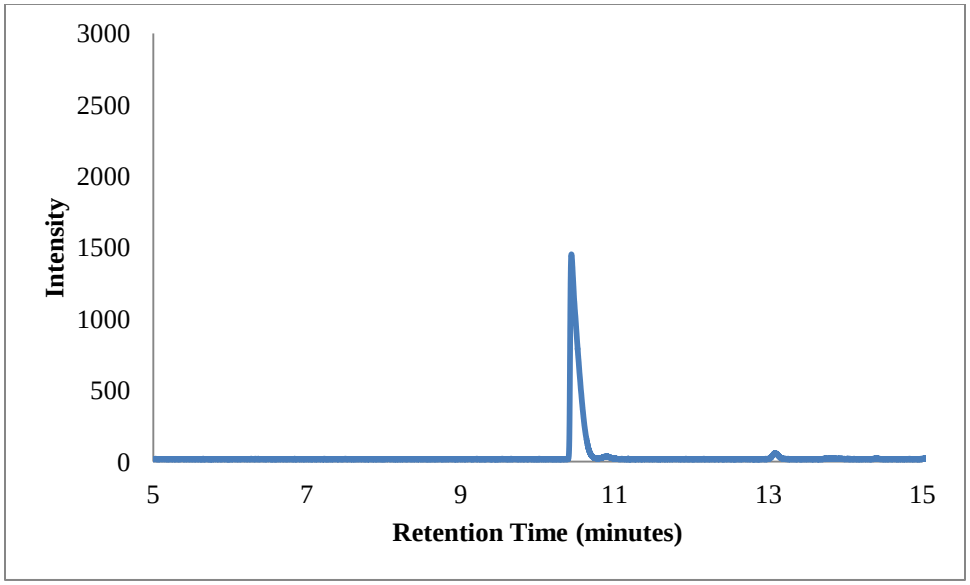

Figure S3.14: AR of 2-acetylthiophene with I86A. Retention time (area): 10.4317 (168.47), 13.0708 (4.36)

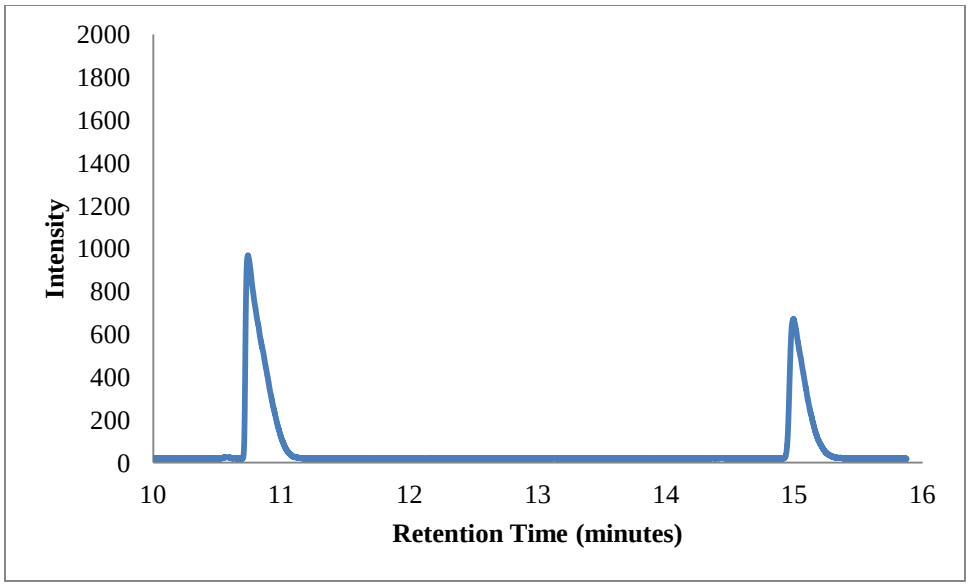

Figure S3.15: AR of 3-acetylthiophene with I86A/C295A. Retention time (area): 10.7342 (147.50), 14.9883 (92.84)

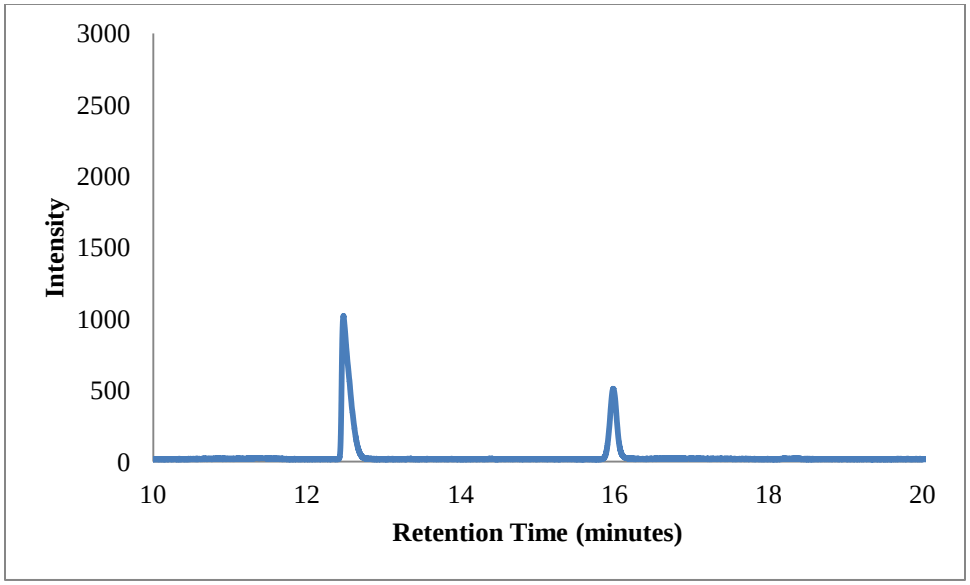

Figure S3.16: AR of propiophenone with I86A/C295A. Retention time (area): 12.4658 (118.79), 15.97 (53.64)

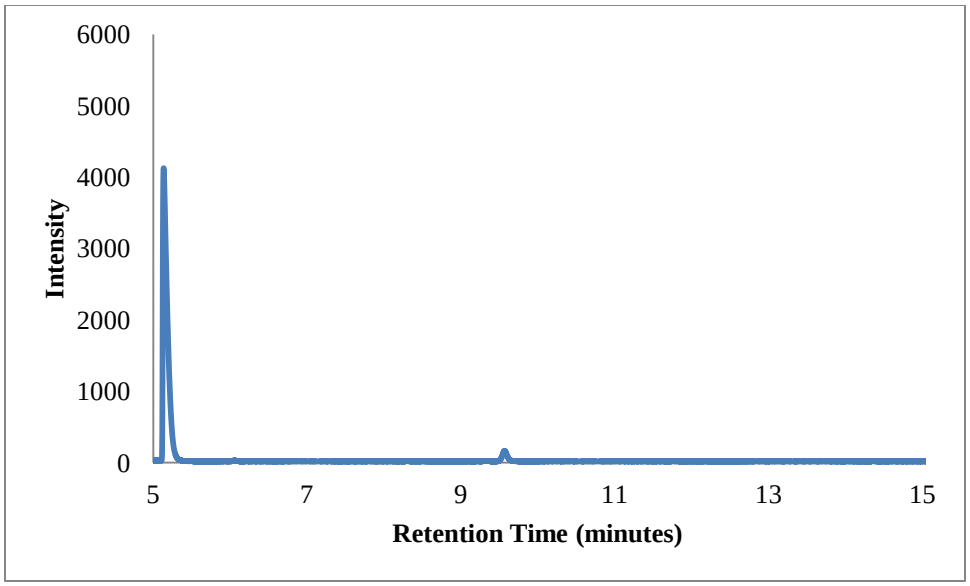

Figure S3.17: AR of 2',4'-difluoroacetophenone with I86A/C295A. Retention time (area): 5.1342 (282.34), 9.5642 (11.83)

S3.2. I86A/C295A Hammett-Taft Plot

Table S3.1: I86A/C295A Hammett-Taft Plot Data [1,2,3]

	σ	E_S	$\log(k/k_o)$	$\log(k/k_o)$ error	$\log((k/K_M)/(k/K_M)_o)$	$\log((k/K_M)/(k/K_M)_o)$ error
Acetophenone	0	0	0	0	0	0
3'-Chloro	0.37	-0.97	-0.109	0.195	-0.165	0.198
3'-Bromo	0.39	-1.16	-0.386	0.174	-0.466	0.181
3'-Iodo	0.35	-1.4	-1.413	0.124	-1.075	0.195
3'-Methyl	-0.07	-1.24	-0.898	0.171	-1.023	0.171
3'-Methoxy	0.12	-0.55	-2.3	0.241	-0.949	0.197
3'-Trifluoromethyl	0.43	-2.4	-2.59	0.199	-1.88	0.385
2',4'-Difluoro	0.35	-0.92	-0.736	0.233	-0.917	0.255
2'-Methyl	0.003	-1.24	-1.94	0.217	-2.02	0.179

S3.3. Kinetic Assay Raw Data

Table S3.2: Acetone with I86A/C295A

Conc. of Substrate	Run 1 Slope	Run 2 Slope	Run 3 Slope
1mM	0.0083	-	-

2mM	0.0295	0.0235	0.0306
4mM	0.0547	0.05	0.0701
8mM	0.1026	0.1483	0.1330
16mM	0.1786	0.2364	0.2426
32mM	-	0.3047	0.3103

Table S3.3: Acetone with I86A

Conc. of Substrate	Run 1 Slope	Run 2 Slope
0.15mM	0.0165	0.0335
0.3mM	0.0634	0.0722
0.6mM	0.0765	0.0540
1.2mM	0.1237	0.1235
2.4mM	0.1157	0.1618

Table S3.4: Acetophenone with I86A/C295A

Conc. of Substrate	Run 1 Slope	Run 2 Slope
1mM	0.0071	0.0095
2mM	0.0143	0.0164
4mM	0.0326	0.0378
8mM	0.0436	0.0469
16mM	0.0654	0.0589

Table S3.5: Acetophenone with I86A

Conc. of Substrate	Run 1 Slope
0.3mM	0.0397
0.6mM	0.0678
1.2mM	0.0697
2.4mM	0.0974
4.8mM	0.1050

Table S3.6: 3’-Chloroacetophenone with I86A/C295A

Conc. of Substrate	Run 1 Slope	Run 2 Slope	Run 3 Slope	Run 4 Slope
1mM	0.0039	0.0081	0.0052	0.0044
2mM	0.0049	0.0063	0.0074	0.0064

4mM	0.0130	0.0135	0.0176	0.0051
8mM	0.0118	0.0080	0.0192	0.0167
16mM	0.0217	0.0237	0.0223	0.0298

Table S3.7: 3'-Chloroacetophenone with I86A

Conc. of Substrate	Run 1 Slope	Run 2 Slope	Run 3 Slope
0.3mM	0.0059	0.0038	0.0013
0.6mM	0.0094	0.0097	0.0066
1.2mM	0.0170	0.0091	0.0105
2.4mM	0.0169	0.0156	0.0147
4.8mM	0.0177	0.0341	0.0194

Table S3.8: 3'-Bromoacetophenone with I86A/C295A

Conc. of Substrate	Run 1 Slope	Run 2 Slope	Run 3 Slope
1mM	0.0040	0.0042	0.0053
2mM	0.0051	0.0108	0.0100
4mM	0.0042	0.0137	0.0104
8mM	0.0152	0.0154	0.0197
16mM	0.0245	0.0235	0.0258

Table S3.9: 3'-Methylacetophenone with I86A/C295A

Conc. of Substrate	Run 1 Slope	Run 2 Slope	Run 3 Slope	Run 4 Slope
1mM	0.0030	0.0017	0.003	0.0041
2mM	0.0058	0.0042	0.0051	0.0059
4mM	0.0097	0.0103	0.0121	0.0132
8mM	0.0154	0.0109	0.0149	0.0128
16mM	0.0189	0.0179	0.0272	0.0237

Table S3.10: 3'-Iodoacetophenone with I86A/C295A

Conc. of Substrate	Run 1 Slope	Run 2 Slope
1mM	0.0239	0.0224
2mM	0.0310	0.0468
4mM	0.0621	0.0569
8mM	0.0695	0.0647

16mM	0.0814	0.1026

Table S3.11: 2'-Methylacetophenone with I86A/C295A

Conc. of Substrate	Run 1 Slope	Run 2 Slope	Run 3 Slope	Run 4 Slope	Run 5 Slope	Run 6 Slope
1mM	-	0.0041	0.0025	0.0058	0.0059	0.0005
2mM	0.0035	-	0.0011	0.0090	0.0045	0.0018
4mM	0.0124	0.0079	0.0042	0.0172	0.0150	0.0027
8mM	0.0158	0.0189	0.0086	0.0152	0.0147	0.0109
16mM	0.0210	-	0.0152	0.0178	-	0.0263

Table S3.12: 2-Acetylpyridine with I86A/C295A

Conc. of Substrate	Run 1 Slope	Run 2 Slope
1mM	0.0033	0.0036
2mM	0.0074	0.0074
4mM	0.0155	-
8mM	0.0192	0.0173
16mM	0.0268	0.0270

Table S3.13: 2-Acetylpyridine with I86A

Conc. of Substrate	Run 1 Slope	Run 2 Slope	Run 3 Slope
0.3mM	0.0025	0.0172	0.0284
0.6mM	0.0103	0.0531	0.0374
1.2mM	0.0208	0.0557	0.0944
2.4mM	0.1221	0.1170	0.1094
4.8mM	0.1612	0.1496	0.1430

Table S3.14: 3-Acetylpyridine with I86A/C295A

Conc. of Substrate	Run 1 Slope	Run 2 Slope	Run 3 Slope	Run 4 Slope	Run 5 Slope
1mM	0.0036	-	-	-	-
1.5mM	-	-	-	0.0128	0.0055
2mM	0.0121	0.0149	0.0202	-	-
3mM	-	-	-	0.0234	0.0361
4mM	0.0423	0.0339	0.0423	-	-
6mM	-	-	-	0.0978	0.0635

8mM	0.0764	0.0822	0.0930	-	-
12mM	-	-	-	0.0983	0.1292
16mM	0.1841	0.1709	0.1157	-	-
24mM	-	-	-	0.0566	0.1182
32mM	-	0.1314	0.0935	-	-

Table S3.15: 3-Acetylpyridine with I86A

Conc. of Substrate	Run 1 Slope	Run 2 Slope
0.3mM	0.0204	0.0103
0.6mM	0.0254	0.0012
1.2mM	0.0337	0.0879
2.4mM	0.1262	0.1595
4.8mM	0.1076	0.1130

Table S3.16: 4-Acetylpyridine with I86A/C295A

Conc. of Substrate	Run 1 Slope	Run 2 Slope
1mM	0.0354	0.0211
2mM	0.0941	0.0453
4mM	0.1034	0.0963
8mM	0.1536	0.1302
16mM	0.1747	-

Table S3.17: 4-Acetylpyridine with I86A

Conc. of Substrate	Run 1 Slope	Run 2 Slope
0.3mM	-	0.0497
0.6mM	-	0.0623
1mM	0.127	-
1.2mM	-	0.1363
2mM	0.1909	-
2.4mM	-	0.1699
4mM	0.2264	-
4.8mM	-	0.2199
8mM	0.2621	-
16mM	0.2755	-

Table S3.18: 2-Acetylthiophene with I86A/C295A

Conc. of Substrate	Run 1 Slope	Run 2 Slope
1mM	0.0052	0.0437
2mM	0.0371	0.0758
4mM	0.1347	0.1178
8mM	0.1772	0.1670
16mM	0.1683	0.2135

Table S3.19: 2-Acetylthiophene with I86A

Conc. of Substrate	Run 1 Slope	Run 2 Slope	Run 3 Slope	Run 4 Slope	Run 5 Slope	Run 6 Slope	Run 7 Slope	Run 8 Slope
0.3mM	0.0048	0.0046	0.0027	0.0050	0.0034	-	-	-
0.6mM	0.0101	0.0053	0.0056	0.0083	0.0087	0.0095	0.0131	0.0054
1.2mM	0.0174	0.0131	0.0069	0.0213	0.0175	0.0143	0.0441	0.0148
2.4mM	0.0260	0.0268	0.0255	0.0334	0.0264	0.0348	0.0417	0.0203
4.8mM	0.0399	0.0403	0.0373	0.0593	0.0547	0.0408	0.0751	0.0385
9.6mM	-	-	-	-	-	0.0369	0.0540	0.0443

Table S3.20: 3-Acetylthiophene with I86A/C295A

Conc. of Substrate	Run 1 Slope	Run 2 Slope	Run 3 Slope	Run 4 Slope	Run 5 Slope	Run 6 Slope	Run 7 Slope
1mM	0.0067	0.0196	0.0217	0.0037	0.0157	-	-
2mM	0.0185	0.0271	0.0513	0.0201	0.0214	0.0231	0.0359
4mM	0.1036	0.0568	0.0483	0.0759	0.0720	0.0639	0.0616
8mM	0.1157	0.0616	0.0884	0.0895	0.1355	0.1193	0.1249
16mM	0.3159	0.2045	0.1087	0.0188	0.2385	0.1396	0.1148
32mM	-	-	-	-	-	0.2505	0.1924

Table S3.21: 3-Acetylthiophene with I86A

Conc. of Substrate	Run 1 Slope	Run 2 Slope
0.3mM	0.0130	0.0169
0.6mM	0.0193	0.0051
1.2mM	0.0507	0.0460

2.4mM	0.0680	0.1389
4.8mM	0.1125	0.1106

Table S3.22: Propiophenone with I86A/C295A

Conc. of Substrate	Run 1 Slope	Run 2 Slope	Run 3 Slope	Run 4 Slope
1mM	0.0001	0.0051	0.0026	0.0034
2mM	0.0059	0.0070	0.0163	0.0124
4mM	0.0245	0.0182	0.0362	0.0218
8mM	0.0387	0.0306	0.0892	0.0512
16mM	0.0551	0.0577	0.0663	0.0849

Table S3.23: Propiophenone with I86A

Conc. of Substrate	Run 1 Slope	Run 2 Slope
0.3mM	0.0157	0.0213
0.6mM	0.0412	0.0421
1.2mM	0.0609	0.0681
2.4mM	0.0535	0.0668
4.8mM	0.0845	0.0788

Table S3.24: 2,4-Difluoroacetophenone with I86A/C295A

Conc. of Substrate	Run 1 Slope	Run 2 Slope	Run 3 Slope	Run 4 Slope	Run 5 Slope
1mM	0.0024	0.0057	-	-	-
2mM	0.0094	0.0088	0.0039	0.0025	-
4mM	0.021	0.0142	0.0049	0.0202	0.0099
8mM	0.0390	0.0251	0.0034	0.0241	0.0024
16mM	0.0324	0.0385	0.0282	0.0403	0.0119
32mM	-	-	0.0478	0.0314	0.0328

Table S3.25: 2,4-Difluoroacetophenone with I86A

Conc. of Substrate	Run 1 Slope	Run 2 Slope
0.3mM	0.0085	0.0108
0.6mM	0.0116	0.0246
1.2mM	0.0212	0.0235
2.4mM	0.0474	0.0188

4.8mM	0.0571	0.0555

Table S3.26: 3'-Methoxyacetophenone with I86A/C295A

Conc. of Substrate	Run 1 Slope	Run 2 Slope	Run 3 Slope	Run 4 Slope	Run 5 Slope
0.3mM	-	0.0045	0.0074	0.0029	-
0.6mM	-	0.0063	0.0059	0.0081	-
1mM	0.0027	-	-	-	-
1.2mM	-	0.0093	0.0056	0.0096	0.0095
2mM	0.0130	-	-	-	-
2.4mM	-	0.0172	0.0218	0.0222	0.0079
4mM	0.0176	-	-	-	-
4.8mM	-	0.0186	-	-	0.0159
8mM	0.0239	-	-	-	-

Table S3.27: 3'-Trifluoromethylacetophenone with I86A/C295A

Conc. of Substrate	Run 1 Slope	Run 2 Slope	Run 3 Slope
0.3mM	0.0057	-	-
0.6mM	0.0046	-	-
1mM	-	0.0031	0.0042
1.2mM	0.0084	-	-
2mM	-	0.0058	0.0070
2.4mM	0.1040	-	-
4mM	-	0.0099	0.0073
4.8mM	0.0190	-	-
8mM	-	-	0.0095
16mM	-	-	0.0134

S3.4. References

[1] Charton, M. The Quantitative Treatment of the Ortho Effect. In *Progress in Physical Organic Chemistry*, Volume 8; Taft, R. W., Ed.; John Wiley and Sons: New York, 1971; pp 240.

[2] Hansch, C.; Leo, A. *Substituent Constants for Correlation Analysis in Chemistry and Biology*; John Wiley and Sons: New York, 1979.

[3] Unger, S. H.; Hansh, C. Quantitative Models of Steric Effects. In *Progress in Physical Organic Chemistry*, Volume 12; Taft, R. W., Ed.; John Wiley and Sons: New York, 1976; pp 92-95.

APPENDIX B

CHAPTER 4 SUPPORTING INFORMATION

TABLE OF CONTENTS

Page

S4.1. Kinetic Resolution Chromatographic Data After Acetylation

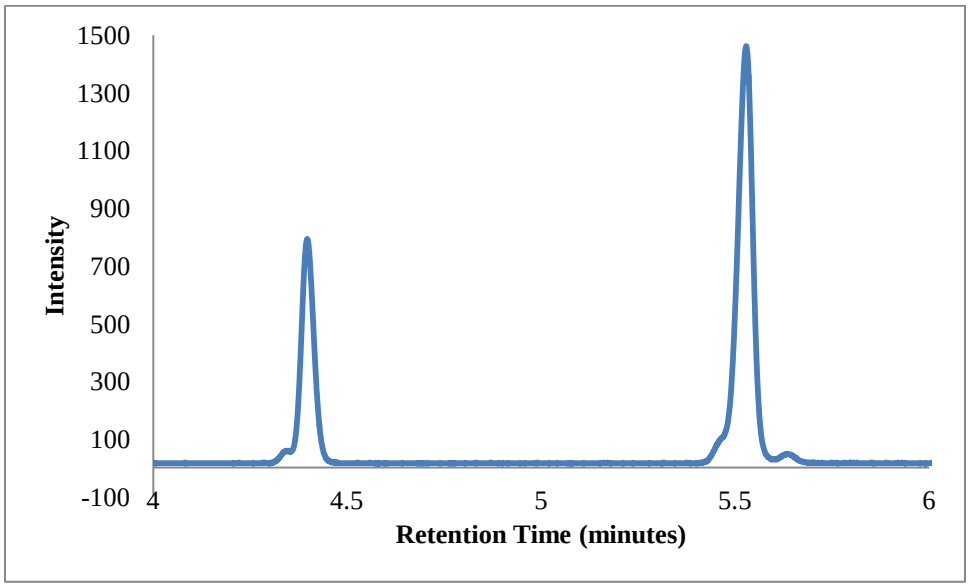

Figure S4.1: KR of 1-phenylethanol (**a**) with I86A. Retention time (area): 4.3950 (31.6372), 5.5258 (71.5237), 5.6325 (3.8548)

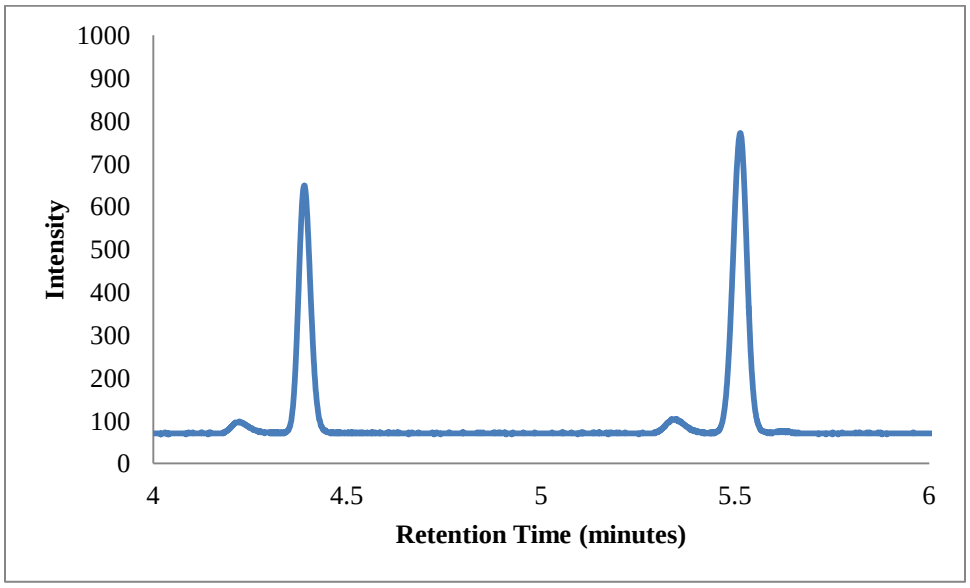

Figure S4.2: KR of 1-phenylethanol (**a**) with I86A/C295A. Retention time (area): 4.3867 (21.7113), 5.51 (31.6976)

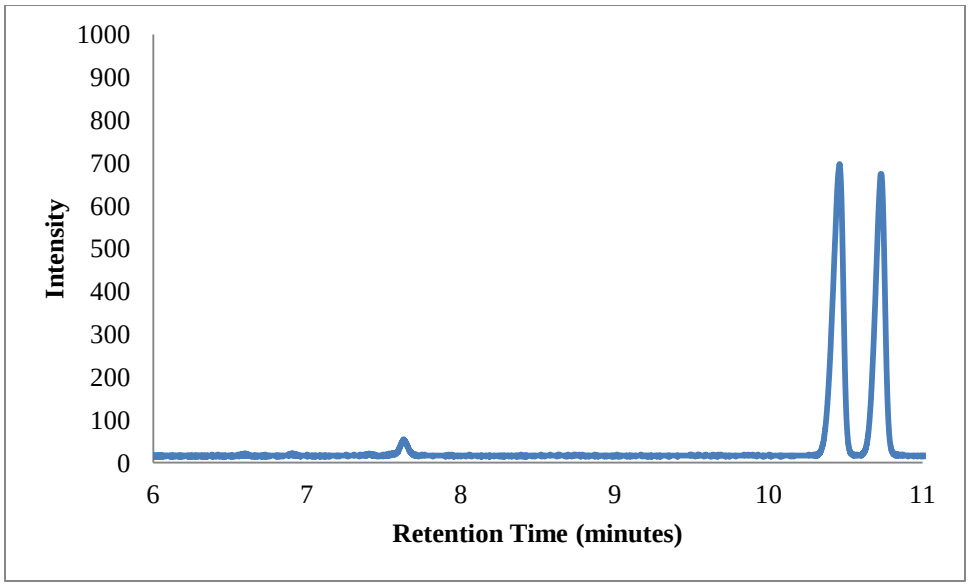

Figure S4.3: KR of 3'-chloro-1-phenylethanol (**b**) with I86A. Retention time (area): 7.6242 (3.5233), 10.4575 (54.4787), 10.7292 (49.7022)

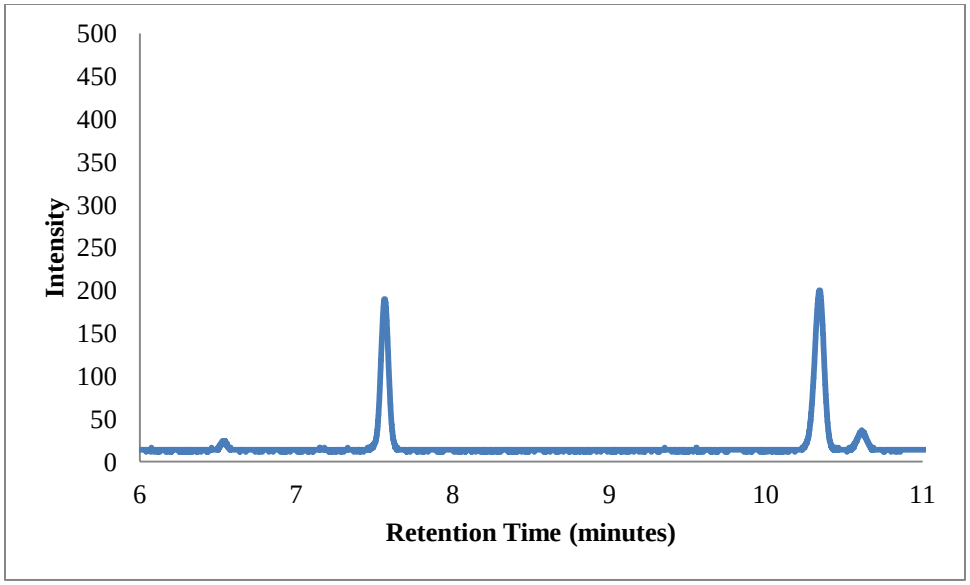

Figure S4.4: KR of 3'-chloro-1-phenylethanol (**b**) with I86A/C295A. Retention time (area): 7.5633 (12.3676), 10.3425 (14.0485), 10.6075 (5.5027)

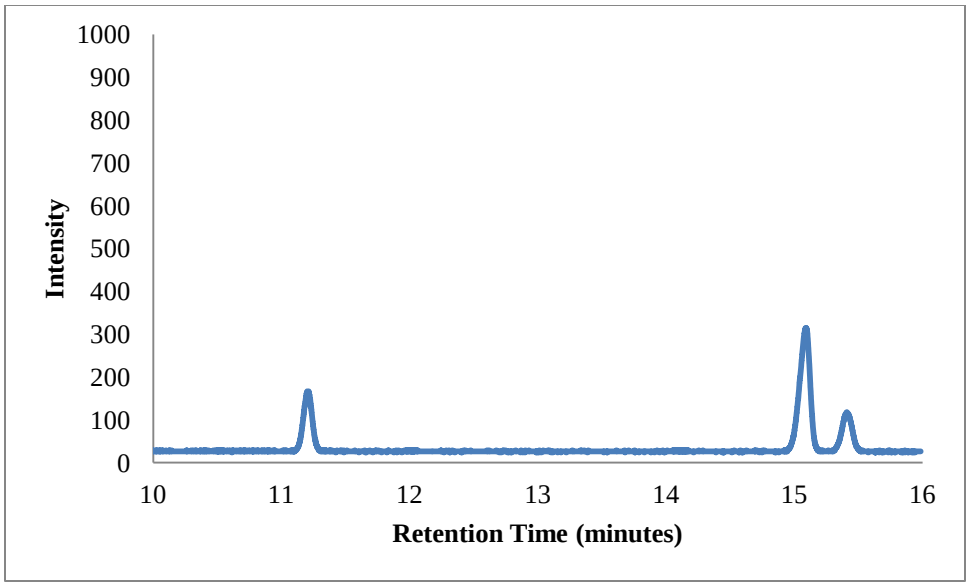

Figure S4.5: KR of 3'-bromo-1-phenylethanol (**c**) with I86A/C295A. Retention time (area): 11.1967 (11.4793), 15.0825 (27.8058), 15.2608 (8.54)

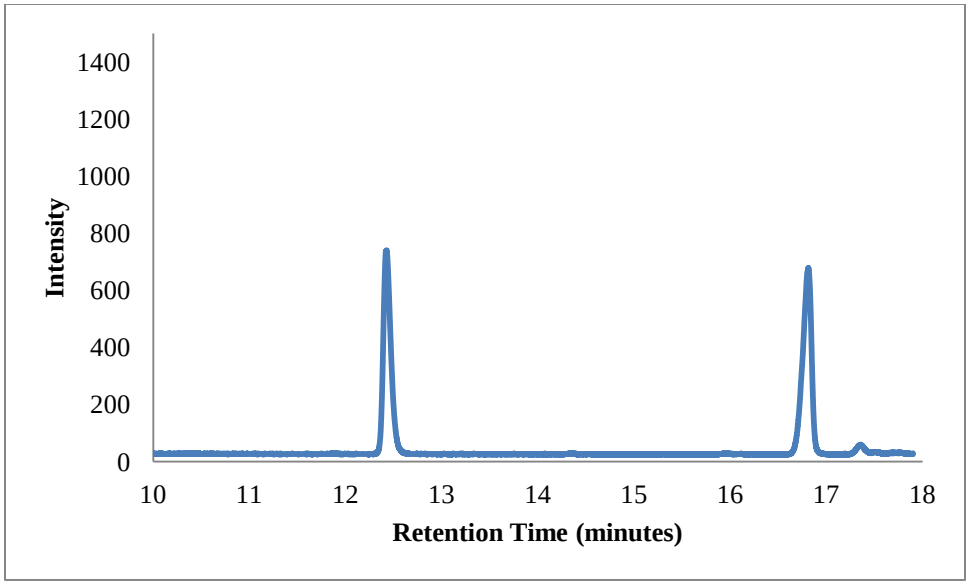

Figure S4.6: KR of 3'-methyl-1-phenylethanol (**d**) with I86A/C295A. Retention time (area): 12.42 (67.8560), 16.8075 (71.2868), 17.3533 (4.3478)

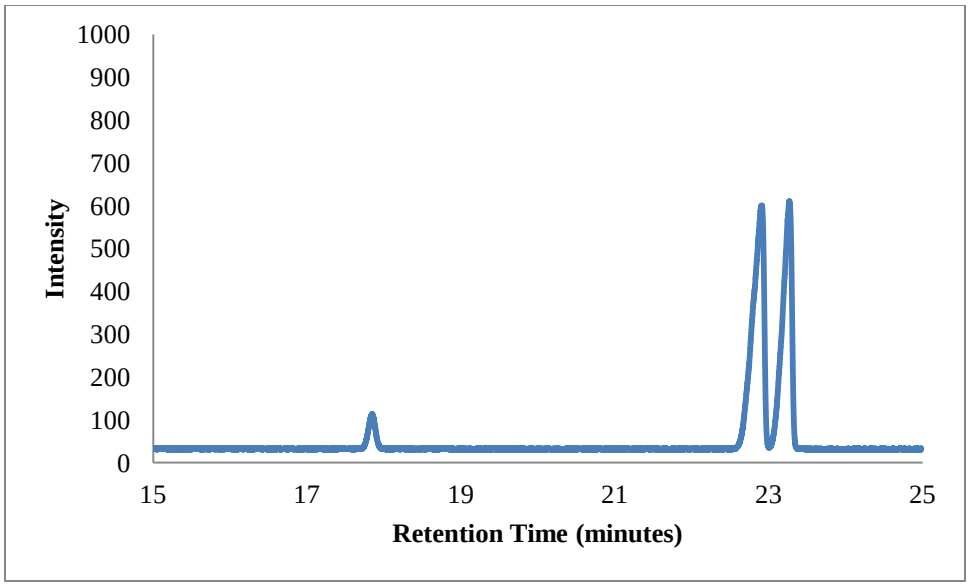

Figure S4.7: KR of 3'-iodo-1-phenylethanol (**e**) with I86A/C295A. Retention time (area): 17.835 (8.8188), 22.8967 (98.6835), 23.2608 (81.6048)

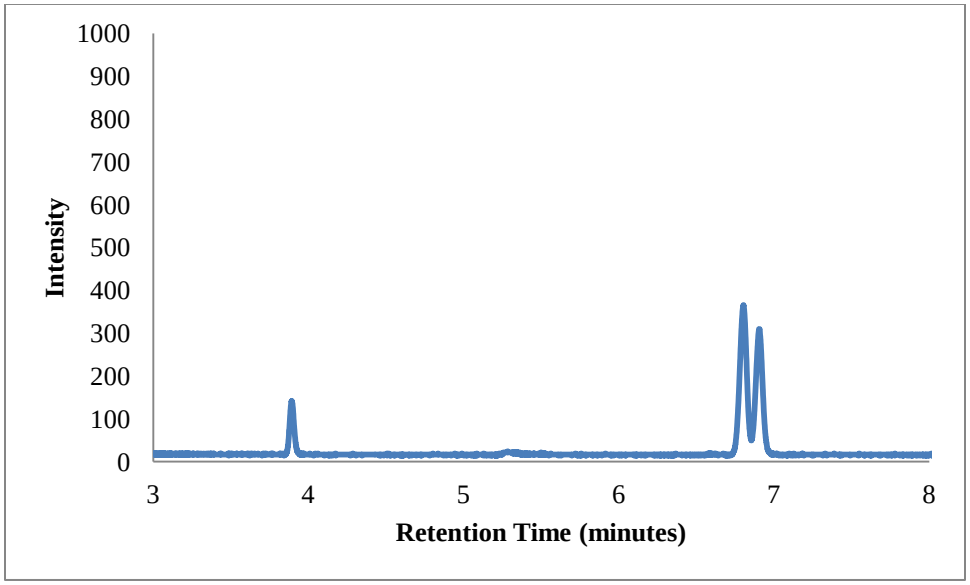

Figure S4.8: KR of 2-pyridinyl-1-ethanol (**f**) with I86A. Retention time (area): 3.8883 (7.5342), 6.8 (18.9753), 6.9 (15.9057)

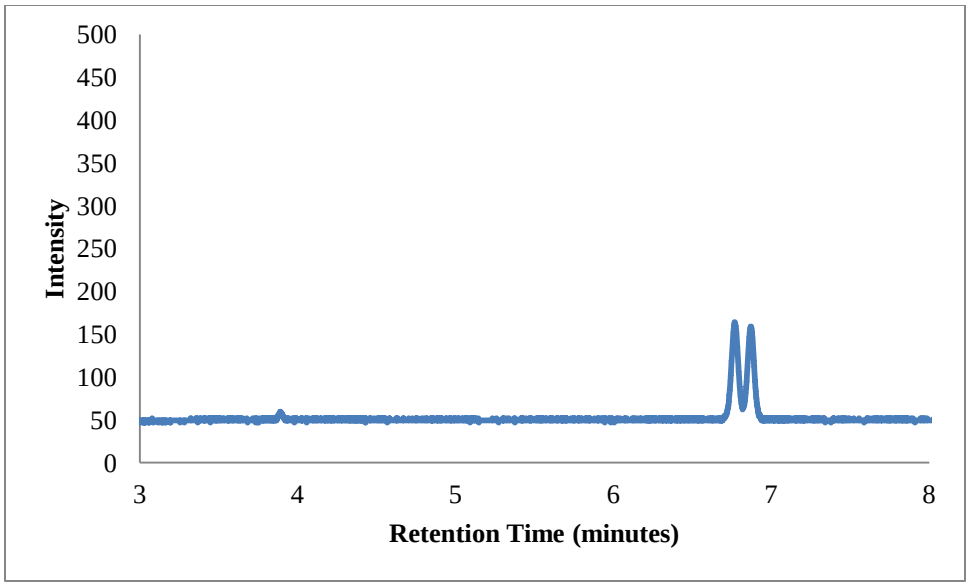

Figure S4.9: KR of 2-pyridinyl-1-ethanol (**f**) with I86A/C295A. Retention time (area): 3.885 (0.3379), 6.7642 (6.0797), 6.8658 (5.7758)

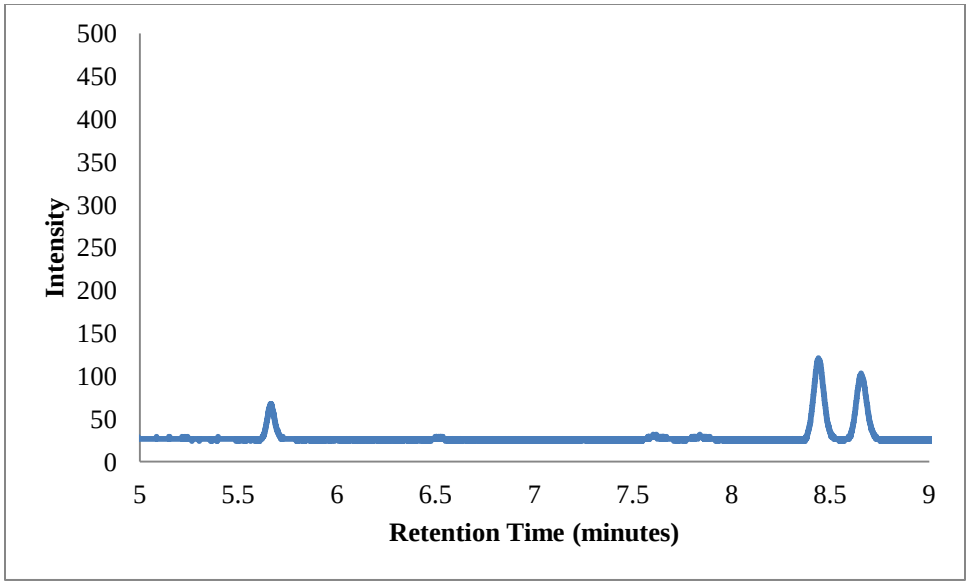

Figure S4.10: KR of 3-pyridinyl-1-ethanol (**g**) with I86A. Retention time (area): 5.6592 (2.6106), 8.4367 (6.2146), 8.6525 (5.2764)

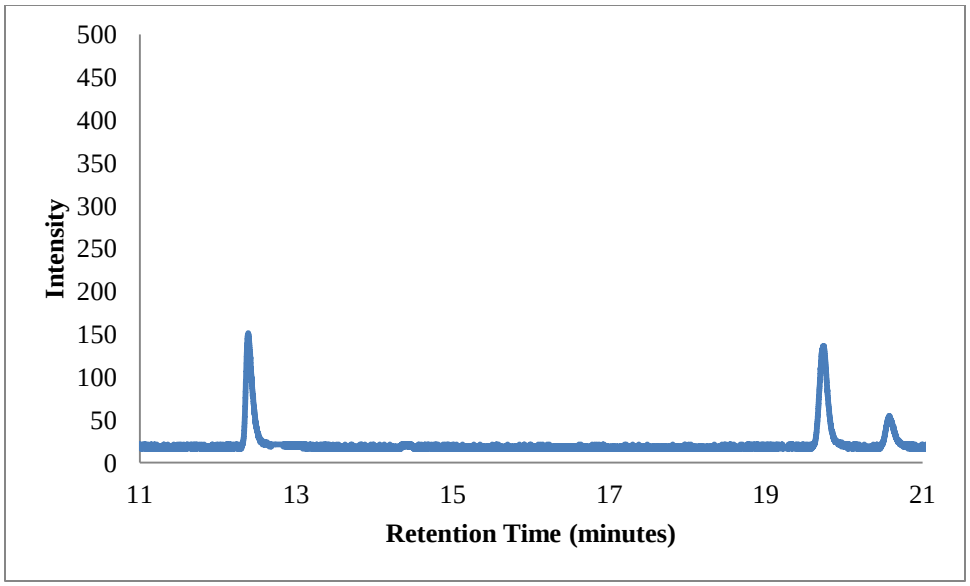

Figure S4.11: KR of 3-pyridinyl-1-ethanol (**g**) with I86A/C295A. Retention time (area): 12.3792 (13.1602), 19.7217 (14.6690), 22.5658 (3.9143)

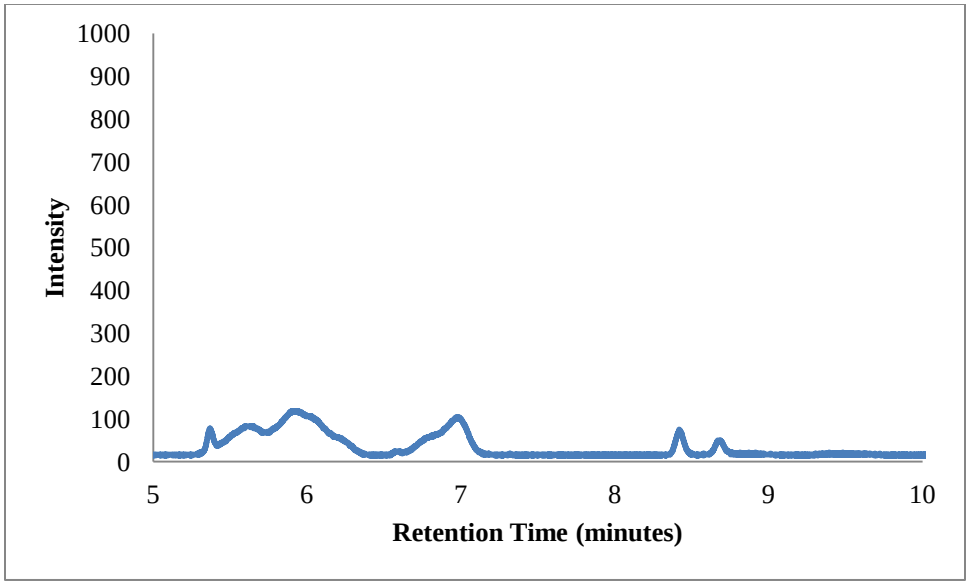

Figure S4.12: KR of 4-pyridinyl-1-ethanol (**h**) with I86A. Retention time (area): 5.3642 (2.0751), 8.4142 (3.9993), 8.6650 (2.9378)

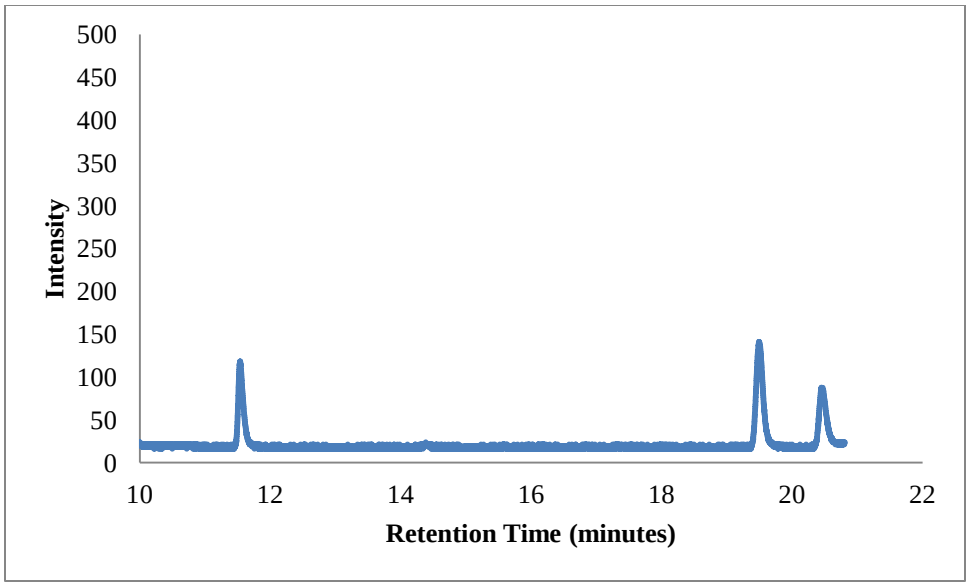

Figure S4.13: KR of 4-pyridinyl-1-ethanol (**h**) with I86A/C295A. Retention time (area): 11.5309 (9.5403), 19.4875 (15.1237), 20.4458 (9.1939)

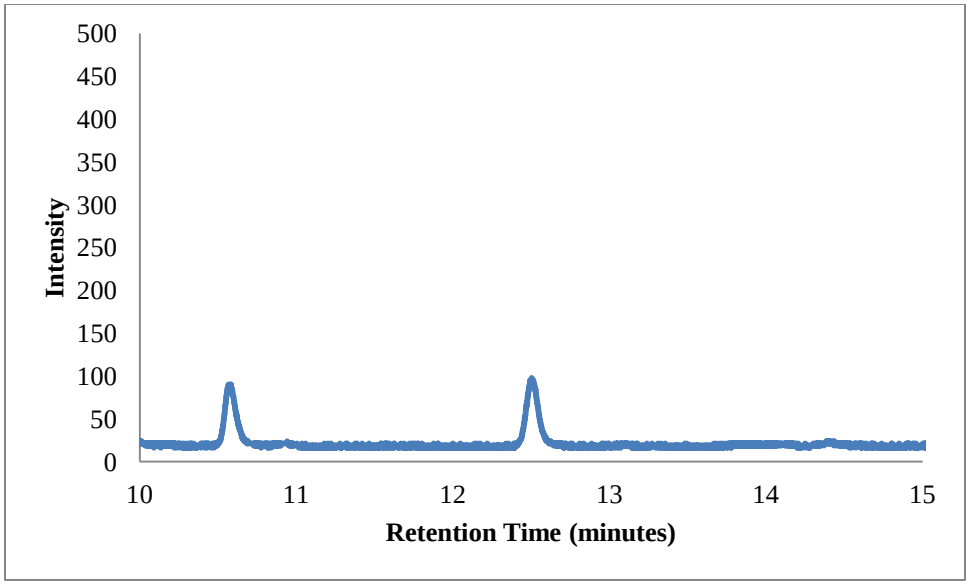

Figure S4.14: KR of 2-thiophenyl-1-ethanol (**i**) with I86A. Retention time (area): 10.5617 (6.6237), 12.4983 (7.5109)

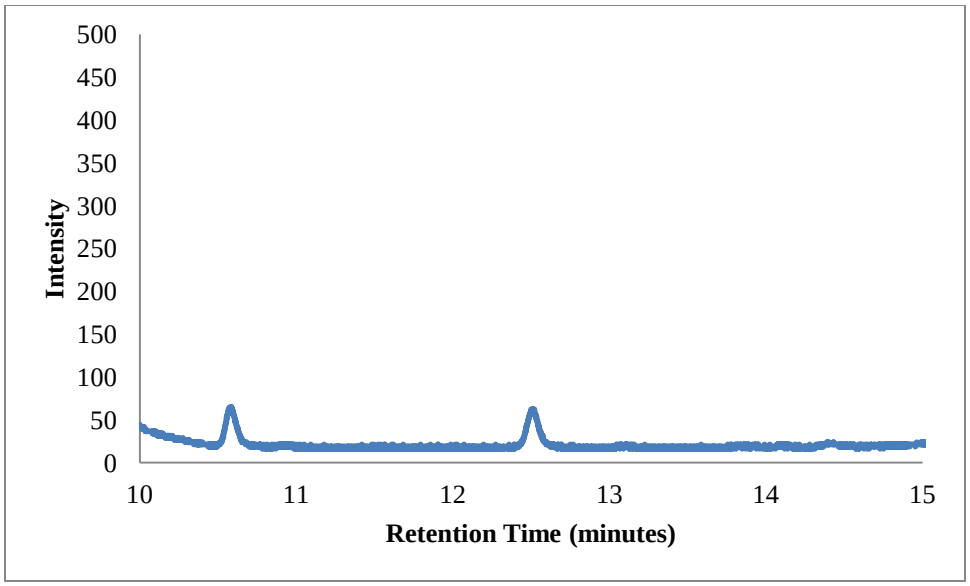

Figure S4.15: KR of 2-thiophenyl-1-ethanol (**i**) with I86A/C295A. Retention time (area): 10.5683 (3.9398), 12.4950 (4.5497)

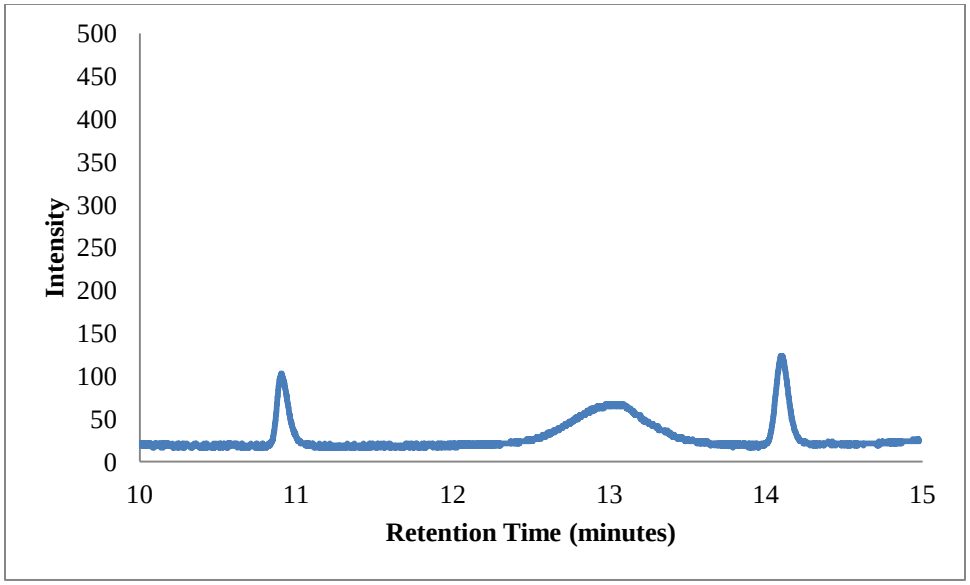

Figure S4.16: KR of 3-thiophenyl-1-ethanol (**j**) with I86A. Retention time (area): 10.8975 (7.6373), 14.0892 (11.0798)

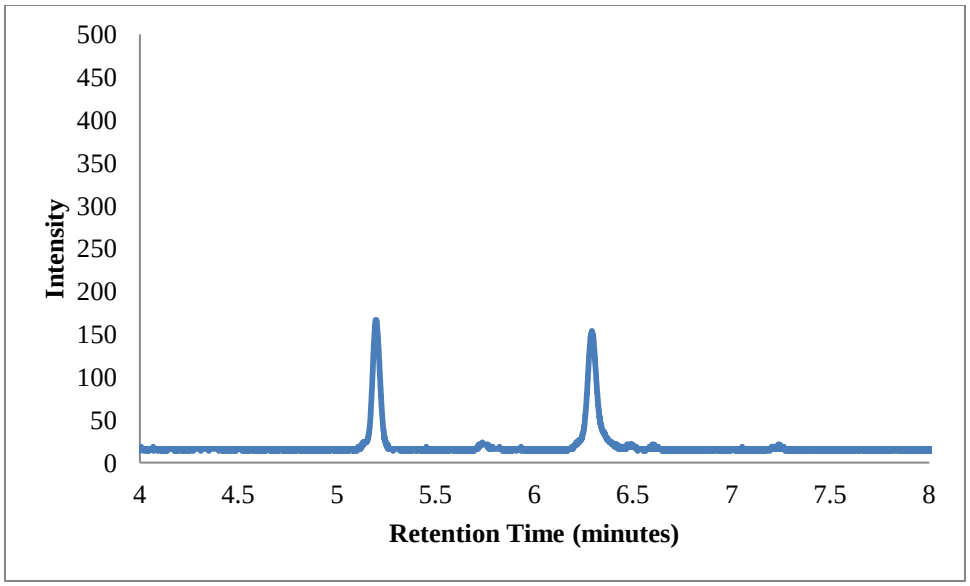

Figure S4.17: KR of 3-thiophenyl-1-ethanol (**j**) with I86A/C295A. Retention time (area): 5.1908 (7.8562), 6.2875 (9.6731), 6.5925 (0.3485)

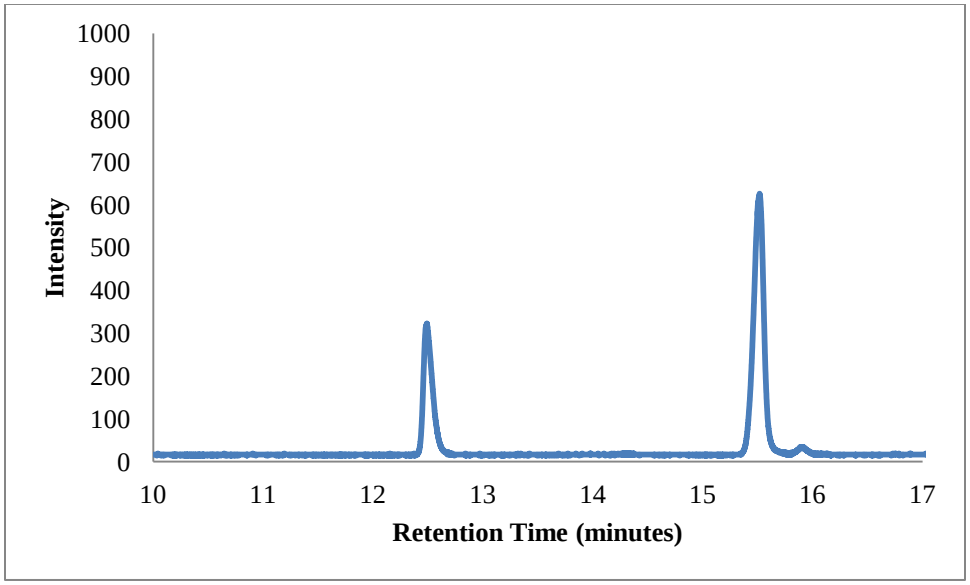

Figure S4.18: KR of 1-phenylpropanol (**k**) with I86A. Retention time (area): 12.4858 (31.6234), 15.5133 (66.5873), 15.8817 (1.9274)

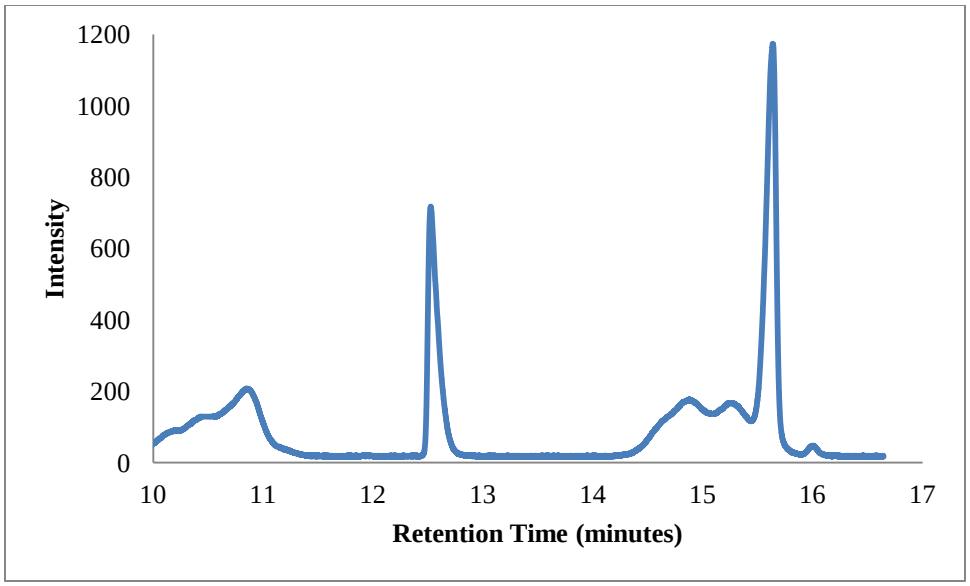

Figure S4.19: KR of 1-phenylpropanol (**k**) with I86A/C295A. Retention time (area): 12.5208 (76.4952), 15.6342 (120.8243), 16.0067 (2.8879)

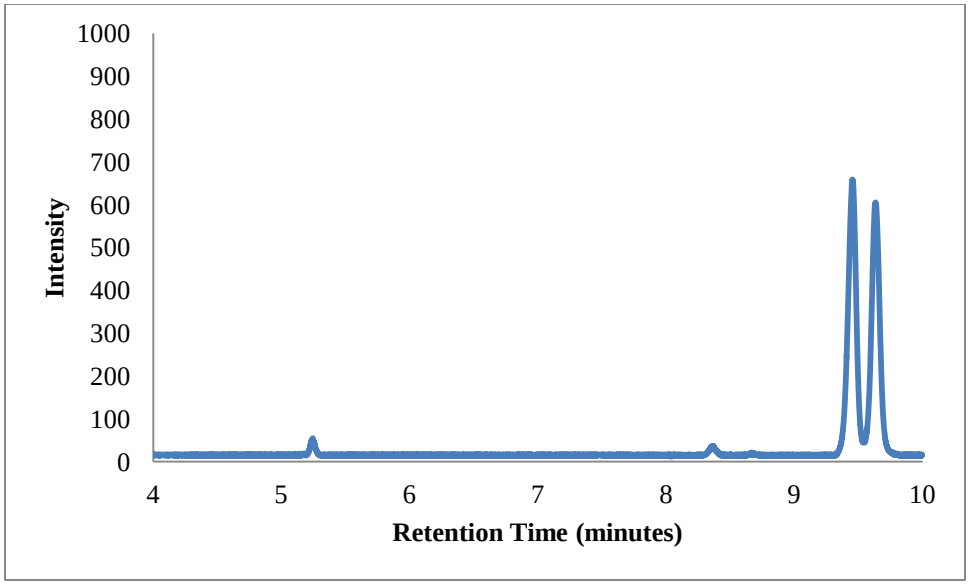

Figure S4.20: KR of 2',4'-difluoro-1-phenylethanol (**l**) with I86A. Retention time (area): 5.2425 (2.0039), 9.4517 (48.9455), 9.6317 (45.8068)

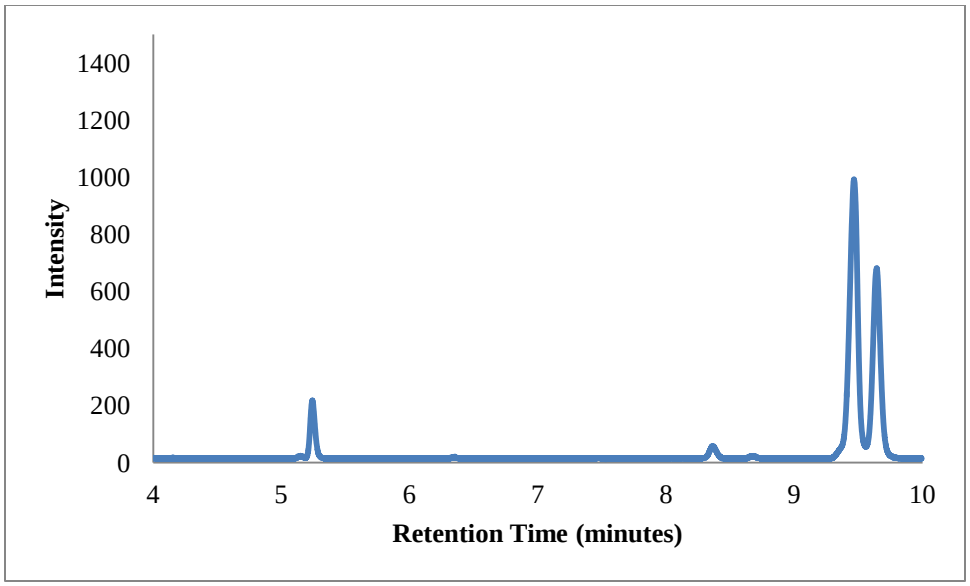

Figure S4.21: KR of 2',4'-difluoro-1-phenylethanol (**l**) with I86A/C295A. Retention time (area): 5.2375 (9.3947), 9.4625 (75.6654), 9.64 (48.5311)

APPENDIX C

CHAPTER 5 SUPPORTING INFORMATION

TABLE OF CONTENTS

Page

S5.1. Asymmetric Reduction Chromatographic Data After Acetylation

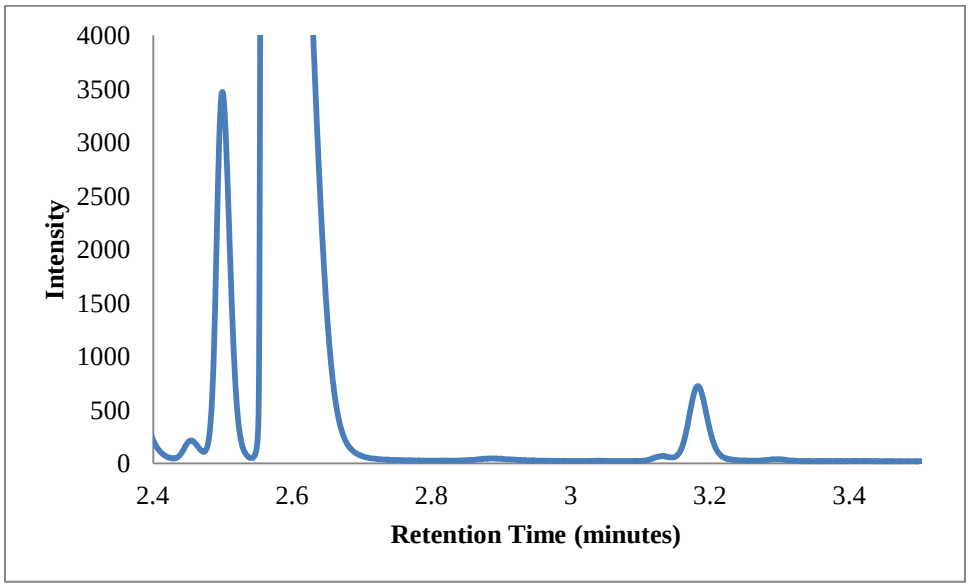

Figure S5.1: AR of 2-hexanone with wild-type. Retention time (area): 2.4875 (82.85), 3.1808 (24.98), 3.2958 (1.09)

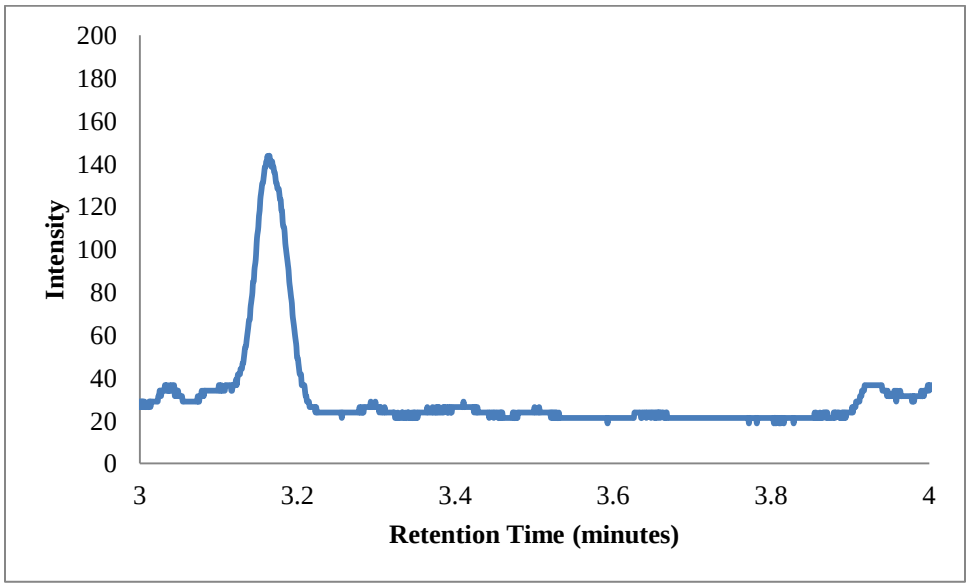

Figure S5.2: AR of 2-hexanone with T153A. Retention time (area): 2.48, 3.1625 (6.16), 3.2908 (0.23)

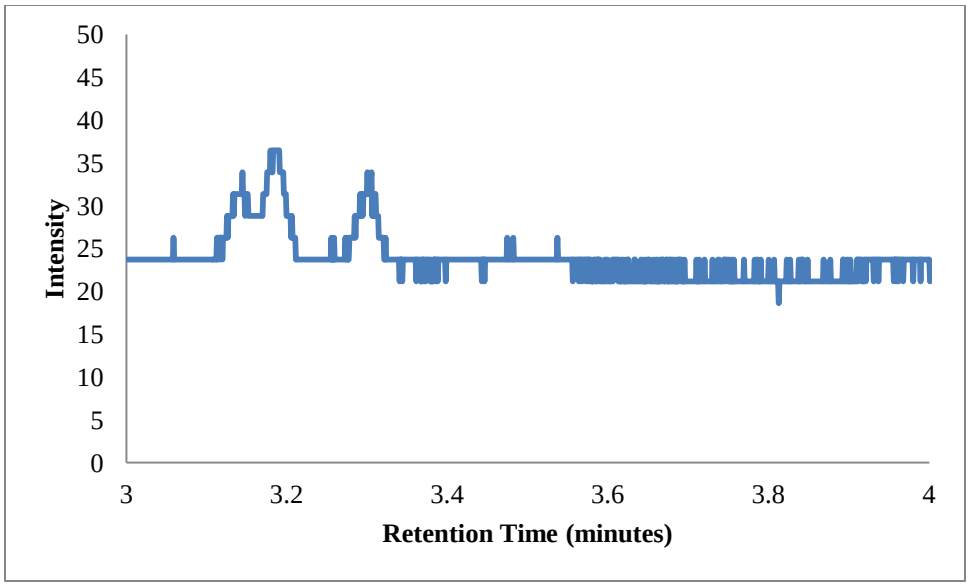

Figure S5.3: AR of 2-hexanone with M151A. Retention time (area): 2.5025 (51.61), 3.1883 (0.65), 3.3033 (0.23)

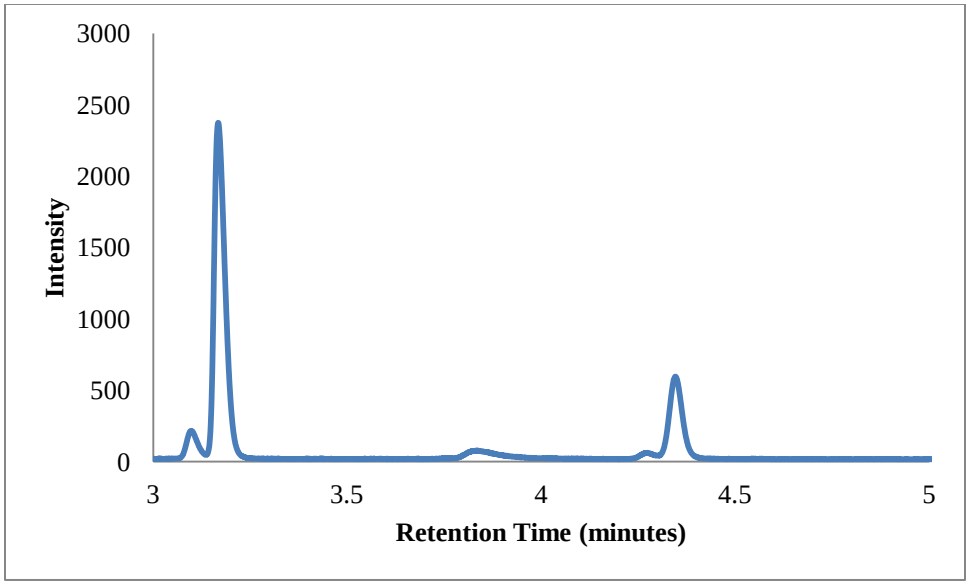

Figure S5.4: AR of 2-heptanone with wild-type. Retention time (area): 3.165 (78.39), 4.3433 (25.58)

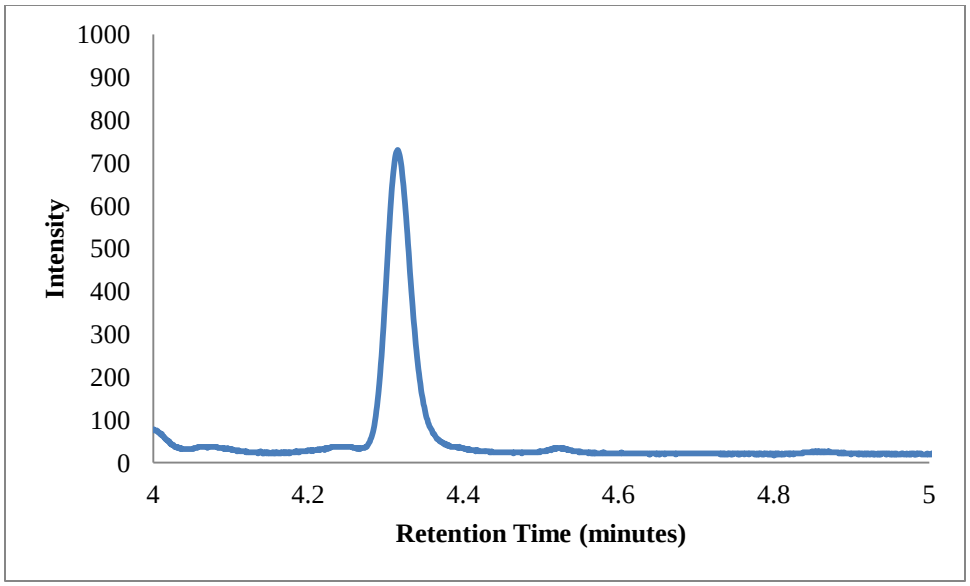

Figure S5.5: AR of 2-heptanone with T153A. Retention time (area): 3.0862, 4.3183 (29.31), 4.5141 (0.55)

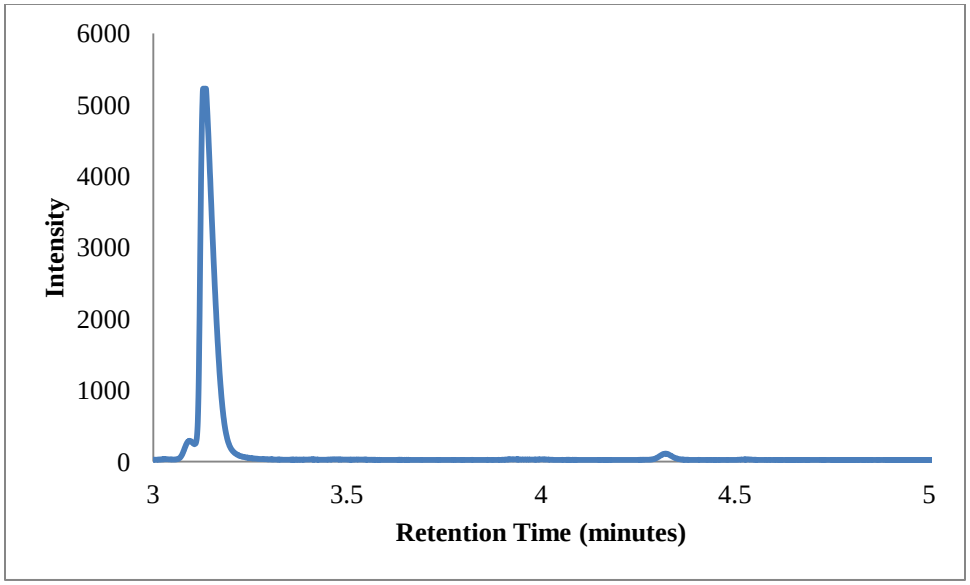

Figure S5.6: AR of 2-heptanone with M151A. Retention time (area): 3.1267 (218.89), 4.32 (3.7995)

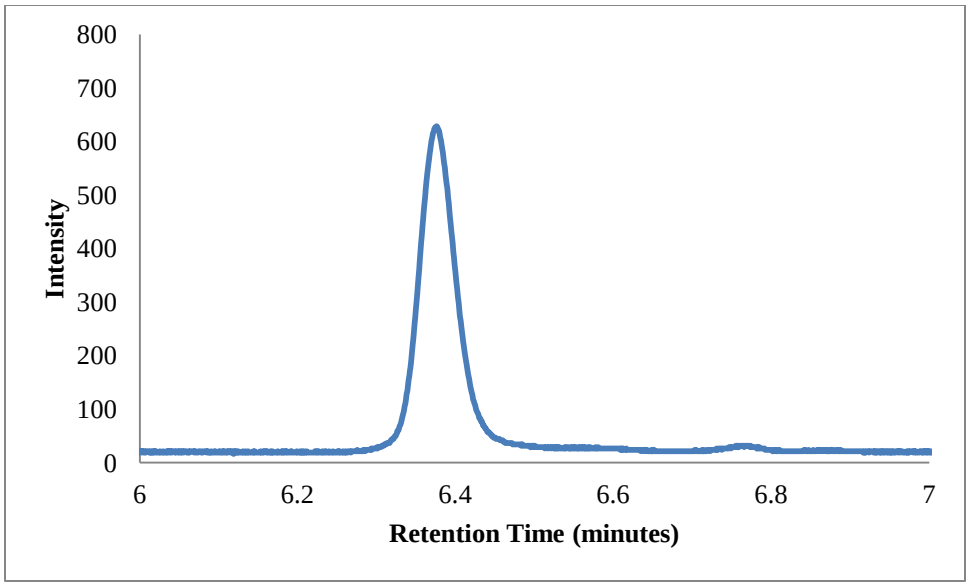

Figure S5.7: AR of 2-octanone with wild-type. Retention time (area): 4.2717 (272.36), 6.3733 (35.01), 6.7525 (0.52)

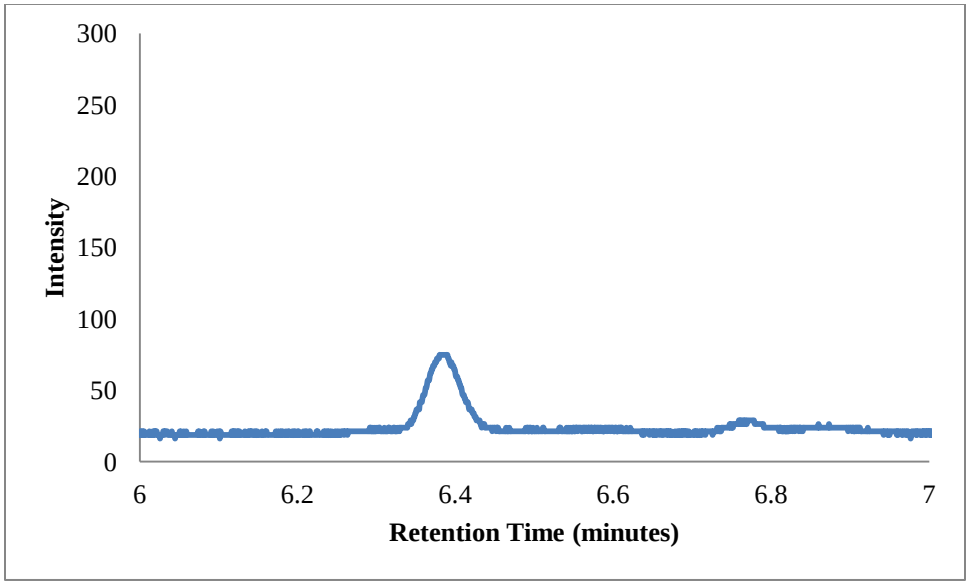

Figure S5.8: AR of 2-octanone with T153A. Retention time (area): 4.2725 (310.14), 6.3775 (2.89), 6.7567 (0.64)

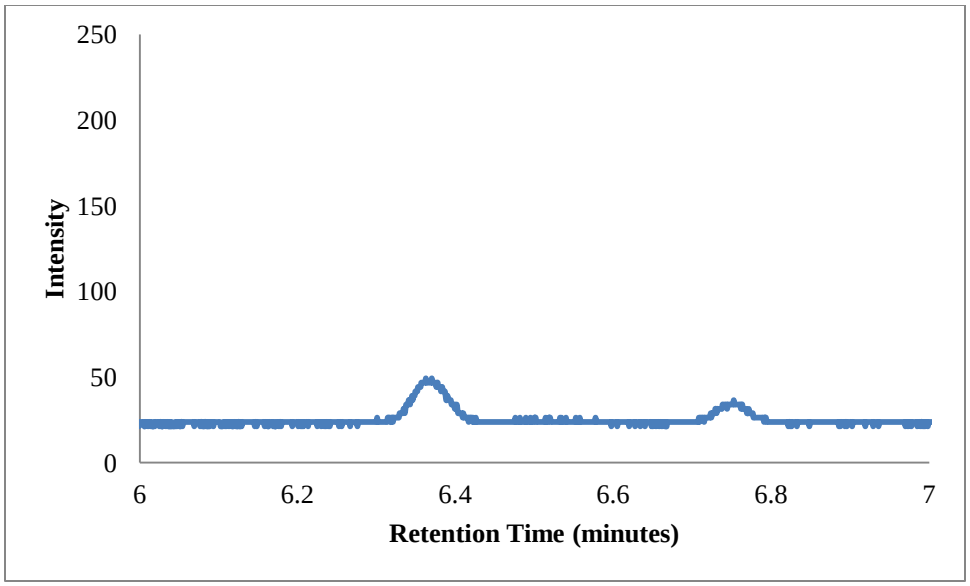

Figure S5.9: AR of 2-octanone with M151A. Retention time (area): 4.2767 (182.31), 6.3675 (1.37), 6.5750 (0.40)

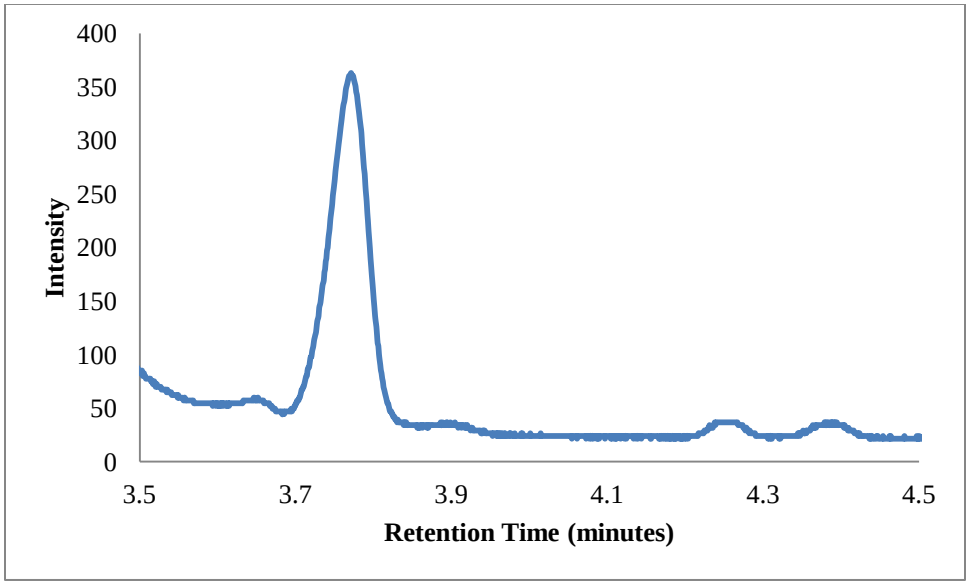

Figure S5.10: AR of 4-methyl-2-pentanone with wild-type. Retention time (area): 2.6308, 3.7692 (19.43), 3.8949 (1.46)

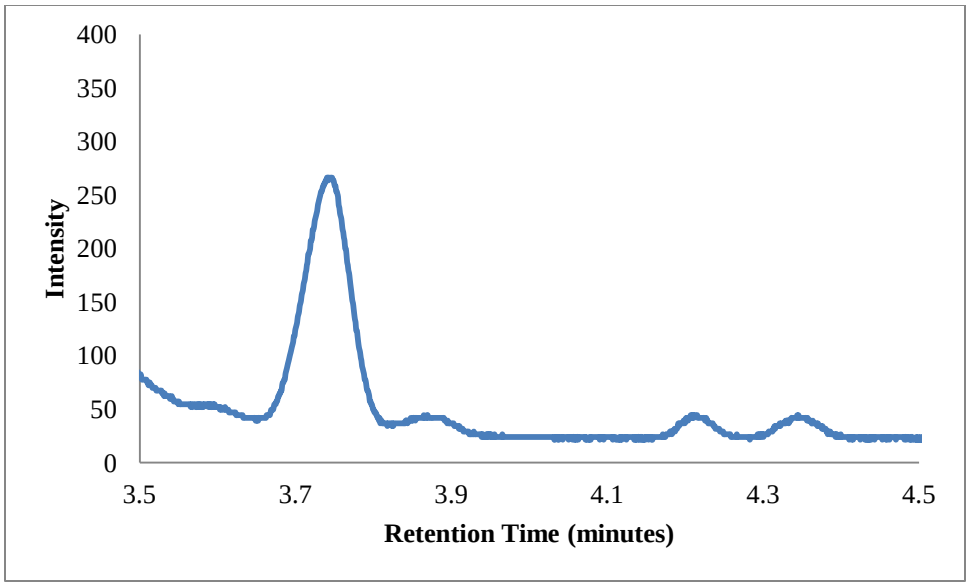

Figure S5.11: AR of 4-methyl-2-pentanone with T153A. Retention time (area): 2.6058, 3.745 (16.71), 3.8675 (1.15)

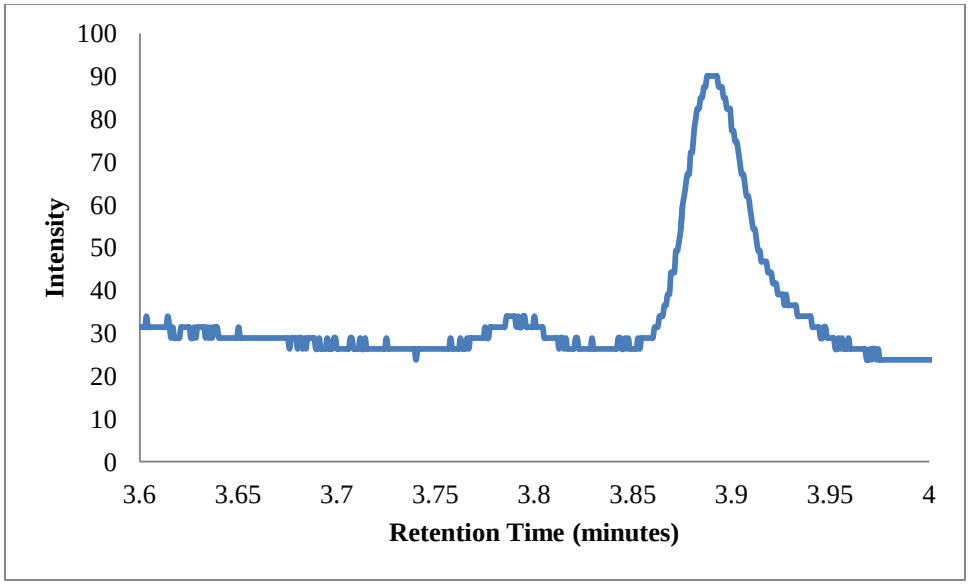

Figure S5.12: AR of 4-methyl-2-pentanone with M151A. Retention time (area): 2.6908 (146.65), 3.7842 (0.32), 3.8908 (3.00)

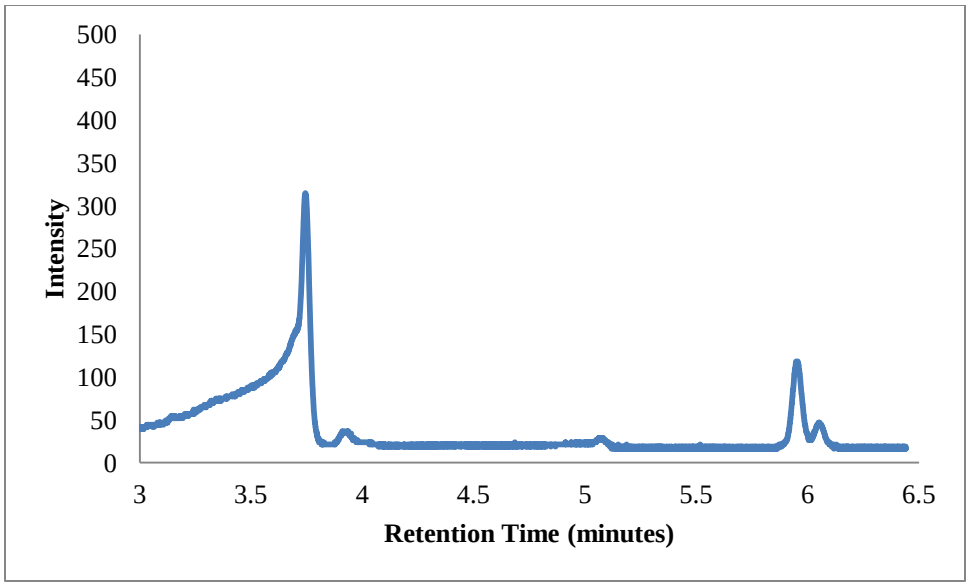

Figure S5.13: AR of methyl acetoacetate with wild-type. Retention time (area): 3.7425 (42.96), 5.9458 (5.59), 6.0467 (1.89)

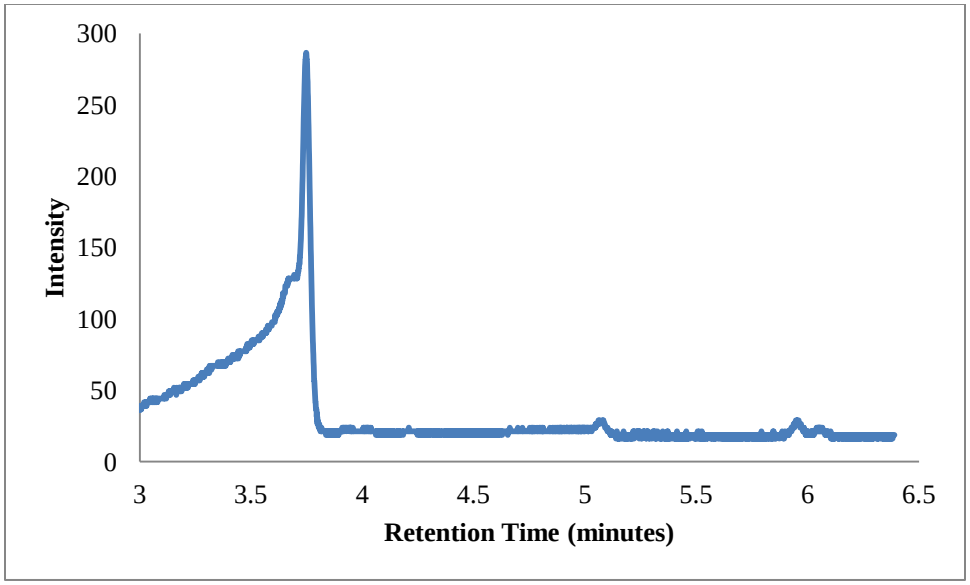

Figure S5.14: AR of methyl acetoacetate with T153A. Retention time (area): 3.7458 (39.31), 5.9442 (0.69), 6.0375 (0.57)

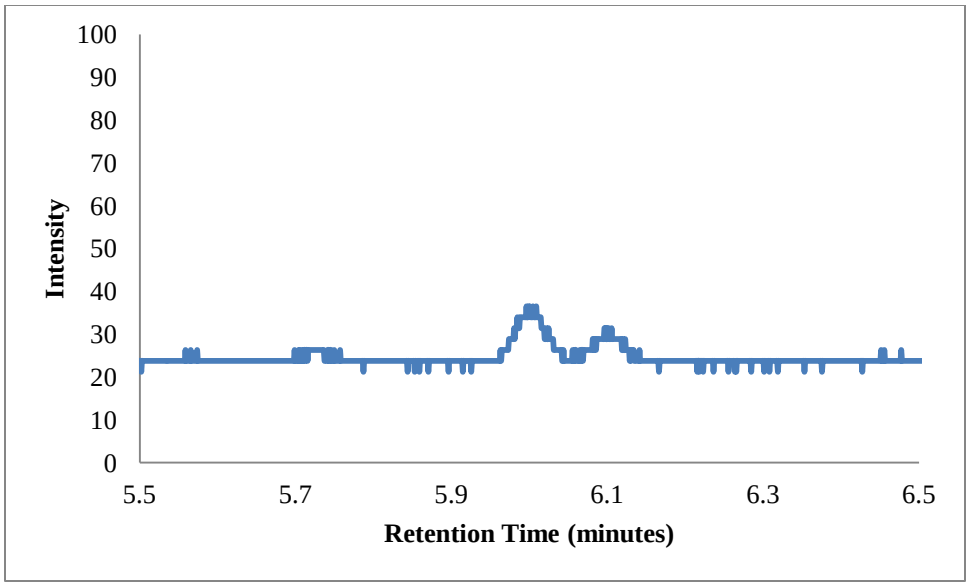

Figure S5.15: AR of methyl acetoacetate with M151A. Retention time (area): 3.7742 (24.15), 5.9942 (1.16), 6.0942 (0.62)

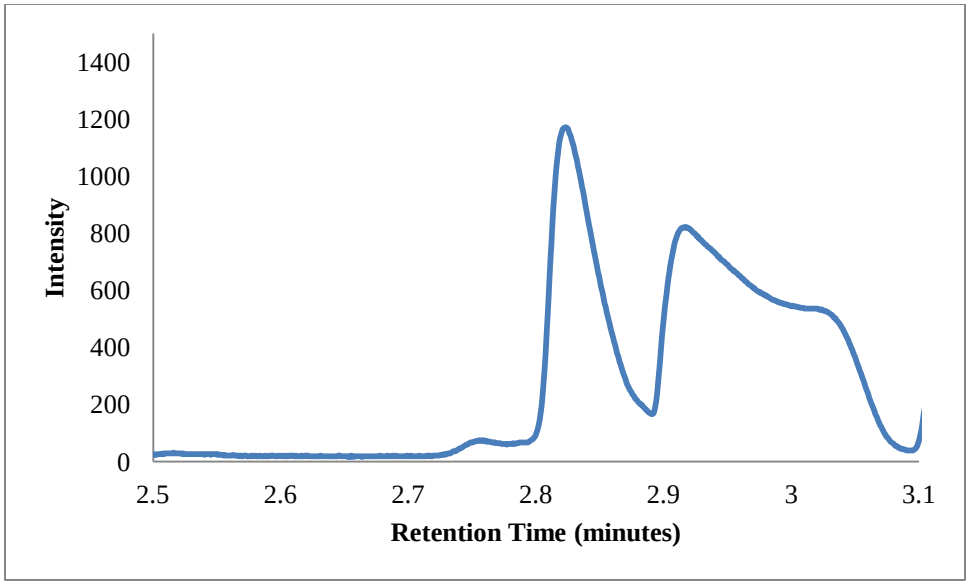

Figure S5.16: AR of 3-methyl-2-butanone with wild-type. Retention time (area): 2.2842 (34.58), 2.8208 (44.35), 2.9158 (81.14)

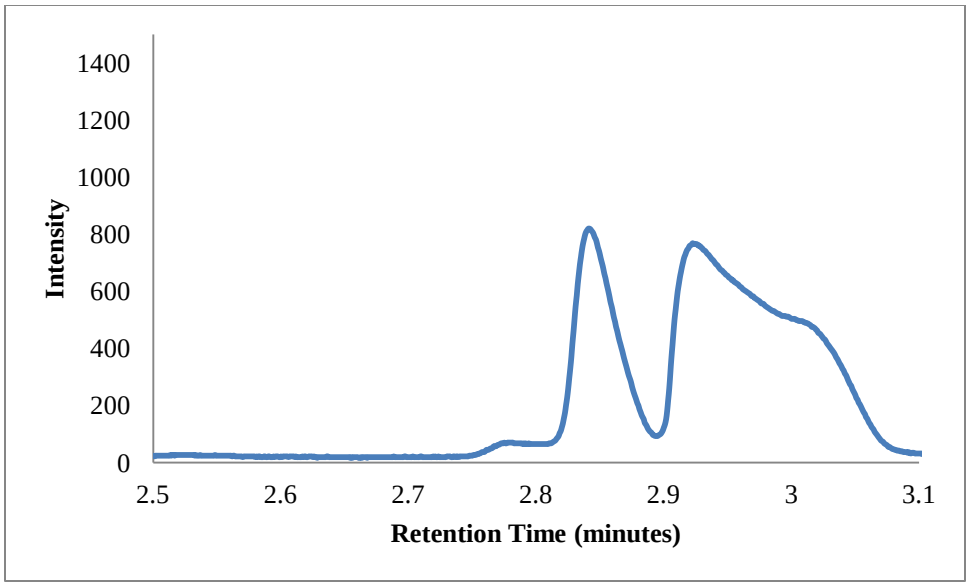

Figure S5.17: AR of 3-methyl-2-butanone with T153A. Retention time (area): 2.2933 (17.12), 2.8392 (28.76), 2.9208 (73.16)

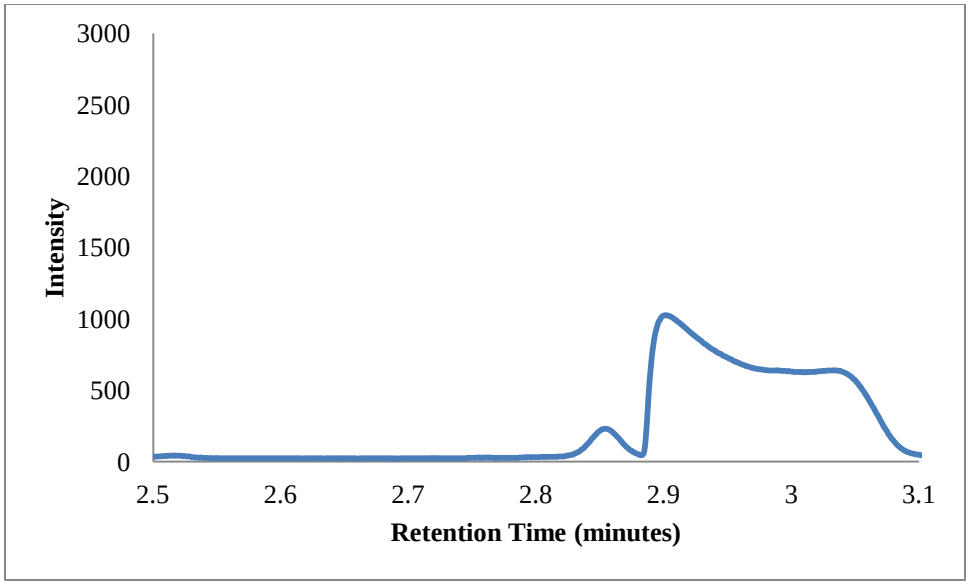

Figure S5.18: AR of 3-methyl-2-butanone with M151A. Retention time (area): 2.2833 (49.33), 2.8517 (5.55), 2.9 (122.91)

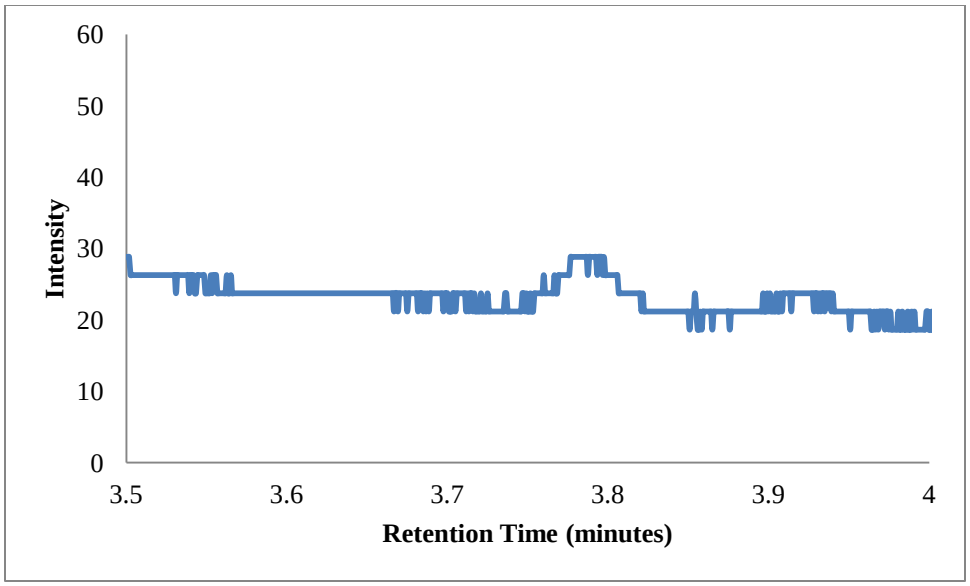

Figure S5.19: AR of 3,3-dimethyl-2-butanone with wild-type. Retention time (area): 2.5867 (105.42), 3.7958 (0.49), 3.8525 (0.33)

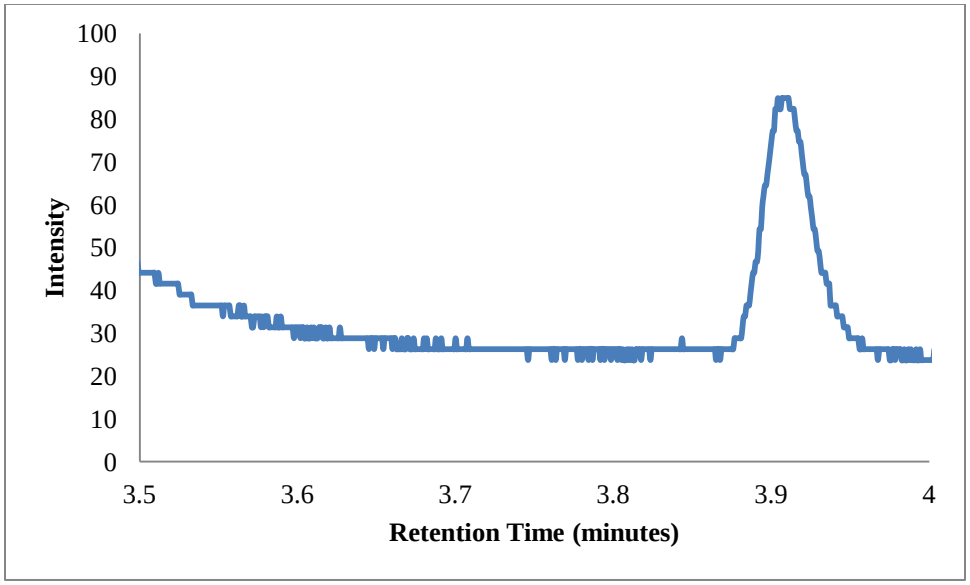

Figure S5.20: AR of 3,3-dimethyl-2-butanone with M151A. Retention time (area): 2.6 (28.98), 3.9 (2.46)

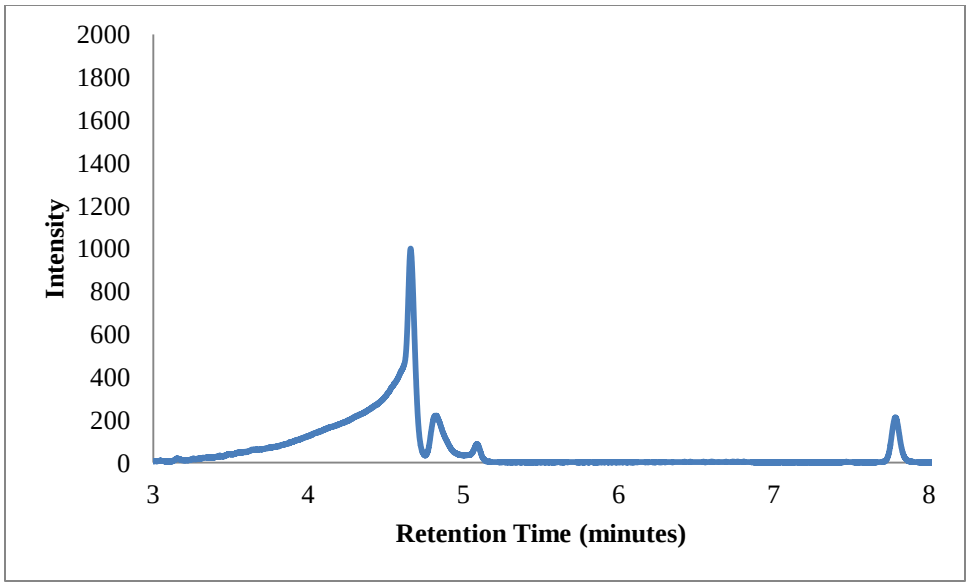

Figure S5.21: AR of ethyl acetoacetate with wild-type. Retention time (area): 4.655 (217.47), 7.7792 (13.531)

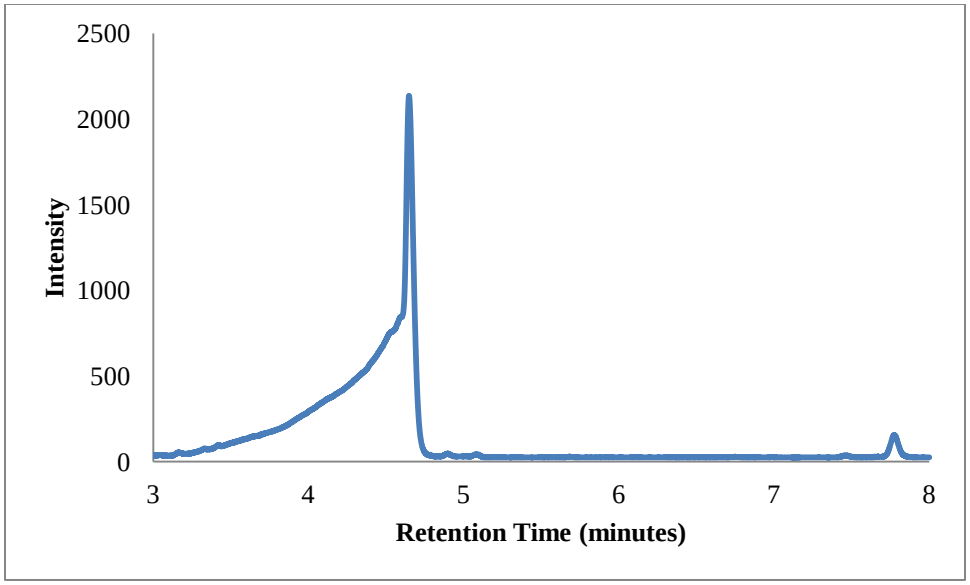

Figure S5.22: AR of ethyl acetoacetate with T153A. Retention time (area): 4.6475 (481.17), 7.7750 (8.84)

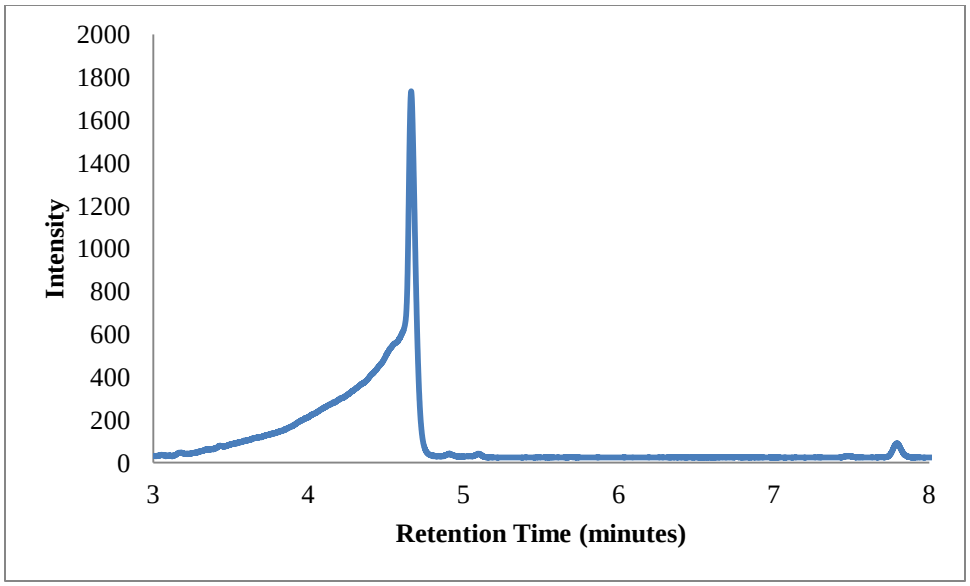

Figure S5.23: AR of ethyl acetoacetate with M151A. Retention time (area): 4.6592 (370.7), 7.7925 (7.06)

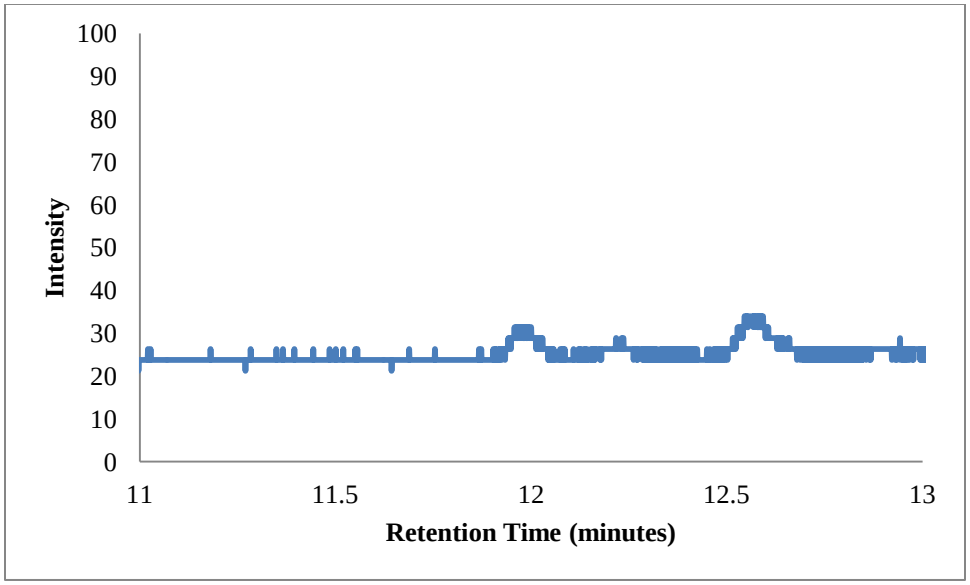

Figure S5.24: AR of acetophenone with T153A. Retention time (area): 8.3133, 12.5417 (0.79)

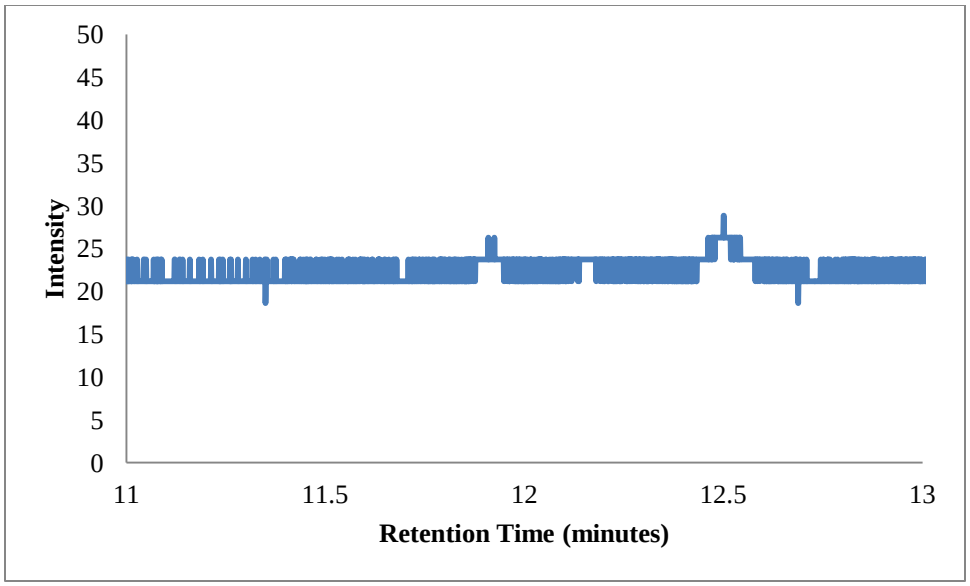

Figure S5.25: AR of acetophenone with M151A. Retention time (area): 8.32, 12.5 (0.16)

S5.2. Kinetic Assay Raw Data

Table S5.1: Acetone with Wild Type

Conc. of Substrate	Run 1 Slope	Run 2 Slope
0.3mM	-	0.0547
0.6mM	-	0.0876
1.2mM	-	0.1143
2mM	0.0982	-
2.4mM	-	0.1203
4mM	0.0971	-
4.8mM	-	0.158
8mM	0.1320	-
16mM	0.1363	-
32mM	0.1450	-

Table S5.2: Acetone with T153A

Conc. of Substrate	Run 1 Slope	Run 2 Slope
0.15mM	-	0.0210
0.3mM	0.0741	0.0480

0.6mM	0.0824	0.0612
1.2mM	0.0867	0.0514
2.4mM	0.0877	-
4.8mM	0.0991	-

Table S5.3: 4-Methyl-2-pentanone with Wild Type

Conc. of Substrate	Run 1 Slope	Run 2 Slope	Run 3 Slope	Run 4 Slope	Run 5 Slope
0.3mM	-	-	0.0087	-	-
0.6mM	-	-	0.0107	0.0122	-
1mM	0.0153	0.0123	-	-	0.0137
1.2mM	-	-	0.0139	0.0117	-
2mM	0.0237	0.0214	-	-	0.0211
2.4mM	-	-	0.0164	0.0206	-
4mM	0.027	0.0182	-	-	0.0314
4.8mM	-	-	0.0175	0.0262	-
8mM	0.0408	0.0327	-	-	0.0285
16mM	0.0417	0.0231	-	-	0.0386

Table S5.4: 4-Methyl-2-pentanone with T153A

Conc. of Substrate	Run 1 Slope	Run 2 Slope	Run 3 Slope	Run 4 Slope
0.3mM	0.0056	-	0.0046	-
0.6mM	0.0053	0.0024	0.0059	-
1mM	-	-	-	0.0098
1.2mM	0.0124	0.0132	0.0111	-
2mM	-	-	-	0.0104
2.4mM	0.0255	-	0.0172	-
4mM	-	-	-	0.0223
4.8mM	0.024	0.0343	0.0313	-
8mM	-	-	-	0.0297

Table S5.5: Methyl acetoacetate with Wild Type

Conc. of Substrate	Run 1 Slope	Run 2 Slope	Run 3 Slope
1mM	0.026	0.0221	-
2mM	0.0492	0.0329	0.0259
4mM	0.0459	0.07	0.0449
8mM	0.0516	0.0517	0.0737
16mM	0.1001	0.1122	0.0922

32mM	-	-	0.0705

Table S5.6: Methyl acetoacetate with T153A

Conc. of Substrate	Run 1 Slope	Run 2 Slope	Run 3 Slope
0.15mM	0.0052	-	-
0.3mM	0.0074	-	-
0.6mM	0.0055	0.012	-
1mM	-	-	0.0067
1.2mM	0.0174	-	-
2mM	-	-	0.0377
2.4mM	0.0342	-	-
4mM	-	-	0.0467
4.8mM	-	0.0327	-
8mM	-	-	0.0607
16mM	-	-	0.1021

Table S5.7: Ethyl acetoacetate with Wild Type

Conc. of Substrate	Run 1 Slope	Run 2 Slope	Run 3 Slope
0.3mM	-	0.0240	0.0219
0.6mM	-	0.0215	0.0120
1mM	0.0317	-	-
1.2mM	-	0.0286	0.0289
2mM	0.0315	-	-
2.4mM	-	0.0258	-
4mM	0.0411	-	-
4.8mM	-	0.0403	-

Table S5.8: Ethyl acetoacetate with T153A

Conc. of Substrate	Run 1 Slope	Run 2 Slope	Run 3 Slope
2mM	-	0.0227	0.0099
4mM	-	0.0205	0.0207
8mM	-	0.0399	0.0334
16mM	0.0412	-	0.0378
32mM	-	-	0.0475

Table S5.9: 3-Methyl-2-butanone with Wild Type

Conc. of Substrate	Run 1 Slope	Run 2 Slope	Run 3 Slope
0.3mM	0.0307	0.0139	0.0112
0.6mM	0.0456	0.0215	0.0238
1.2mM	0.0605	0.0336	0.0386
2.4mM	0.0698	0.0403	0.0548
4.8mM	0.0395	0.0765	0.0807

Table S5.10: 3-Methyl-2-butanone with T153A

Conc. of Substrate	Run 1 Slope	Run 2 Slope	Run 3 Slope	Run 4 Slope
0.15mM	-	0.0207	0.0173	0.0252
0.3mM	0.0327	0.0485	0.0222	0.0311
0.6mM	0.0716	0.0866	0.0299	0.0445
1.2mM	0.0590	0.0747	0.0451	0.0538
2.4mM	0.0707	0.0713	0.0522	0.0671
4.8mM	0.0927	-	-	-

Table S5.11: 2-Hexanone with Wild Type

Conc. of Substrate	Run 1 Slope	Run 2 Slope
0.3mM	0.0086	-
0.6mM	0.0181	-
1mM	-	0.0226
1.2mM	0.0184	-
2mM	-	0.0359
2.4mM	0.0293	-
4mM	-	0.0493
4.8mM	0.0425	-
8mM	-	0.067
16mM	-	0.075

Table S5.12: 2-Hexanone with T153A

Conc. of Substrate	Run 1 Slope	Run 2 Slope	Run 3 Slope
0.3mM	-	0.0094	-
0.6mM	-	0.0084	-
1mM	0.0234	-	-

1.2mM	-	0.0102	-
2mM	0.0182	-	0.0163
4mM	0.0406	-	-
4.8mM	-	0.0267	-
8mM	0.0520	-	-
16mM	0.0303	-	-

Table S5.13: 2-Heptanone with Wild Type

Conc. of Substrate	Run 1 Slope	Run 2 Slope
0.3mM	0.0242	0.0091
0.6mM	0.0523	0.0557
1.2mM	0.0771	0.0905
2.4mM	-	0.1148
4.8mM	0.1294	0.1129

Table S5.14: 2-Heptanone with T153A

Conc. of Substrate	Run 1 Slope	Run 2 Slope
0.3mM	-	0.0205
0.6mM	-	0.0245
1mM	0.0354	-
2mM	0.0883	-
2.4mM	-	0.0654
4mM	0.0744	-
4.8mM	-	0.0588
8mM	0.1165	-
16mM	0.1235	-

Table S5.15: 2-Octanone with Wild Type

Conc. of Substrate	Run 1 Slope	Run 2 Slope
0.3mM	0.0064	0.0081
0.6mM	0.0161	0.0175
1.2mM	0.0288	0.0321
2.4mM	0.0359	0.0394
4.8mM	0.0328	0.0488

Table S5.16: 2-Octanone with T153A

Conc. of Substrate	Run 1 Slope	Run 2 Slope
0.3mM	0.0156	0.0201
0.6mM	0.0339	0.0259
1.2mM	0.0386	0.0273
2.4mM	0.0495	0.0300
4.8mM	0.0514	0.0234

Table S5.17: 3,3-Dimethyl-2-butanone with Wild Type

Conc. of Substrate	Run 1 Slope	Run 2 Slope
0.3mM	0.0029	0.0033
0.6mM	0.0032	0.0039
1.2mM	0.0077	0.0038
2.4mM	0.0057	0.0061
4.8mM	0.0046	0.0084

Table S5.18: Acetophenone with Wild Type

Conc. of Substrate	Run 1 Slope	Run 2 Slope	Run 3 Slope
0.3mM	0.0009	-	-
0.6mM	0.0021	-	-
1mM	-	0.0151	-
1.2mM	0.0003	-	-
2mM	-	0.0116	0.0125
2.4mM	0.0073	-	-
4mM	-	0.0059	0.0050
4.8mM	0.0130	-	-
8mM	-	0.0082	0.0133
16mM	-	0.0097	0.0124
32mM	-	-	0.0076

S5.3. M151A Acetone Reaction Data

Table S5.19. M151A Acetone Reaction Data

2mM Acetone		4mM Acetone		8mM Acetone		16mM Acetone		32mM Acetone	
Time (min)	Abs	Time (min)	Abs	Time (min)	Abs	Time (min)	Abs	Time (min)	Abs

0.008	2.048	0.075	2.270	0.125	2.129	0.192	2.193	0.242	1.985
0.408	2.047	0.458	2.263	0.508	2.129	0.558	2.189	0.608	1.982
0.775	2.037	0.825	2.254	0.875	2.122	0.925	2.187	0.975	1.981
1.142	2.025	1.208	2.247	1.258	2.122	1.308	2.182	1.358	1.977
1.525	2.015	1.575	2.240	1.625	2.123	1.675	2.176	1.725	1.975
1.892	2.008	1.942	2.231	2.008	2.116	2.058	2.173	2.108	1.971
2.275	1.998	2.325	2.222	2.375	2.115	2.425	2.166	2.475	1.970
2.642	1.988	2.692	2.211	2.742	2.112	2.792	2.158	2.858	1.965
3.025	1.980	3.075	2.198	3.125	2.110	3.175	2.152	3.225	1.962
3.392	1.970	3.442	2.188	3.492	2.107	3.542	2.144	3.592	1.958
3.775	1.960	3.825	2.179	3.875	2.101	3.925	2.137	3.975	1.953
4.142	1.952	4.192	2.166	4.242	2.101	4.292	2.131	4.342	1.948
4.508	1.939	4.575	2.154	4.625	2.091	4.675	2.123	4.725	1.946
4.892	1.928	4.942	2.138	4.992	2.089	5.042	2.116	5.092	1.939
5.258	1.920	5.308	2.126	5.358	2.085	5.425	2.107	5.475	1.933
5.642	1.909	5.692	2.114	5.742	2.079	5.792	2.099	5.842	1.926
6.008	1.898	6.058	2.098	6.108	2.076	6.158	2.092	6.208	1.921
6.375	1.885	6.442	2.087	6.492	2.071	6.542	2.082	6.592	1.918
6.758	1.876	6.808	2.068	6.858	2.065	6.908	2.071	6.958	1.908
7.125	1.864	7.175	2.054	7.225	2.057	7.275	2.063	7.342	1.902
7.508	1.853	7.558	2.044	7.608	2.051	7.658	2.053	7.708	1.891
7.875	1.842	7.925	2.027	7.975	2.042	8.025	2.046	8.075	1.884
8.258	1.829	8.308	2.010	8.358	2.033	8.408	2.032	8.458	1.877
8.625	1.819	8.675	1.993	8.725	2.028	8.775	2.022	8.825	1.866
8.992	1.806	9.042	1.976	9.108	2.018	9.158	2.011	9.208	1.858
9.375	1.795	9.425	1.962	9.475	2.008	9.525	2.000	9.575	1.846
9.742	1.783	9.792	1.948	9.842	1.999	9.892	1.987	9.958	1.837
10.125	1.771	10.175	1.927	10.225	1.990	10.275	1.978	10.325	1.825
10.492	1.759	10.542	1.914	10.592	1.978	10.642	1.966	10.692	1.814
10.875	1.745	10.925	1.894	10.975	1.969	11.025	1.955	11.075	1.804
11.242	1.734	11.292	1.876	11.342	1.958	11.392	1.940	11.442	1.791
11.608	1.721	11.658	1.859	11.725	1.948	11.775	1.929	11.825	1.778
11.992	1.709	12.042	1.842	12.092	1.935	12.142	1.917	12.192	1.766
12.358	1.699	12.408	1.827	12.458	1.923	12.508	1.902	12.558	1.752
12.742	1.684	12.792	1.807	12.842	1.911	12.892	1.887	12.942	1.738
13.108	1.673	13.158	1.791	13.208	1.896	13.258	1.876	13.308	1.725
13.492	1.660	13.542	1.771	13.592	1.883	13.642	1.862	13.692	1.709
13.858	1.647	13.908	1.755	13.958	1.869	14.008	1.851	14.058	1.696
14.225	1.636	14.292	1.736	14.342	1.856	14.392	1.837	14.442	1.680
14.608	1.623	14.658	1.719	14.708	1.842	14.758	1.824	14.808	1.665
14.975	1.610	15.025	1.701	15.075	1.829	15.125	1.809	15.192	1.651
15.358	1.597	15.408	1.684	15.458	1.812	15.508	1.795	15.558	1.635

15.725	1.585	15.775	1.666	15.825	1.798	15.875	1.783	15.925	1.618
16.092	1.573	16.158	1.648	16.208	1.782	16.258	1.769	16.308	1.603
16.475	1.560	16.525	1.631	16.575	1.768	16.625	1.754	16.675	1.586
16.842	1.548	16.892	1.614	16.942	1.751	17.008	1.739	17.058	1.570
17.225	1.535	17.275	1.597	17.325	1.734	17.375	1.725	17.425	1.554
17.592	1.522	17.642	1.579	17.692	1.718	17.742	1.712	17.792	1.537
17.975	1.510	18.025	1.562	18.075	1.702	18.125	1.695	18.175	1.519
18.342	1.499	18.392	1.546	18.442	1.686	18.492	1.682	18.542	1.504
18.708	1.485	18.775	1.528	18.825	1.670	18.875	1.668	18.925	1.487
19.092	1.471	19.142	1.509	19.192	1.655	19.242	1.652	19.292	1.470
19.458	1.461	19.508	1.494	19.558	1.635	19.608	1.640	19.675	1.453
19.842	1.448	19.892	1.478	19.942	1.620	19.992	1.624	20.042	1.436
20.208	1.436	20.258	1.461	20.308	1.603	20.358	1.610	20.408	1.421
20.575	1.425	20.625	1.445	20.692	1.587	20.742	1.597	20.792	1.403
20.958	1.413	21.008	1.430	21.058	1.569	21.108	1.583	21.158	1.385
21.325	1.400	21.375	1.412	21.425	1.552	21.475	1.567	21.542	1.370
21.708	1.388	21.758	1.396	21.808	1.537	21.858	1.554	21.908	1.352
22.075	1.375	22.125	1.381	22.175	1.519	22.225	1.541	22.275	1.335
22.458	1.364	22.508	1.365	22.558	1.503	22.608	1.527	22.658	1.319
22.825	1.351	22.875	1.349	22.925	1.486	22.975	1.515	23.025	1.303
23.192	1.342	23.242	1.333	23.308	1.469	23.358	1.500	23.408	1.286
23.575	1.328	23.625	1.318	23.675	1.453	23.725	1.486	23.775	1.269
23.942	1.316	23.992	1.304	24.042	1.436	24.092	1.471	24.142	1.254
24.325	1.305	24.375	1.288	24.425	1.420	24.475	1.458	24.525	1.237
24.692	1.295	24.742	1.274	24.792	1.403	24.842	1.445	24.892	1.222
25.058	1.283	25.125	1.259	25.175	1.387	25.225	1.432	25.275	1.205
25.442	1.272	25.492	1.245	25.542	1.372	25.592	1.418	25.642	1.191
25.808	1.260	25.875	1.230	25.925	1.355	25.975	1.405	26.025	1.175
26.192	1.249	26.242	1.216	26.292	1.339	26.342	1.392	26.392	1.160
26.558	1.239	26.608	1.203	26.658	1.324	26.708	1.380	26.775	1.144
26.942	1.227	26.992	1.189	27.042	1.308	27.092	1.365	27.142	1.129
27.308	1.216	27.358	1.175	27.408	1.293	27.458	1.353	27.508	1.115
27.675	1.207	27.742	1.162	27.792	1.277	27.842	1.340	27.892	1.100
28.058	1.195	28.108	1.149	28.158	1.262	28.208	1.328	28.258	1.086
28.425	1.184	28.475	1.137	28.525	1.246	28.575	1.316	28.642	1.071
28.808	1.175	28.858	1.122	28.908	1.233	28.958	1.302	29.008	1.058
29.175	1.163	29.225	1.109	29.275	1.218	29.325	1.291	29.375	1.044
29.542	1.153	29.608	1.097	29.658	1.203	29.708	1.279	29.758	1.030
29.925	1.144	29.975	1.085	30.025	1.188	30.075	1.266	30.125	1.016
30.292	1.133	30.342	1.073	30.392	1.173	30.458	1.255	30.508	1.003
30.675	1.123	30.725	1.061	30.775	1.160	30.825	1.244	30.875	0.989
31.042	1.112	31.092	1.049	31.142	1.146	31.192	1.232	31.242	0.976

31.425	1.102	31.475	1.037	31.525	1.132	31.575	1.221	31.625	0.963
31.792	1.093	31.842	1.025	31.892	1.119	31.942	1.209	31.992	0.951
32.158	1.085	32.208	1.014	32.258	1.106	32.325	1.197	32.375	0.938
32.542	1.074	32.592	1.002	32.642	1.094	32.692	1.186	32.742	0.926
32.908	1.065	32.958	0.992	33.008	1.079	33.058	1.176	33.108	0.914
33.275	1.054	33.342	0.980	33.392	1.067	33.442	1.165	33.492	0.902
33.658	1.046	33.708	0.970	33.758	1.054	33.808	1.154	33.858	0.890
34.025	1.037	34.075	0.958	34.142	1.041	34.192	1.143	34.242	0.879
34.408	1.026	34.458	0.948	34.508	1.029	34.558	1.132	34.608	0.866
34.775	1.018	34.825	0.937	34.875	1.017	34.925	1.123	34.992	0.855
35.158	1.009	35.208	0.927	35.258	1.005	35.308	1.111	35.358	0.845
35.525	1.000	35.575	0.916	35.625	0.994	35.675	1.100	35.725	0.834
35.908	0.991	35.958	0.906	36.008	0.982	36.058	1.091	36.108	0.823
36.275	0.982	36.325	0.897	36.375	0.970	36.425	1.080	36.475	0.813
36.642	0.973	36.708	0.886	36.758	0.958	36.808	1.071	36.858	0.802
37.025	0.965	37.075	0.877	37.125	0.947	37.175	1.061	37.225	0.792
37.392	0.957	37.442	0.867	37.492	0.936	37.558	1.050	37.608	0.781
37.775	0.947	37.825	0.858	37.875	0.925	37.925	1.041	37.975	0.772
38.142	0.940	38.192	0.848	38.242	0.915	38.292	1.032	38.342	0.762
38.525	0.932	38.575	0.840	38.625	0.905	38.675	1.023	38.725	0.752
38.892	0.924	38.942	0.830	38.992	0.893	39.042	1.014	39.092	0.743
39.258	0.916	39.308	0.822	39.358	0.883	39.425	1.004	39.475	0.734
39.642	0.907	39.692	0.814	39.742	0.873	39.792	0.996	39.842	0.724
40.008	0.900	40.058	0.805	40.108	0.865	40.158	0.986	40.208	0.716
40.392	0.891	40.442	0.796	40.492	0.854	40.542	0.978	40.592	0.707
40.758	0.883	40.808	0.788	40.858	0.844	40.908	0.968	40.958	0.698
41.125	0.877	41.175	0.779	41.225	0.836	41.292	0.960	41.342	0.690
41.508	0.869	41.558	0.771	41.608	0.825	41.658	0.952	41.708	0.682
41.875	0.861	41.925	0.763	41.975	0.816	42.025	0.944	42.092	0.673
42.258	0.854	42.308	0.756	42.358	0.808	42.408	0.935	42.458	0.665
42.625	0.846	42.675	0.748	42.725	0.798	42.775	0.928	42.825	0.658
43.008	0.839	43.058	0.741	43.108	0.790	43.158	0.919	43.208	0.649
43.375	0.832	43.425	0.734	43.475	0.780	43.525	0.911	43.575	0.642
43.742	0.825	43.792	0.726	43.858	0.771	43.908	0.903	43.958	0.635
44.125	0.818	44.175	0.718	44.225	0.764	44.275	0.895	44.325	0.627
44.492	0.811	44.542	0.712	44.592	0.756	44.658	0.887	44.708	0.620
44.875	0.804	44.925	0.705	44.975	0.747	45.025	0.879	45.075	0.613
45.242	0.797	45.292	0.698	45.342	0.740	45.392	0.872	45.442	0.605
45.625	0.791	45.675	0.691	45.725	0.733	45.775	0.864	45.825	0.600
45.992	0.784	46.042	0.685	46.092	0.724	46.142	0.858	46.192	0.592
46.375	0.777	46.425	0.677	46.475	0.717	46.525	0.850	46.575	0.585
46.742	0.771	46.792	0.672	46.842	0.710	46.892	0.844	46.942	0.579

47.108	0.765	47.158	0.665	47.225	0.702	47.275	0.835	47.325	0.573
47.492	0.758	47.542	0.658	47.592	0.695	47.642	0.828	47.692	0.566
47.858	0.752	47.908	0.653	47.958	0.688	48.025	0.821	48.075	0.561
48.242	0.746	48.292	0.647	48.342	0.681	48.392	0.815	48.442	0.555
48.608	0.739	48.658	0.641	48.708	0.675	48.758	0.809	48.808	0.548
48.992	0.734	49.042	0.635	49.092	0.666	49.142	0.802	49.192	0.543
49.358	0.728	49.408	0.629	49.458	0.661	49.508	0.795	49.558	0.537
49.742	0.722	49.792	0.624	49.842	0.654	49.892	0.789	49.942	0.531
50.108	0.716	50.158	0.617	50.208	0.647	50.258	0.782	50.308	0.526
50.475	0.711	50.525	0.612	50.592	0.642	50.642	0.777	50.692	0.520
50.858	0.705	50.908	0.607	50.958	0.636	51.008	0.770	51.058	0.516
51.225	0.700	51.275	0.602	51.325	0.629	51.375	0.764	51.425	0.511
51.608	0.694	51.658	0.597	51.708	0.624	51.758	0.758	51.808	0.505
51.975	0.689	52.025	0.591	52.075	0.619	52.125	0.751	52.175	0.500
52.342	0.683	52.392	0.587	52.458	0.613	52.508	0.745	52.558	0.496
52.725	0.678	52.775	0.581	52.825	0.607	52.875	0.740	52.925	0.491
53.092	0.673	53.142	0.577	53.192	0.601	53.258	0.734	53.308	0.486
53.475	0.668	53.525	0.572	53.575	0.596	53.625	0.729	53.675	0.482
53.842	0.662	53.892	0.568	53.942	0.589	53.992	0.723	54.058	0.477
54.225	0.657	54.275	0.562	54.325	0.585	54.375	0.718	54.425	0.472
54.592	0.652	54.642	0.558	54.692	0.579	54.742	0.711	54.792	0.468
54.975	0.648	55.025	0.553	55.075	0.576	55.125	0.707	55.175	0.464
55.342	0.642	55.392	0.548	55.442	0.569	55.492	0.701	55.542	0.460
55.708	0.638	55.758	0.545	55.808	0.565	55.875	0.696	55.925	0.456
56.092	0.633	56.142	0.540	56.192	0.559	56.242	0.691	56.292	0.452
56.458	0.629	56.508	0.536	56.558	0.556	56.608	0.686	56.658	0.448
56.842	0.623	56.892	0.532	56.942	0.551	56.992	0.680	57.042	0.443
57.208	0.619	57.258	0.528	57.308	0.546	57.358	0.675	57.408	0.440
57.592	0.615	57.642	0.523	57.692	0.542	57.742	0.671	57.792	0.436
57.958	0.610	58.008	0.520	58.058	0.537	58.108	0.666	58.158	0.432
58.325	0.606	58.392	0.516	58.442	0.534	58.492	0.662	58.542	0.429
58.708	0.601	58.758	0.512	58.808	0.530	58.858	0.656	58.908	0.426
59.075	0.597	59.125	0.508	59.175	0.525	59.242	0.651	59.292	0.422
59.458	0.593	59.508	0.505	59.558	0.521	59.608	0.647	59.658	0.419
59.825	0.589	59.875	0.501	59.925	0.516	59.975	0.642	60.025	0.415
60.208	0.584	60.258	0.497	60.308	0.513	60.358	0.638	60.408	0.412